



MEDICAL UNIVERSITY
OF VIENNA

Genetic synthetic rescue interactions for the Fanconi anemia pathway of DNA repair

Doctoral thesis at the Medical University of Vienna
to obtain the academic degree

Doctor of Philosophy

Submitted by

Lydia Robinson García, MSc

Supervisor:

Dr. Joanna I. Loizou

CeMM Research Centre for Molecular Medicine
of the Austrian Academy of Science
Lazarettgasse 14, AKH BT 25.3
1090 Vienna, Austria

Vienna, 08/2019

Declaration

The experimental part of the work that I present here was carried out in the laboratory of Dr. Joanna Loizou, DNA damage signaling group, CeMM Research Center for Molecular Medicine of the Austrian Academy of Sciences, Vienna, Austria. Additional experiments were carried out by the collaborator laboratories of Stephen P. Jackson and Haico van Attikum. The computational data analysis was carried out in the Center for Computational Biology & Bioinformatics, Department of Medicine, University of California.

The project was conceived by Dr. Joanna Loizou. The experimental part of the project was designed by Dr. Joanna Loizou and Dr. Georgia Velimezi with input from myself.

I performed the experimental work together with Dr. Georgia Velimezi, with assistance from Mag. Marc Wiedner, Dr. Michel Owusu and Dr. Martin Moder. MSc. Joana Ferreira da Silva helped with the visualization of the data. Dr. Francisco Muñoz-Martínez performed complementary experiments in the Jackson laboratory and Dr. Wouter W. Wiegant performed complementary experiments in the van Attikum laboratory. Dr. Sara Brin Rosenthal and Dr. Kathleen M. Fisch carried out the data analysis. We received advice on data analysis from Jörg Menche and USP48 constructs from the laboratory of Prof. Jason Moffat.

Dr Georgia Velimezi, Dr. Joanna Loizou and I wrote the manuscript, with input from all authors.

The manuscript resulting from this project is my first-author publication. It constitutes this thesis and has been reprinted according to the reprint and permission policies of the Nature Publishing Group. The article can be found in *Nature Communications*:

Map of synthetic rescue interactions for the Fanconi anemia pathway identifies USP48. Georgia Velimezi*, Lydia Robinson-Garcia*, Francisco Muñoz-Martínez, Wouter W. Wiegant, Joana Ferreira da Silva, Michel Owusu, Martin Moder, Marc Wiedner, Sara Brin Rosenthal, Kathleen M. Fisch, Jason Moffat, Jörg Menche, Haico van Attikum, Stephen P. Jackson, Joanna I. Loizou (*: these authors contributed equally)

Nature Communications, volume 9, article 2280 (2018)

<https://doi.org/10.1038/s41467-018-04649-z>

I, the author, wrote all the chapters of this thesis.

Table of Contents

Declaration	ii
Table of contents	iii
List of figures	vi
List of tables	vii
Abstract	viii
Zusammenfassung	ix
Publications arising from this thesis	x
List of abbreviations	xi
Acknowledgments	xvii
CHAPTER ONE: INTRODUCTION	1
1. DNA damage and genome instability	1
1.1. Inter-strand crosslinks	3
1.2. Replication-independent repair	4
2. The Fanconi anemia disease	6
2.1. History and origins	6
2.2. Classification of FA patients	7
2.3. Clinical features of FA	8
• Bone marrow failure	8
• Cancer predisposition	9
• Congenital abnormalities	10
2.4. Approaches to detect and treat FA patients	10
3. The Fanconi anemia pathway	13
3.1. Evolution and conservation of the FA pathway	13
3.2. Step 1: Detection of the lesion	13
• Activation and signaling	13
• Core Complex formation	14

3.3. Step 2: Downstream activation	15
• ID Complex	15
3.4. Step 3: Repair effectors	16
• Excision of the ICL and DSB generation	16
• Translesion synthesis	17
• DSB repair through Homologous Recombination	18
4. Ubiquitylation and the DNA damage response	23
4.1. Ubiquitin signaling in the FA pathway	24
5. Model systems for investigating the FA disease/pathway	27
5.1. Animal models of FA disease	27
• <i>Danio rerio</i>	27
• <i>Caenorhabditis elegans</i>	28
• <i>Mus musculus</i>	28
• <i>Sus scrofa domesticus</i>	30
5.2. Induced pluripotent stem cells	30
5.3. Mammalian cells	30
• Genetic synthetic lethal approaches	31
• Genetic synthetic rescue approaches	32
6. Mapping synthetic rescue interactions for the FA pathway	35
7. Aims	36
CHAPTER 2: RESULTS	37
1. Prologue	37
2. Research article	38
2.1. Supplementary information	52
CHAPTER 3: DISCUSSION	60
1. HAP1 as an ideal tool for genetic screens	60
2. How does USP48 function in the FA pathway	60
2.1. The role of USP48 in the Nf-κB pathway	61

2.2. The role of USP48 in p53 regulation	63
2.3. The role of USP48 in chromatin regulation	64
2.4. At which step in the FA pathway does USP48 exert its function?	66
3. Consequences of the discovery of USP48	69
3.1. In the context of the FA pathway	69
3.2. In the context of FA disease	70
4. Conclusions	71
CHAPTER 4: MATERIALS & METHODS	72
1.1. Materials	72
1.2. Methods	73
REFERENCES	76
CURRICULUM VITAE	93

List of figures

Figure 1. Types of ICLs	4
Figure 2. Timeline of discovery of FA genes (22 identified up to date)	6
Figure 3. Classification of FA genes according to their clinical manifestations (listed in order of discovery)	8
Figure 4. Evolutionary conservation of FA genes	13
Figure 5. Diagram depicting the repair of an ICL by the FA pathway	22
Figure 6. Schematic representation of a synthetic lethal interaction in the context of the DDR	32
Figure 7. Schematic representation of a synthetic rescue interaction in the context of the DDR	33
Figure 8. Workflow for the identification of synthetic rescue interactions in FA-deficient cells	35
Figure 9. USP48 catalytic dead clones in FA-deficient cells rescues MMC-induced sensitivity	61
Figure 10. USP48 does not promote p65/RELA nuclear translocation after MMC treatment	63
Figure 11. USP48 does not bind specifically to any region of the chromatin	65
Figure 12. Loss of USP48 uncovers a novel ubiquitin moiety on H2A	66
Figure 13. FAN1 depletion is not possible in a <i>USP48</i> -deficient background	67
Figure 14. <i>USP48</i> -deficient cells do not have a de-regulation in cell cycle progression but are sensitive to ATR inhibition	68

List of tables

Table 1. List of DNA repair pathways known to be functional in mammalian cells (adapted from Jeggo et al, 2016).	2
Table 2. List of tests performed to monitor FA patients	11
Table 3. List of materials employed in the experiments described in the Discussion section	72

Abstract

Fanconi anemia (FA) is a rare disease that results from defects in the DNA repair machinery, more specifically in the repair of inter-strand crosslinks (ICLs). It is characterized by bone marrow failure, developmental abnormalities, and increased cancer risk. To identify suppressor genes that function within this pathway, we have performed whole genome loss-of-function screens across a panel of 5 human haploid isogenic FA-deficient cells (FANCA, FANCC, FANCG, FANCI, FANCD2). As a result, we have identified the deubiquitylating enzyme, USP48, as synthetic viable for FA deficiencies. FA-deficient cells alone are sensitive to genotoxic stress, however, additional loss of USP48 confers resistance to ICL-inducing agents. FA-USP48-deficient cells show increased clearance of DNA damage and restoration of DNA repair as marked by enhanced BRCA1 and RAD51 recruitment to sites of damage and increase clearance of DNA damage. Hence, depletion of USP48 reduces chromosomal instability of FA-deficient cells. Our results reveal a new role for USP48 in controlling DNA repair and suggest it is a potential therapeutic target in the treatment of FA.

Zusammenfassung

Die Fanconi-Anämie (FA) ist eine seltene Erbkrankheit, welche auf Defekte in den DNA-Reparaturmechanismen zurückzuführen ist. Insbesondere die Reparatur von Interstrand Crosslinks (ICLs) scheint gestört. Häufige Symptome der FA sind Knochenmarkinsuffizienz, Entwicklungsstörungen und ein erhöhtes Krebsrisiko. Zur Identifizierung von Suppressor-Genen innerhalb dieses Pfades/Reparaturmechanismus, haben wir Whole-Genom-Loss-of-Function-Screens über ein Genpanel von fünf menschlichen, haploiden, isogenen, FA-defizienten Zellen (FANCA, FANCC, FANCG, FANCI, FANCD2) durchgeführt. Hierdurch konnte das ubiquitylierende Enzym USP48 als synthetisch lebensfähig geeignet für FA-Defizite identifiziert werden. FA-defiziente Zellen allein reagieren empfindlich auf genotoxischen Stress. Der zusätzliche Verlust von USP48 verleiht ihnen jedoch Resistenz gegen ICL-induzierende Substanzen. FA-USP48-defiziente Zellen weisen eine erhöhte Beseitigung von DNA-Schäden und die Wiederherstellung der DNA-Reparatur auf. Dies zeigt sich in einer erhöhten Rekrutierung von BRCA1 und RAD51 an geschädigten Stellen und einer erhöhten Beseitigung von DNA-Schäden. Dadurch reduziert der Schwund von USP48 die chromosomale Instabilität von FA-defizienten Zellen. Unsere Ergebnisse zeigen eine neue Rolle von USP48 in der Kontrolle der DNA-Reparatur. Darüber hinaus deuten sie darauf hin, dass USP48 ein potenzielles therapeutisches Ziel bei der Behandlung der FA ist.

Publications arising from this thesis

Title: Map of synthetic rescue interactions for the Fanconi anemia pathway identifies USP48

Authors: Gergia Velimezi*, Lydia Robinson-Garcia*, Francisco Muñoz-Martínez, Wouter W. Wiegant, Joana Ferreira da Silva, Michel Owusu, Martin Moder, Marc Wiedner, Sara Brin Rosenthal, Kathleen M. Fisch, Jason Moffat, Jörg Menche, Haico van Attikum, Stephen P. Jackson, Joanna I. Loizou

(*: these authors contributed equally)

Journal: Nature Communications, volume 9, article 2280 (2018)

Title: Synthetic lethal interactions for kinase deficiencies to DNA damage chemotherapeutics

Authors: Lydia Robinson-Garcia*, Joana Ferreira da Silva*, Joanna I. Loizou

(*: these authors contributed equally)

Journal: Cancer Research (accepted), Review

List of abbreviations

53BP1	Tumor Protein p53 Binding Protein 1
AGT/MGMT	O6-Alkylguanine-DNA Alkyl-Transferase
ALDH2	Aldehyde Dehydrogenase 2 Family Member
ALKB	α -Ketoglutarate-Dependent Dioxygenase
AML	Acute Myeloid Leukemia
ATP	Adenosine Triphosphate
ATR	Ataxia Telangiectasia and Rad3 Related Kinase
ATRIP	ATR Interacting Protein
BARD1	BRCA1 Associated Ring Domain 1
BCR-ABL	Fusion Protein of RhoGEF And GTPase Activating Protein And Proto-Oncogene Tyrosine-Protein Kinase
BER	Base Excision Repair
BLM	BLM Helicase REQ-Like
BMF	Bone Marrow Failure
BRCT	BRCA1 C-Terminus Domain
CDK1	Cyclin Dependent Kinase 1
cDNA	Complementary DNA
CHK1	Checkpoint Kinase 1
CIS	Cisplatin
CMG	Helicase Complex Cdc45–MCM–GINS
CML	Chronic Myeloid Leukemia
CPD	Cyclobutene Pyrimidine Dimer
cREL	REL Proto-Oncogene NF- κ B Subunit
CSA	ERCC Excision Repair 8, Csa Ubiquitin Ligase Complex Subunit
CSB	ERCC Excision Repair 6, Chromatin Remodeling Factor
CtIP	Retinoblastoma Binding Protein 8
DAPI	4',6-Diamidino-2-Phenylindole
DEB	1,2,3,4-Diepoxybutane
DDR	DNA Damage Response
DNA	Deoxyribonucleic Acid
DNA2	DNA Replication Helicase/Nuclease 2
DNAPKcs	DNA-Dependent Protein Kinase Catalytic Subunit
DOC	Deoxycholate Lysis Buffer
DR	Direct Reversal
DSB	Double Strand Breaks
DSBR	Double Strand Break Repair
dTAG	Degradation Tag

FCS	Fetal Calf Serum
GEN1	GEN1 Holliday Junction 5' Flap Endonuclease
GLI1	Glioma-Associated Oncogene Homolog 1, Zinc Finger Protein
gRNA	Guide RNA
H2A	Histone H2A
H2A.X	H2A Histone Family Member X
HAP1	Haploid cells derived from KBM-7
HCLK2	Telomere Maintenance 2
HDR	Homologous Directed Repair
HELQ	Helicase POLQ-Like
HEPES	4-(2-Hydroxy-Ethyl)-1-Piperazine Ethane Sulfonic Acid
HJ	Holliday Junction Structure
HLA	Human Leukocyte Antigen
HR	Homologous Recombination
HSC	Hematopoietic Stem Cell
HSCT	Hematopoietic Stem Cell Transplantation
HU	Hydroxyurea
ICL	Inter-Strand Crosslink
IκBs	Inhibitor of Nuclear Factor kappa B Kinase complex
iPSCs	Induced Pluripotent Stem Cells
IR	Ionizing Radiation
KBM7	Chronic Myelogenous Leukemia derived cells
KOH	Potassium Hydroxide
KU70	X-Ray Repair Cross Complementing 6
LIG4	DNA Ligase 4
LMNA	Lamin A
MDC1	Mediator of DNA Damage Checkpoint Protein 1
MDM2	Mouse Double Minute 2, proto-oncogene, E3 ligase
MDS	Myelodysplastic Syndrome
MGI	Mice Genome Informatics Database
MHF1-2	FANCM Interacting Histone Fold Protein 1-2
MLH1-3	MutL Homolog 1-3
MMC	Mitomycin C
MMR	Mismatch Repair
MRE11	MRE11 Homolog Double Strand Break Repair Nuclease
MSH2-6	MutS Homolog 2-6
MUS81	MUS81 Structure Specific Endonuclease Subunit
MUTYH	MutY DNA Glycosylase
NaOH	Sodium Hydroxide

NAT10	N-Acetyltransferase 10
NBS1	Nibrin
NEIL1-3	Nei Like DNA Glycosylase 1-3
NER	Nucleotide Excision Repair
NF-κB	Nuclear Factor Kappa B
NGS	Next Generation Sequencing
NHEJ	Non-Homologous End-Joining
NP-40	Nonidet P-40
OGG1	8-Oxoguanine DNA Glycosylase
p21	Cyclin Dependent Kinase Inhibitor 1A
p50	Nuclear Factor Kappa B Subunit 1
p52	Nuclear Factor Kappa B Subunit 2
p53	Tumor Protein P53
p100	Nuclear Factor Kappa B Subunit 2
p105	Nuclear Factor Kappa B Subunit 1
PARK6	PTEN induced Kinase 1
PARP1	Poly(ADP-Ribose) Polymerase 1
PBS	Phosphate Buffered Saline
PCNA	Proliferating Cell Nuclear Antigen
PFA	Paraformaldehyde
PI	Propidium Iodide
PNK	Proteinase K
POLD2	DNA Polymerase Delta 2, Accessory Subunit
POLD3	DNA Polymerase Delta 3, Accessory Subunit
Pol ϵ	DNA Polymerase Epsilon
Pol ζ	DNA Polymerase Zeta
Pol η	DNA Polymerase Eta
Pol ι	DNA Polymerase Iota
Pol κ	DNA Polymerase Kappa
Pol ς	DNA Polymerase Sigma
Pol ν	DNA Polymerase Upsilon
Pol ϕ	DNA Polymerase Phi
PRC1	Polycomb Repressive Complex 1
PTM	Post-Translational Modification
PUVA	Psoralen UV-A
qRT-PCR	Quantitative Reverse Transcription Polymerase Chain Reaction
RAD6	Ubiquitin Conjugating Enzyme E2B
RAD18	RAD18 E3 Ubiquitin Protein Ligase

RAD50	RAD50 Double Strand Break Repair Protein
RAD52	RAD52 Homolog, DNA Repair Protein
REV1	DNA Directed Polymerase
RELA	Nuclear Factor NF-Kappa-B p65 Subunit
RELB	Transcription Factor
RING	Really Interesting New Gene Finger Domain
RING1B	RING-Type E3 Ubiquitin Transferase RING2
RIPA	Radio-Immunoprecipitation assay
RMI1	RecQ Mediated Genome Stability 1
RNF8	Ring Finger Protein 8
RNF168	Ring Finger Protein 168
ROS	Reactive Oxygen Species
RPA	Replication Protein A
SCC	Squamous Cell Carcinoma
SCE	Sister Chromatid Exchange
SDS	Sodium Dodecyl Sulfate
SDS-PAGE	Sodium Dodecyl Sulfate–Polyacrylamide Gel Electrophoresis
SLX1	SLX1 Structure Specific Endonuclease Subunit
SNM1A	DNA Crosslink Repair 1A
SSB	Single Strand Break
SSBR	Single Strand Break Repair
ssDNA	Single Stranded DNA
TLS	Translesion Synthesis
TNF-α	Tumor Necrosis Factor alpha
TOPBP1	DNA Topoisomerase II Binding Protein 1
TOPIIIA	DNA Topoisomerase III Alpha
TRIS	Tris(hydroxymethyl)aminomethane
TUNEL	Terminal Deoxynucleotidyl Transferase dUTP Nick End Labeling
U2OS	Human Bone Osteosarcoma Epithelial Cell Line
UAF1	USP1 Associated Factor 1
Ub	Ubiquitin Moiety
UBC13	Ubiquitin Conjugating Enzyme E2N
UBD	Ubiquitin-Binding Domain
UBM	Ubiquitin Binding Motif
UBZ	Ubiquitin-Binding Zinc Finger Domain
UHRF1	Ubiquitin Like with PHD and Ring Finger Domains 1
USP1	Ubiquitin Specific Peptidase 1
USP48	Ubiquitin Specific Peptidase 48
UV	Ultra Violet

WES	Whole Exome Sequencing
WRN	Werner Syndrome ATP-Dependent Helicase
WT	Wild-Type
XPC	Xeroderma Pigmentosum Complementing Group C
XPF	Xeroderma Pigmentosum Complementing Group F
XPG	Xeroderma Pigmentosum Complementing Group G
XRCC4	X-Ray Repair Cross Complementing 4
XP-V	Xeroderma Pigmentosum Variant

Acknowledgments

I would like to begin by thanking my PhD supervisor Dr. Joanna I. Loizou. I am extremely grateful for the opportunity that she gave me 4 years ago. It has been a truly amazing adventure which has helped me grow as a scientist and as a person.

I would, of course, also like to thank Dr. Georgia Velimezi. She has been my constant companion and mentor during this period and I would not have been able to accomplish this without her. I am also grateful for the scientific and moral support of my colleagues (and friends) Joanna Ferreira da Silva and Dr. Michel Owusu. They have helped make the hard times easier to bare. Marc Wiedner has played a key role in the management of the lab and has supported my project, along with many others, pushing them towards success.

I am very grateful to have worked in such a stimulating environment as CeMM. It has been a pleasure to share space with my colleagues from the 6th floor and to have interacted with many other great scientists, always ready to help, assist and advice.

I would also like to thank my dear year of 2015: Michael Caldera, Ruochen Jia, Alexander Lercher, Robert Pazdzior, Julia Pazmandi, Federica Quattrone and Martin Watzenböck. I am very happy to have met you and to have shared with you this exciting experience. Also, I am grateful to my Spanish Support Group (Azahara Rodríguez y Adrián Cesar Razquin), who have made Vienna a home even when it was cold outside. I would also like to thank Rico Ardy and Tamara Casteels for sharing such fun times.

I cannot describe in words how grateful I am to my parents and my brother who have always supported me in any decision I have made, helping me arrive where I now stand. They have always felt close even in the distance. Finally, I am grateful to have had the support of Lorenz Sprich since the beginning of my PhD; he has been essential on this journey.

CHAPTER ONE: INTRODUCTION

1. DNA Damage and genome instability

Genome instability is inherently common in all living beings. The extreme complexity of the processes that an individual cell undergoes, in a steady state, can already produce a complex selection of by-products that alters the deoxyribonucleic acid (DNA) sequence. The biology of this molecule renders it highly vulnerable to chemical modifications, also known as mutations. If these changes cannot be reverted, they will be transmitted to future daughter cells, giving rise to deleterious/lethal or advantageous effects. Therefore, it is important to create a balance to promote a healthy progression of the cells throughout the cell cycle and, in a broader sense, a healthy individual during their entire life.

Throughout evolution, from unicellular organisms — archaea and eukaryotic — to multicellular organisms, different more advanced DNA repair mechanisms have appeared in order to maintain genome homeostasis. One of the first processes, discovered in the early 1960s, was the so-called photo-reactivation required for the repair of lesions induced by ultraviolet (UV) light from sunlight (Hanawalt, 2016). This exogenous source of damage can induce up to 10^5 DNA lesions per cell per day (Hoeijmakers, 2009). This repair process has been lost in the evolution of higher organisms and in some bacteria, and has been replaced with what is known as the Nucleotide Excision Repair pathway (NER), a more complex yet more efficient and versatile mechanism.

UV light is just one of the many sources of damage that can attack our DNA. For example, ionizing radiation (IR), to which we are generally exposed to through the use of X-rays or radiotherapy, can induce oxidation of the DNA bases and result in the generation of single-strand breaks (SSBs) or double-strand breaks (DSBs). Additionally, the use of different chemical therapies together with exposure to diagnostic techniques or cigarette smoke renders humans vulnerable to a plethora of DNA lesions that can be mutagenic (e.g. pyrimidine dimers or aromatic DNA adducts) or cytotoxic/cytostatic (SSBs, DSBs, inter-strand cross-links (ICLs)) (Hoeijmakers, 2009; Ciccia & Elledge, 2010).

It is essential we determine the type of lesions different agents can induce in our DNA because in doing so we can reduce our exposure to them. However, there are also endogenous sources of damage that are not so easily avoided. On the one hand, we can suffer from spontaneous reactions (i.e. hydrolysis), mis-incorporation of nucleotides during replication or alkylation of bases. On the other hand, products of our endogenous metabolism can also harm our genome: reactive oxygen species (ROS); nitrogen species; or products resulting from lipid peroxidation, like formaldehyde (Ciccia & Elledge, 2010;

Hoeijmakers, 2009; Niedernhofer *et al*, 2005; Moldovan & D'Andrea, 2009). Additionally, certain processes, such as replication, will induce stress in the DNA helix, stalling replication forks and eventually resulting in spontaneous DSBs.

In mammalian cells, a collection of repair pathways have evolved to specifically tackle each type of lesion (**Table 1**). In doing so, cells have developed a fine-tuned system in which they can specifically activate a pathway according to the lesion in place and, promote the utmost fidelity of repair. Note that these pathways do not exert their function in an isolated fashion but, on the contrary, a complex signaling network intertwines them allowing for narrow crosstalk between pathways. The most prominent example of these collaborative efforts takes place when ICLs occur in the DNA.

Table 1. List of DNA repair pathways known to be functional in mammalian cells (adapted from Jeggo *et al*, 2016).

Repair pathway	Lesion	Key players
Direct reversal (DR)	O-alkylated bases	O ₆ -alkylguanine-DNA alkyltransferase (AGT/MGMT)
	N-alkylated bases	α-ketoglutarate-dependent dioxygenase (AlkB)
Translesion Synthesis (TLS)	Replication past lesions	REV1, Pol η, Pol ι, Pol κ
Mismatch Repair (MMR)	Mismatched bases	MSH2/MSH6, MLH1 and MLH3
Base Excision Repair (BER)	Oxidative bases Deaminated bases Alkylated bases Abasic bases	Mono-functional or bi-functional glycosylases (MUTYH, OGG1, NEIL1-3)
Nucleotide excision repair (NER)	Bulky lesions (i.e. CPDs)	Global-genome NER: XPC, XPF-ERCC1, XPG Transcriptional-coupled NER: CSA and CSB
Fanconi Anemia (FA)	ICLs	FA core complex, ID complex, BRCA1
Single Strand Break Repair (SSBR)	SSBs	PARP1, Pol ε, PCNA
Double Strand Break Repair (DSBR)	DSBs	Homologous recombination (error-free repair): BRCA1, RPA, RAD51
		Non-homologous end-joining (error-prone repair): 53BP1, XRCC4, LIG4

1.1. Inter-strand crosslinks

As mentioned before, a variety of lesions can occur in the DNA. One of the most deleterious types of damage are ICLs; one single cell can only tolerate between 20-60 at a time (Clauson *et al*, 2013). These lesions induce the blockage of essential processes, such as replication and transcription, through the formation of a covalent bond between opposite strands of the DNA that is irreversible.

Cross-linking agents can arise from either exogenous or endogenous sources. They are bifunctional, since they can bind to both DNA strands, requiring the repair machinery to repair both strands in contrast to their monofunctional analogues. Hence, they are extremely genotoxic by nature. These agents typically produce damage at the chromosomal level and induce DNA strand breakage, increasing recombination events such as sister chromatid exchanges (SCE) (Noll *et al*, 2006).

The main drugs that induce this type of lesions are bifunctional alkylating agents (nitrogen mustards), mitomycin C (MMC) and platinum compounds (i.e. cisplatin (CIS)). Psoralen and psoralen derivatives can also induce ICLs after UV light exposure (**Figure 1**). Due to their high toxicity, especially to highly active replicating cells, these drugs are used as chemotherapeutic agents. MMC is mainly used for the treatment of early stage bladder cancer but also for the treatment of aggressive cancers such as adenocarcinoma of the stomach and pancreas (Tuinmann *et al*, 2004; Schunke *et al*, 2018; Ferrarotto *et al*, 2012); additionally, it has been used in combination with other anticancer treatments. CIS has shown an effect against cancers of the ovaries and testes, as well as blood cancers and other solid tumors (Shaloam & Tchounwou, 2014). Psoralen treatment, also known as Psoralen and UV-A (PUVA), is well established for the treatment of psoriasis, a skin condition by which cells on the skin's surface divide at high speed (Zhang & Wu, 2018). Due to its resemblance to certain skin cancers, the use of psoralen as a potential anti-cancer drug is also being explored (Wang *et al*, 2016; Oldham *et al*, 2016).

Endogenously, it has been proposed that by-products of the lipid peroxidation pathway could be a source of ICLs, due to their structure (i.e. aldehydes, malonaldehydes) (Noll *et al*, 2006; Deans & West, 2011). Most recently, it has been shown that acetaldehyde and formaldehyde can induce specific sensitivity to those cells lacking proteins involved in the repair of ICLs (Langevin *et al*, 2011; Rosado *et al*, 2011). Formaldehyde and acetaldehyde are generated as by-products of cell metabolism (ethanol metabolism), demonstrating that both molecules are the source of endogenous ICLs.

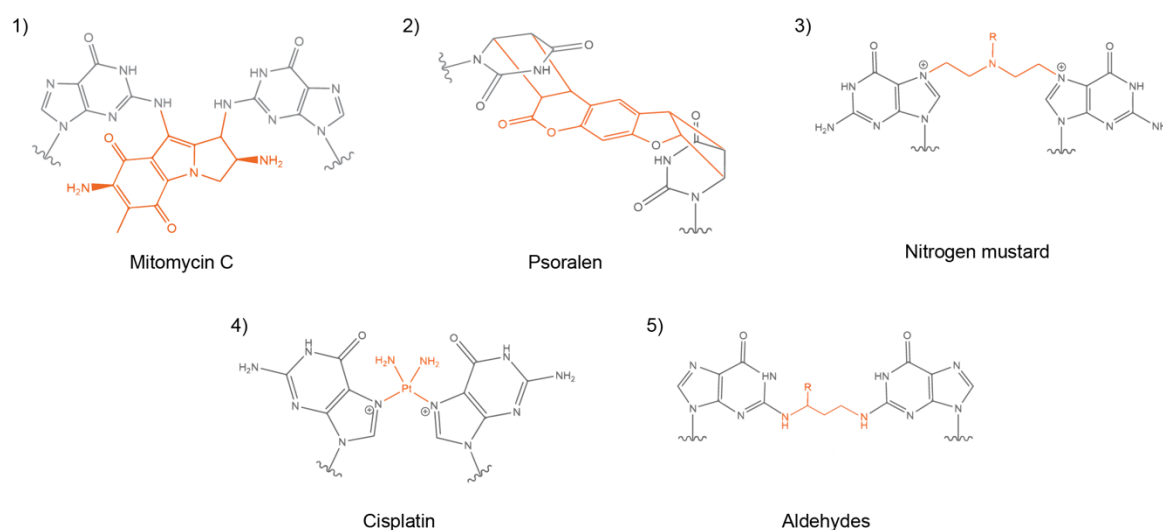


Figure 1. Types of ICLs. Depending on the damaging agent ICLs can adopt many different structures that can deform or not the double DNA helix. Orange depicts a crosslink between two base pairs.

1.2. Replication-independent repair

Repair of ICLs is generally studied in the context of replication, since it is during S-phase that ICLs are going to have their most deleterious effect. Nevertheless, un-repaired ICLs during G1-phase can also present negative effects for cell cycle progression. It has been suggested that this is because ICLs may be blocking the transcription of essential genes.

In vitro studies have shown that NER is involved in the repair of ICLs in G1. This correlates with the clinical features described in patients deficient in NER repair or XP-V (Xeroderma pigmentosum variant). These patients show mild sensitivity to ICL-inducing agents, suggesting a possible role for NER in ICL repair (Ho & Schärer, 2010; Enoiu *et al*, 2012). To distinguish which NER pathway is involved in ICL repair, specific knock-out cells for the global-genome NER (i.e. Xeroderma pigmentosum complementing group C (XPC)-deficient) or transcription-coupled NER (i.e. Excision repair 8/6 (CSA/CSB)-deficient) were tested for their capacity to repair an ICL. Interestingly, and in line with the hypothetical toxicity of ICL due to transcription blockage, transcription-coupled NER-deficient cells were unable to deal with these lesions. This indicates that NER is activated when an ICL is blocking the transcription of a gene (Enoiu *et al*, 2012).

After the ICL is excised through the activity of the nucleases Xeroderma Pigmentosum complementing group F (XPF) and Excision Repair 1 (ERCC1), the gap is filled by TLS polymerases. In particular, DNA polymerases κ , ζ and DNA directed polymerase (REV1) have been shown to have a predominant role in this step (Hashimoto *et al*, 2016; Enoiu *et al*,

2012). However, it remains unclear whether they have overlapping functions. In order to exert their function, TLS polymerases need to be recruited to the site of damage. It has been shown that mono-ubiquitylated Proliferating Cell Nuclear Antigen (PCNA) is essential for the correct repair of replication-independent ICLs, promoting the recruitment of TLS polymerases (Williams *et al*, 2012; Ho & Schärer, 2010). It is also known that during replication, PCNA is ubiquitylated by the E3 ligase RAD18. Furthermore, for the recruitment of RAD18 to the site of damage, the presence of Replication Protein A (RPA) coated single-stranded (ssDNA) is required. This could occur during G1-phase due to the presence of RPA while the lesion is being excised by the NER nucleases.

Note that different studies have reported that upon loss of the NER pathway, there is a reactivation in the repair of ICLs. Suggesting the presence of tolerance mechanisms such as MMR that can take over in order to reduce genome instability (Enoiu *et al*, 2012; Hashimoto *et al*, 2016).

2. The Fanconi anemia disease

2.1. History and origins

Defects in genes involved in the repair of ICLs give rise to the development of a monogenic rare disease called Fanconi anemia (FA). This illness was first identified by the Swiss pediatrician Guido Fanconi in 1927 (Garaycochea & Patel, 2013). He described three siblings suffering from birth abnormalities and severe anemia. He also hypothesized that the complexity of this disease had to be due to chromosomal translocations. However, it was only later in the 1960s, that the underlying cause of the disease was discovered to be due to chromosomal instability (Lobitz & Velleuer, 2006).

Phenotype-complementing assays were developed in the effort to determine the origin of the disease. These assays allowed researchers to stratify patients by fusing cells from two independent FA individuals. After treatment with MMC, if the resulting cell remained sensitive to the damage, both patients would belong to the same complementation group. On the other hand, if the cell became resistant to the damage, the patients had different causing mutations and, hence, they could complement each other (Joenje & Patel, 2001).

60 years after the discovery of the disease only three complementation groups had been identified and it was not until 1992 that the *FANCC* gene associated with complementation group C was identified, as a result of the development of complementation-cloning technology (Strathdee *et al*, 1992). This assay employs immortalized lymphoblasts of an FA patient that are then transfected with a cDNA library. Transfected cells are subjected to MMC selection and those that are resistant to the lesion have incorporated the DNA of a complementary gene that can restore their phenotype (Joenje & Patel, 2001). This revolutionary tool has allowed for an exponential increase in the discovery rate of FA genes (Figure 2).

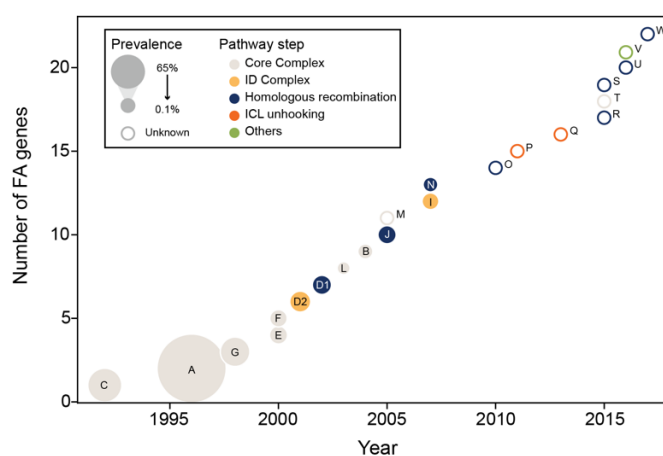


Figure 2. Timeline of discovery of FA genes (22 identified up to date). Bubble size indicates the prevalence of mutations in FA patients of a specific gene. The bubble color indicates the step of the pathway.

The main reason for this arduous path is the lack of a phylogenetic root amongst these genes. The sole link between them is the FA-like pathophysiology that their loss causes. It is important to understand that other genes are involved in the repair of ICLs, even though no FA patient has been identified as bearing a mutation in these genes.

2.2. Classification of FA patients

As mentioned before, FA is a rare monogenic disease. Its prevalence varies depending on the population from 1:200 000 to 1:400 000, with higher incidence in Ashkenazi and Afrikaners (Dong *et al*, 2015). Founding mutations have been identified for different populations although it has been determined that FA Complementing genes A, C and G (*FANCA*, *FANCC* and *FANCG*) constitute ~85% of all FA cases (Dong *et al*, 2015). FA patients manifest a plethora of clinical pathologies. Interestingly, their symptoms are not only dependent on the gene affected but, also, on the type of mutation. Efforts have been invested in developing classification tables to stratify patients although the rare presence of some mutations and the complexity of the clinical features confounds this procedure (Morales *et al*, 2008). Clearly, predicting disease development remains difficult. Nevertheless, some complementation groups have a higher predisposition to certain types of cancer — such as FA Complementing group D1, N and J (*FANCD1/BRCA2*, *FANCN* and *FANCI*), which are related to breast and ovarian cancer (Bogliolo & Surrallés, 2015). The high clinical diversity correlates to the complex functionality of each complementation group at the molecular level. Surprisingly, this extensive heterogeneity is counter-balanced at the cellular level, where FA-cells manifest a unique phenotype: (1) sensitivity to crosslinking agents, (2) cell cycle arrest, (3) chromosome breakage and (4) dysregulated apoptosis (Neveling *et al*, 2009). This serves as a tool for the diagnosis of FA patients, even if they do not present one of the known mutations. Additionally, 15 of the 22 FA genes identified have been classified as *bona fide* FA genes. This classification follows the criteria that at least two patients must present the same gene mutant and show chromosomal instability and bone marrow failure (BMF). These genes cover each step of the pathway: detection of the lesion (Core Complex), signaling (ID Complex), unhooking of the ICL (nucleases), and controlled DSB repair (HR) (Bogliolo & Surrallés, 2015). This reflects the essentiality, in humans, of the correct resolution of lesions (**Figure 2 & Figure 3**).

	<i>Bona Fide</i>	FA-like	FBOC
FANCC	Light Blue	Grey	Grey
FANCA	Light Blue	Grey	Grey
FANCG	Light Blue	Grey	Grey
FANCE	Light Blue	Grey	Grey
FANCF	Light Blue	Grey	Grey
FANCD2	Light Blue	Grey	Grey
FANCD1/BRCA2	Light Blue	Grey	Orange
FANCL	Light Blue	Grey	Grey
FANCB	Light Blue	Grey	Grey
FANCJ/BRIP1	Light Blue	Grey	Orange
FANCM	Grey	Grey	Orange
FANCI	Light Blue	Grey	Grey
FANCN/PALB2	Light Blue	Grey	Orange
FANCO/RAD51C	Grey	Teal	Orange
FANCP/SLX4	Light Blue	Grey	Grey
FANCQ/ERCC4	Light Blue	Teal	Grey
FANCR/RAD51	Grey	Teal	Grey
FANCS/BRCA1	Grey	Teal	Orange
FANCT/UBE2T	Light Blue	Grey	Grey
FANCU/XRCC2	Grey	Grey	Grey
FANCV/REV7	Grey	Grey	Grey
FANCW/RFWD3	Grey	Grey	Grey

Figure 3. Classification of FA genes according to their clinical manifestations (listed in order of discovery). Each of the 22 FA genes identified can be classified in three categories: *Bona Fide* genes, which fulfil the criteria of the FA pathophysiology; FA-like genes, which give rise to some but not all the clinical features; and FBOC genes, which are associated with familial breast and ovarian cancer.

2.3. Clinical features of FA

- **Bone marrow failure**

BMF is the main hallmark of FA disease. FA patients are born with complete blood counts that rapidly deplete and result in the manifestation of symptoms at a median of age of 7 years. Generally, they have low levels of platelets, leukocytes, and thrombocytes resulting in aplastic anemia (Garaycoechea & Patel, 2013). The main goal for physicians and scientists has been to restore the hematopoietic stem cell pool (HSC). Thus far, the most successful solution has been progenitor stem cell transplantation (HSCT). Thanks advances in the methodology and use of drugs like fludarabine, this procedure has improved the survival rate by up to 5 years in ~94% of patients undergoing this procedure (Gluckman, 2015). However, it has certain drawbacks: HSCT requires human leukocyte antigen (HLA)-matched HSC

cells from an (un)related donor and this is often available. Additionally, this approach is associated with the unsolicited side-effect of increased cancer risk, especially in FA patients who are deficient in DNA repair (Bogliolo & Surrallés, 2015).

The fact that all blood lineages are depleted suggests that there is a defect in the hematopoietic stem cell pool (HSC). This is due to the high basal levels of replication stress intrinsic to FA cells that activates the tumor suppressor protein P53 (p53) and its downstream effector the cyclin dependent kinase inhibitor 1A (p21) inducing cell death (Ceccaldi *et al*, 2012). In addition, these defects are not only due to replication stress but also to the presence of ICLs induced by by-products of cell metabolism i.e. aldehydes, compromising the functionality of the HSCs (Garaycochea *et al*, 2018, 2012). Defects in the stem cell pool have also been assumed to be the cause of infertility in FA patients. More specifically, defects during the development of the primordial germ cell (PGC), the precursors of sperm and eggs, resulting in a reduced number of gametes (Tsui & Crismani, 2019). Around 50% of female FA patients and the majority of all male FA patients have been shown to be infertile. And their chances of conceiving are reduced to 15% for female FA patients compared to the 50% chances of non-FA individuals. The cause of the reduced number of gametes has also been associated with the ataxia telangiectasia and Rad3 related kinase (ATR)-p53-p21 pathway, in line with defects in proliferation due to endogenous damage (Luo *et al*, 2014).

- **Cancer predisposition**

The enormous efforts invested in tackling BMF symptoms have successfully improved survival rates although this has led to cancer becoming the next main cause of death. The deficiency in the blood lineages of FA patients provides the ideal environment for clonal blood cancers. Most characteristically, patients with FA develop leukemias and myelodysplastic syndromes (MDS). These tumors generally appear in patients at an early age in contrast to solid tumors such as head and neck, esophageal or vulvar carcinomas (Alter, 2003). Interestingly, there is a high incidence of liver cancers. The liver is the central organ for lipid metabolism which results in by-products such as formaldehyde that, as mentioned before, have been shown to be the endogenous source of damage (Moldovan & D'andrea, 2009). It is still unclear how the different cancers develop: Is it solely dependent on the DNA damage repair defects or is there a clear causal effect from the treatment patients are subjected to? which makes them extremely vulnerable to classical chemotherapy.

- **Congenital abnormalities**

Lastly, congenital abnormalities have been shown to be another hallmark of FA. These malformations can range from hearing impairment to microcephaly, covering a wide variety of affected organs (Arleen D. Auerbach, 2010). However, one third of all FA patients do not have this pathology. It has been hypothesized that defects in the FA pathway do not cause malformations although they can increase the risk patients presenting this pathology.

2.4. Approaches to detect and treat FA patients

Taking into consideration the previous clinical features of FA, the first diagnosis is suggested by the presence of BMF and congenital abnormalities. Nevertheless, the presence of one of these afflictions alone is enough to suspect that the patient might suffer from FA. To confirm this, a chromosomal fragility test is performed after exposing the patient's blood cells to crosslinking inducing agents (MMC or 1,2,3,4-diepoxybutane (DEB)). In some cases, it is impossible to determine chromosomal fragility due to somatic mosaicism. Mosaicism is a consequence of the molecular adaptation of HSCs or lymphocyte progenitors which revert the FA gene to a wild-type (WT) gene. In these cases, chromosomal fragility is tested on skin fibroblasts, where mosaicism is better appreciated. The next step is to perform complementation group assays to determine to which group the patient belongs to. Thus far, 22 genes have been identified as harboring mutations that lead to the development of FA. Additionally, within each gene, a plethora of mutations have been described to give rise to different phenotypic outcomes, all within the clinical spectrum of FA. However, there are still individuals without an identified causing mutation as it has been impossible to determine this through complementation group assays. Next generation sequencing (NGS) has become an efficient and accurate approach aimed at overcoming this. More specifically, whole exome sequencing (WES) is the preferred method of identifying novel genetic mutations in the context of rare diseases and cancer (Knies *et al*, 2012; Tetreault *et al*, 2015).

The application of this technique has exponentially improved the diagnosis of thousands of patients. For example, a cohort of patients with similar clinical features related to infertility, but no known cause, were diagnosed during adulthood through WES as harboring a novel *FANCA* mutation (Krausz *et al*, 2019). Concomitantly, the use of WES has also revealed novel FA genes such as the ubiquitin ligase *RFWD3* (Knies *et al*, 2017). In this case, there were previous reports of this protein being involved in replication stress but no direct link to the disease (Elia *et al*, 2015).

After a patient has been diagnosed with FA, an extremely thorough assessment of their pathology needs to be undertaken (**Table 2**) which is essential for correct treatment (Dufour, 2017). In the case of non-severe manifestation of any clinical features, patients are checked every few months in order to determine the evolution of the disease.

Table 2. List of tests performed to monitor FA patients

Hematological	Bone marrow	Morphology, cytogenetics, immunophenotyping
	Full blood count	Differential count
	Serum	Immunoglobulins, immunophenotyping, vaccine response
Extra hematological	Liver, kidney, heart, urinary tract, hearing and visual function, endocrinology and skeletal evaluation	
Malignancies	Especial attention to cancers of the oral cavity	
HLA test	Typing of the patient and siblings, in the case of no match search for unrelated donor	

For the treatment of the disease, the most efficient option to correct BMF is HSCT. However, it has recently been determined that only those patients with severe cytopenia benefit from this treatment without increasing the risk of death by comparison with non-transplanted patients (Dufour, 2017). The benefits are further improved when the donor is a matched HLA sibling. Indeed, a number of affected families have decided to have an HLA-compatible baby by preimplantation genetic diagnosis of the embryo (Trujillo & Surralles, 2015). These so-called “savior babies” were initially developed to treat an FA patient, and later on this procedure has been applied to the treatment of other diseases of the blood. With advances in stem cell technology, the possibility of autologous cellular therapy has become real. Induced pluripotent stem cells (iPSCs) can be generated from fibroblasts of an FA patient and, after correction of the repair defect they can be differentiated into HSC and potentially be transplanted into the patient. Other techniques have been developed in order to correct the FA defect by performing a short transduction with a therapeutic lentiviral vector. Using this technology Río *et al*, 2017 have shown *in vivo* repopulating properties in immunodeficient mice. Most excitingly, there is currently a Phase II clinical trial for the transplantation of CD34+ cells (marker for hematopoietic progenitors) in *FANCA*-deficient patients (NCT02931071).

In the case of patients that manifest MDS or acute myeloid leukemia (AML), HSCT becomes a risky option. These patients are extremely sensitive to the chemotherapy or radiation

therapy that is necessary for cytoreduction prior to the transplant. However, depending on their individual situation they undergo special pre-transplant treatment to minimize side-effects (Peffault de Latour & Soulier, 2016). An alternative to HSCT is the treatment with growth factors or androgens. In the first case, the treatment is never long-term because of the risk of clonal evolution. In the second case, treatment can vary between 2-4 years depending, mainly, on the patient's liver response and the occurrence of adenomas. Additional supportive treatments exist, based on the transfusion of red blood cells and/or platelets.

3. The Fanconi anemia pathway

3.1. Evolution and conservation of the FA pathway

The FA pathway is a complex DNA repair signaling pathway involved in the detection and clearance of ICLs, in a replication dependent manner (Palovcak *et al*, 2017). Initially, it was thought to be only in vertebrates since many of the essential genes in this phylum were not identified in lower species. However, later on it has been shown that specific proteins, such as the FA Complementing groups M, D2, Q and R (FANCM, FANCD2, FANCD2, FANCD2 and FANCD2), are conserved in other kingdoms (**Figure 4**) (Dong *et al*, 2015). These proteins are essential players in each of the three steps into which the pathway is divided: (1) detection of the lesion, (2) downstream activation and (3) repair effectors.

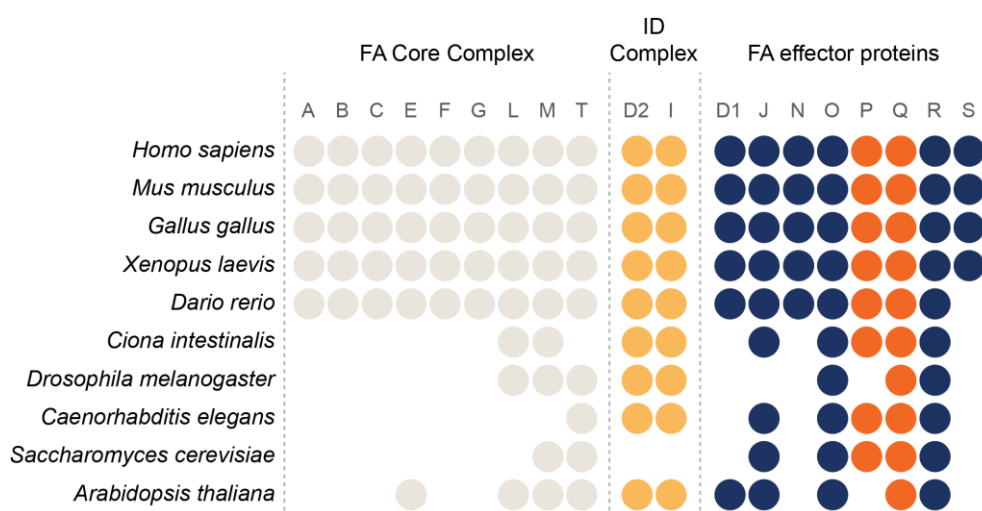


Figure 4. Evolutionary conservation of FA genes. This adaptation from Dong *et al*, 2015 shows the level of conservation of the FA genes within 10 different species from *Homo sapiens* to *Arabidopsis thaliana*.

The FA pathway comprises a group of proteins that, originally, have a role in the repair of other types of lesions. However, the unique interactions between them allow for correct repair. The main role of the FA pathway is to balance the activation of an error-free repair pathway, homologous recombination (HR), while blocking the activity of an error-prone pathway, known as non-homologous end-joining (NHEJ). This shift is due to the correct recognition of the lesion, avoiding replication fork stalling/collapse resulting in spontaneous DSBs, and, through the signaling and direct activation of HR proteins.

3.2. Step 1: Detection of the lesion

- **Activation and signaling**

The FA pathway is activated during S-phase when replication forks are stalled due to the presence of crosslinks. The S-phase checkpoint is controlled by the ATR and checkpoint

kinase 1 (CHK1) pathway, which is essential for maintaining replication fork integrity. When the replication forks converge with an ICL, the CMG helicases (Cdc45-MCM-GINS) (**Figure 5: step 3A**), essential for the unwinding of DNA during replication, presents a physical hindrance to the repair machinery. Breast Cancer Associated protein 1 (BRCA1/FANCS), activated by ubiquitylation signaling, is necessary for the unloading of CMG, hence exposing ssDNA (Long *et al*, 2014). To protect the ssDNA, RPA binds to the DNA followed by ATR and ATR Interacting Protein (ATRIP) (Kennedy & D'Andrea, 2005). Consequently, ATR phosphorylates multiple substrates: CHK1 and nibrin (NBS1), for checkpoint activation (Shiloh, 2001) and FANCM, for FA pathway activation (**Figure 5: step 3B**) (Singh *et al*, 2013). Modified FANCM and direct interaction with DNA topoisomerase II binding protein 1 (TOPBP1), induces a positive feedback loop for efficient ATR/CHK1 signaling in response to ICL-induced damage (Schwab *et al*, 2010; Singh *et al*, 2013).

FANCM is related to the XPF-MUS81 flap/fork endonuclease family. It possesses helicase activity which allows for branch migration throughout the cell cycle (Deans & West, 2009). For FANCM to exert its function it is necessary that it forms an heterodimer with the Fanconi Anemia Associated Protein 24 (FAAP24) (Ciccia *et al*, 2007). When FANCM-FAAP24 are anchored to the DNA they interact with ATR via telomere maintenance 2 protein (HCLK2), both proteins essential for the activation of the FA pathway (Collis *et al*, 2007). Additionally, FANCM interacts with the FANCM interacting histone fold protein 1-2 (MHF1/MHF2), a dimeric complex with putative histone fold domains that confer DNA binding affinity, offering a second DNA binding site for FANCM. Therefore, FANCM is constitutively bound to DNA in order to sense lesions and activate S-phase checkpoint to allow for ICL repair.

Additionally, other members of the FA pathway are also ATR targets: FANCA (Collins *et al*, 2009), FANCE (Wang *et al*, 2007), FANCG (Qiao *et al*, 2004), FANCD2 and FANCI (Andreassen *et al*, 2004). However, these events are essential further downstream in the pathway.

- **Core Complex formation**

Once FANCM is at the damaged site, it acts as the DNA targeting subunit of the FA Core Complex. The Core Complex consists of 10 FA Complementing groups: FANCA, FANCB, FANCC, FANCE, FANCF, FANCG, FANCL, FANCM, together with Fanconi Anemia Associated Proteins FAAP100, FAAP20 (**Figure 5: step 4**) (Clauson *et al*, 2013; Dong *et al*, 2015; Palovcak *et al*, 2017). Within the Core Complex, three individual subcomplexes have been identified: A-G-20, B-L-100 and C-E-F (Huang *et al*, 2014; van Twest *et al*, 2017; Yan *et al*, 2012). Each complex shows differential sensitivities to crosslinking agents indicating

that they have distinct functions (Huang *et al*, 2014). Specifically, to the role that each sub-complex has in the mono-ubiquitylation of FANCD2.

The A-G-20 sub-complex is able to associate to chromatin in the absence of B-L-100, functioning as a support module of the Core Complex (Huang *et al*, 2014). It has been inferred that the A-G-20 complex can bind to chromatin via the UBZ domain of FAAP20 and the DNA binding domain of FANCA (Huang *et al*, 2014).

In vitro, the ubiquitin ligase FANCL, together the ubiquitin conjugase FANCT/UBE2T, can restore FANCD2 mono-ubiquitylation, hence loss of the sub-complex that stabilizes this protein has a major role (Rajendra *et al*, 2014; Meetei *et al*, 2003). FAAP100 seems to function in engaging FANCL to its target and, together with FANCB, they stabilize each other.

The C-E-F sub-complex has a parallel function, but works independently, to the A-G-20 module in promoting the recruitment of the Core Complex (Huang *et al*, 2014). In this case, FANCF interacts with FANCM to induce chromatin enrichment of the complex (Deans & West, 2009).

Once they are recruited to the damaged site via FANCM, their role is to activate the downstream effector complex formed by the FA Complementing groups D2 and I (FANCD2 and FANCI). This activation is done by adding an ubiquitin molecule to each of the proteins.

3.3. Step 2: Downstream activation

- **ID Complex**

After the Core Complex is assembled onto the ICL, phosphorylation of FANCA by ATR and ubiquitylation of FANCI and FANCD2 (lysine 523 and lysine 561, respectively) by FANCL and FANCT/UBE2T allows for pathway progression (**Figure 5: step 5**) (MacKay *et al*, 2010).

FANCI and FANCD2 form what is known as the *ID Complex*. It is an inter-dependent complex at the heart of the pathway (Smogorzewska *et al*, 2007). Direct binding of the ID complex to DNA is required for mono-ubiquitylation of each protein (Joo *et al*, 2011). The C-E-F module, through direct interaction to the ID complex, acts as a sensor of FANCD2 mono-ubiquitylation and then drives the mono-ubiquitylation of FANCI (van Twest *et al*, 2017). In addition, the phosphorylation of FANCI by ATR, further increases the recruitment and interaction between both proteins, thus promoting a correct repair (Smogorzewska *et al*, 2007). The presence of this complex is necessary and essential for the unhooking of the ICL (Knipscheer *et al*, 2009), and further recruitment of other repair proteins.

De-ubiquitylation of the ID Complex by the ubiquitin-specific protease 1 (USP1) is hypothesized to be involved in the resolution of the repair as a way of shutting-down the FA pathway once the repair has been done. Direct interaction of USP1 to the ID complex is only acquired when the complex is no longer bound to chromatin (van Twest *et al*, 2017).

3.4. Step 3: Repair effectors

- **Excision of the ICL and DSB generation**

One major step for the repair of ICLs is the processing of the crosslink into DSBs. This is a key step, since it allows the conversion of an irreversible lesion to a DNA repair acceptable lesion. The XPF-ERCC1 complex – previously identified to have a role in NER – is a 3' DNA flap endonuclease which induces hypersensitivity to ICLs upon its loss (De Silva *et al*, 2002). It is the only nuclease that has been shown to be essential, but not sufficient, for ICL unhooking, and its activity is promoted by the presence of RPA (Klein Douwel *et al*, 2014; Kuraoka *et al*, 2000; Abdullah *et al*, 2017). After XPF-ERCC1 makes an incision near the ICL, the exonuclease DNA crosslink repair 1A (SNM1A) is able to digest nucleotides across the lesion and produce a suitable template for TLS (Wang *et al*, 2011). However, additional excision, at different steps of the repair process, is necessary: (1) ICL unhooking, (2) resolution of Holliday Junctions after HR or (3) the processing/removal of the unhooked adduct. Other nucleases, such as the structure-specific endonuclease MUS81-EME1 have been shown to act in the excision of DNA 3' flaps generated after replication fork conversion to the ICL, hence generating a DSB (Hanada *et al*, 2006).

The interaction of these proteins with the ICL and how they are recruited to DNA have been open questions for some time. The structure specific nuclease SLX4 serves as a scaffold for MUS81-EME1, XPF-ERCC1 and SLX1, amongst other proteins. Looking at mutations in patients, the ubiquitin-binding zinc finger domain (UBZ domain) of SLX4 seems to be greatly affected indicating a prominent role in the repair of ICLs (Stoepker *et al*, 2011; Kim *et al*, 2011). Furthermore, depletion of this domain showed specific sensitivity to MMC compared to other drugs such as poly(ADP-ribose) polymerase (PARP) inhibitors or camptothecin, a topoisomerase I inhibitor (Kim *et al*, 2012b). This could suggest that SLX4 goes to sites of damaged DNA through its UBZ domain and serves as a platform for MUS81-EME1 and XPF-ERCC1. In the first case, it has been shown that loss of the interacting domain between SLX4-MUS81 is dispensable for ICL repair. MUS81-EME1 might have a more predominant role in late-S-phase, to excise ICLs that have not been properly dealt with (Wang *et al*, 2011), and in replication restart by generation of DSBs after replication inhibition and

processing of HR intermediates (Hanada *et al*, 2007, 2006). In the second case, it has been shown that XPF-ERCC1 can be recruited to foci in cells with SLX4- Δ UBZ (Kim *et al*, 2012b). Of note, we refer to foci as DNA repair factories where the repair proteins localize to deal with a lesion. This suggests an independent role of the UBZ domains of SLX4 in ICL repair. The interaction between SLX4 and the nuclease complexes is essential for its localization and, therefore, the ICL excision (**Figure 5: step 6**) (Klein Douwel *et al*, 2017). Its recruitment is dependent on FANCD2 (Klein Douwel *et al*, 2014).

It has additionally been described the presence of a third nuclease, the FANCD2 and FANCI associated nuclease 1 (FAN1), which shows specificity for the excision of 5' DNA flaps (MacKay *et al*, 2010; Liu *et al*, 2010). The UBZ domain of FAN1 is essential for its recruitment to foci (Smogorzewska *et al*, 2010). Loss of ubiquitylated FANCD2 (Ub-FANCD2) depletes FAN1 foci formation, indicating that this modification is used as a scaffold for the recruitment of the nuclease after ICL generation. Recently, it has been shown that restoration of FAN1-UBZ* (with point mutations in the UBZ domain), independently of its localization to foci, rescues cell survival after MMC. However, this is not the case when the cells are treated with replication stress inducing agents such as hydroxyurea (HU). This suggests a more general role for FAN1, having a protective response when replication forks are stalled (Lachaud *et al*, 2016). This complex signaling process allows for independent regulation of the nucleases thus leading to a more fine-tuned excision of the lesions.

- **Translesion synthesis**

TLS is a pathway that allows for replication past DNA lesions, also known as DNA damage tolerance. It is performed by polymerases with a lower fidelity than the normal replicative polymerases. This step is essential to provide a template for repair of the DSBs generated after the excision of the ICL (Roy & Schärer, 2016). As mentioned previously, ICL-inducing agents can form a plethora of lesions in the DNA, affecting the minor or the major groove of the helix, provoking different degrees of distortion and/or crosslinking either the opposite or the same strand of the DNA. Hence, it has been complicated to determine which polymerases have a role in replication-dependent repair and how they function together in order to overcome these hurdles. Independent loss-of-function studies have been performed to address which error-prone polymerases confer sensitivity to ICL-inducing agents.

REV1 and Pol ζ have been shown to be essential for the repair of ICLs during replication, since loss of either polymerase shows an extreme sensitivity to ICL-inducing agents (**Figure 5: step 7A**) (Simpson & Sale, 2003; Sonoda *et al*, 2003). It has been shown that they act epistatically with FANCC (Patel *et al*, 2004). Recruitment studies indicate that the REV1

directly interacts with FANCA via FAAP20, suggesting a role of the Core Complex in recruiting TLS polymerases independently of the ID complex (Kim *et al*, 2012a). Moreover, recent studies have shown that both polymerases tightly interact with each other and they are localized to ICLs (Budzowska *et al*, 2015).

REV1 is a Y-family polymerase, which also interacts with other polymerases of the same family: Pol η , ι , and φ . Supporting the idea that it might work as a scaffold for TLS (Sale *et al*, 2012; Ho & Schärer, 2010). Pol ζ belongs to the B-family of polymerases, it consists of: REV3 and REV7, and the accessory subunits POLD2 and POLD3 (Lee *et al*, 2014). This enzyme lacks the 3' and the 5' proofreading exonuclease activity, has low processivity and a higher error rate on undamaged DNA (McCulloch & Kunkel, 2008). Moreover, studies using *Xenopus laevis* extracts have unequivocally shown that Pol ζ has a direct role in ICL repair. REV3 would be important for the addition of one nucleotide at the lesion position and REV7 would allow for the extension of the intermediates (Räschle *et al*, 2008).

Albeit REV1-pol ζ have a predominant role in bypassing ICLs in a replication dependent manner, other TLS polymerases have also shown to bypass ICLs in a structure specific manner. For example, Pol κ , another Y-family member, shows a sensitivity towards ICL-inducing agents upon depletion. However it has a predisposition to bypass only those lesions that do not significantly distort the DNA helix (minor groove) (Minko *et al*, 2008). Likewise, Pol ν , an A-family polymerase with low fidelity and robust arm displacement, shows high efficiency in bypassing major groove distortions (Yamanaka *et al*, 2010). Similar to Rev1-pol ζ , loss of Pol ν shows sensitivity to CIS. To determine the specific role of this enzyme, interactions study have revealed that it binds to FA and HR proteins: the recombinase RAD51 and PCNA. Additionally, Pol ν , together with the helicase POLQ-like (HELQ), have an epistatic effect with FANCD2 towards ICLs, showing that they are involved in allowing DNA synthesis in the FA pathway (Moldovan *et al*, 2010).

- **DSB repair through Homologous Recombination**

The last step of the process entails the repair of a DSB that is generated after the ICL adduct is excised via the nucleases. Spontaneously generated DSBs can be repaired by either NHEJ or HR, depending on the cell phase of the cell cycle. Yet again, proteins of an independent repair pathway have an essential role in the repair of ICLs. Considering that loss of the FA pathway results in high genomic instability, it has been hypothesized that NHEJ is blocked in the presence of FA proteins allowing for the activation of the HR pathway after nuclease-induced DSBs (Adamo *et al*, 2010a). Over time, many studies have aimed to determine the connection between these two pathways. Thus, the cross-talk between them

has become more and more apparent since they both have an important role in the maintenance of genome integrity in response to endogenous replication stress. Replication forks can be blocked due to the formation of ICLs from endogenous aldehydes, but also through the formation of R-loops in transcription or DNA secondary structures (García-Rubio *et al*, 2015). This results in overlapping functions between the proteins of each pathway, and one example is the BRCA1 interacting C-terminal helicase (BRIP1/BACH1/FANCI). This protein is a RECQ-like helicase required for the repair of IR or HU-induced DSBs, however it has been shown to interact with FANCD2 and is essential for FANCD2 foci formation (Zhang *et al*, 2010). Additionally, FANCD2 foci formation also fails in the absence of BRCA1 after MMC damage (Taniguchi *et al*, 2002).

Furthermore, mutations in individual genes from each pathway can result in similar phenotypic outcomes. On the one hand, mutations in known HR proteins such as BRCA1/2 and RAD51 resemble some FA pathologies (Michl *et al*, 2016). However, it is important to understand that complete abrogation of BRCA1/2 is lethal, so only hypomorphic mutations have been identified which do not recapitulate all the hallmarks of FA disease (Biswas *et al*, 2011). There appears to be a stronger link between BRCA2 mutations leading to hematological defects. In the case of BRCA1 mutants, no hematological defects are encountered even though the cells show sensitivity to the ICL-inducing agent carboplatin, so it would be more appropriate to associate BRCA1 mutations to an FA-like syndrome (Freire *et al*, 2018). Other HR proteins such as the partner and localizer of BRCA2 (PALB2/FANCD1) or RAD51 have been found to have biallelic or dominant negative mutations, respectively. Some of these examples present distinct separation of function between DSB and ICL repair. On the other hand, mutations in FANCD3 have been associated with a slightly increased predisposition to breast cancer (Michl *et al*, 2016).

The HR proteins are generally described as participating in the last steps of the FA pathway in order to repair the DSB and promote its resolution. However, different studies have reported the early presence of HR proteins during ICL repair. After replication fork conversion and prior to the recruitment of the Core Complex, BRCA1 promotes the unloading of CMG helicase from chromatin. This action leaves the DNA helix unprotected, a known hallmark of replication stress that induces the phosphorylation of RPA by ATR on serine 33. This phosphorylation mark triggers the additional phosphorylation, by the DNA-dependent protein kinase catalytic subunit (DNA-PKcs), on serines 4/8 which, together with the binding of RPA to ssDNA, in turn, induces cell-cycle checkpoint activation (Toledo *et al*, 2013; Chen & Wold, 2014; Ashley *et al*, 2014). RPA induces RAD51 recruitment to the

ssDNA protecting the replication fork from breakage or degradation and allowing a correctly coordinated incision process (Long *et al*, 2014).

After this initial step, the HR proteins again come into action in order to repair the DSB, as the final step in repairing an ICL. In this case, the canonical steps for DSB repair take place: (1) resection of the DSB, (2) DNA strand invasion and (3) junction resolution. The short-range resection is performed by the MRN (MRE11-RAD50-NBS1) complex, this complex is recruited via the RPA-coated ssDNA, together with the nuclease CtIP. Additionally, exonucleases EXO1/DNA2 and the BLM helicase, induce a more extended resection of the DSB. This function is tightly regulated by the Werner syndrome ATP-dependent helicase (WRN) that blocks MRN activity in order to avoid replication fork degradation (Syed & Tainer, 2018). BRCA2 then facilitates the removal of RPA and, concomitantly, loads RAD51 onto ssDNA, also helping to control MRN function (**Figure 5: step 7B**) (Kottemann & Smogorzewska, 2013).

RAD51-coated DNA filaments guide DNA strand invasion. This step consists on the unwinding and invasion of a homologous untouched dsDNA. This provides a 3' end for DNA synthesis. Consecutively, the second end is captured and the gap is filled, leading to the formation of a double Holliday Junction structure (HJ). This structure is common during meiosis and mitosis, after DSB generation, although in the former genetic crossover is promoted in order to enable genome haploidization (Matos & West, 2014). In the latter case, non-crossovers are preferred since they prevent the loss of heterozygosity and the consequent induction of genome instability. To return the DNA to its natural state, branch migration promotes HJ resolution, via cleavage by the HJ 5' flap endonuclease (GEN1) or SLX4-MUS81-EME1-SLX1 resolvases — resulting in either crossover or non-crossover (**Figure 5: step 8A**)— or HJ dissolution mediated by BLM, the DNA topoisomerase III alpha (TOPIIIa) and RecQ mediated genome stability 1 (RMI1), the BTR complex — resulting in non-crossover (**Figure 5: step 8B**) (Matos & West, 2014; Shah Punatar *et al*, 2017).

In an unperturbed state and after DNA damage, these enzymes are tightly controlled throughout the cell cycle. The BTR complex specifically functions in the dissolution of double HJ and is active during the entire cell cycle. BLM catalyzes the convergent branch migration of the two HJ, while TOPIIIa reduces the stress induced by the supercoiling of the DNA molecule. RMI1 helps TOPIIIa to bind to the DNA and “dissolve” the catenated DNA. Loss of the BLM helicase gives rise to the known rare disease BLM Syndrome, characterized by high SCE. This demonstrates the essential nature of the BTR complex or dissolvasome in the repair of DSBs (Mankouri & Hickson, 2007; Wu & Hickson, 2003; Swiec & Costa, 2014). In contrast, the resolvase enzymes gain a more predominant role after replication, during

mitosis. SLX4-MUS81-EME1-SLX1 (SLX-MUS holoenzyme) is phosphorylated by the cyclin dependent kinase 1 (CDK1) during the G2/M transition enabling it to bind to un-resolved double or single HJ and excise the DNA, blocking the formation of aberrant replication (Szakal & Branzei, 2013). Whereas high levels of phosphorylation on GEN1 block its function until late M phase. Additionally, GEN1 is only imported into the nucleus after nuclear membrane breakdown. Hence, GEN1 is spatially and temporarily regulated to maintain genome stability (Shah Punatar *et al*, 2017).

With the resolution/dissolution of the HJ, the repair of an ICL is completed allowing the cells to proceed to their division and the generation of two daughter cells.

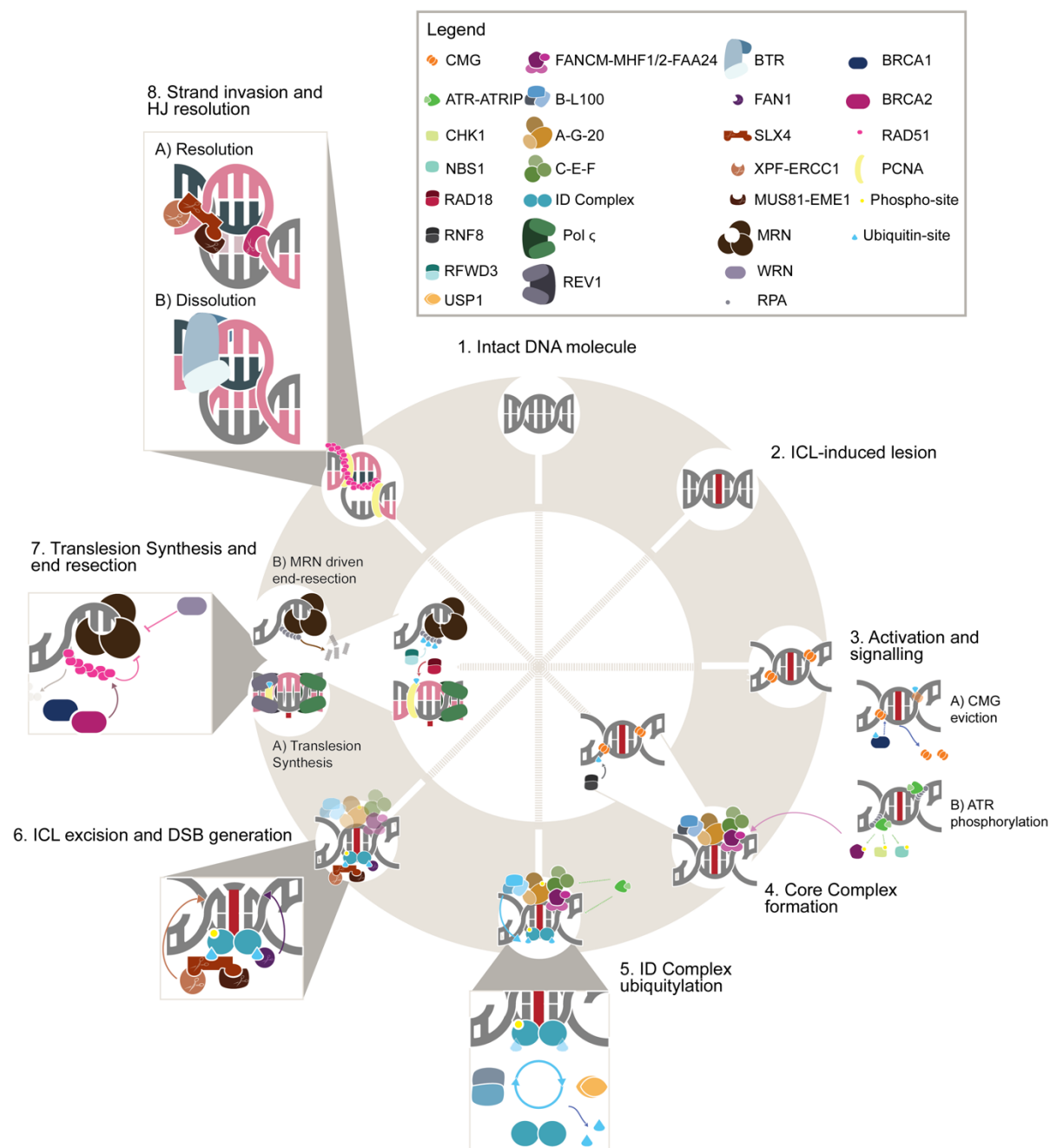


Figure 5. Diagram depicting the repair of an ICL by the FA pathway. An intact DNA molecule (1) is subjected to an ICL lesion (2) induced by endogenous or exogenous damage. ICL induces the activation of the FA pathway resulting in the eviction of CMG by BRCA1 (3A) and the phosphorylation of a variety of proteins by ATR, FANCM among others (3B). FANCM phosphorylation promotes direct binding to chromatin at the site of damage and the recruitment of the Core Complex (4). This is further promoted through the ubiquitylation of H2A by RNF8 (4: inner circle). The Core Complex ubiquitylates the ID Complex (5). This modification is removed by USP1 in order to switch off the pathway (5: amplification). The ubiquitylation of the ID Complex allows for the binding of nucleases and the subsequent excision of the ICL and the generation of a DSB (6). Low fidelity polymerases: REV1 and Pol ζ fill the gap formed after the excision of the ICL (7A); ubiquitylation of PCNA further promotes the binding of REV1 and Pol ζ (inner circle). End resection of the other DNA end is performed by the MRN complex (7B) to generate ssDNA and promote strand invasion by RAD51 (8). Prior to this, RPA is ubiquitylated by RFWD3 to remove it from the DNA and enable RAD51 binding (7: inner circle). Finally, after templated repair, the HJ is either resolved/dissolved resulting in an intact DNA molecule (8: amplification).

4. Ubiquitylation and the DNA damage response

Post-translational modifications (PTMs) play a major role in the regulation of the DNA damage response (Dantuma & van Attikum, 2016). These covalent/reversible modifications of target proteins offer a variety of signaling effects, providing quick and reversible dynamics that allow for fast responses. For example, there is no doubt about the regulatory effects that phosphorylation has in the activation of a wide range of proteins after DNA damage (Owusu *et al*, 2019). This is because of the predominant role that kinases — such as: ataxia telangiectasia mutated (ATM), ATR or DNA-PKcs — have in the activation and signaling of the DNA damage response (DDR) (A. & L., 2013; Hiom, 2005). However, there is emerging evidence that ubiquitylation also plays a major role in the DDR (Panier & Durocher, 2009).

Ubiquitin is a small molecule that is expressed ubiquitously in all tissues. Its structure is extremely conserved: 3/76 amino acids differ between yeast and humans (Panier & Durocher, 2009). The ubiquitin molecules bind to their substrate protein through their carboxy terminal glycine, this amino acid can covalently bind to any lysine residues through isopeptide bonds (Le *et al*. 2019). Ubiquitin itself has 7 lysine residues that can be further modified. This reaction is the result of the concerted activity of three independent enzymes: E1 (ubiquitin-activating enzyme), E2 (ubiquitin-conjugating enzyme) and E3 (ubiquitin ligase enzyme) (Panier & Durocher, 2009; Le *et al*, 2019).

This modification can vary depending on whether one or several ubiquitin moieties are bound to a protein (monoubiquitylation or multi-monoubiquitylation, respectively). Furthermore, several ubiquitin molecules can be consecutively added to a previous ubiquitin, termed poly-ubiquitylation. In this case, poly-ubiquitin chains can present different structures depending on which lysine of the ubiquitin is being modified since all lysine residues serve as acceptor sites. Thus far, one specific structure for proteasome signaling has been identified: K48, K29 and K11-linked poly-ubiquitin chains. Mono-ubiquitylation on K63 generally signals pathways such as DNA repair, signal transduction, protein trafficking and ribosomal protein synthesis (Panier & Durocher, 2009; Al-Hakim *et al*, 2010). The topology of these conformations is going to allow for the specific recognition and binding of ubiquitin-binding domains (UBDs).

These modifications are reversible due to the role of another set of enzymes called: de-ubiquitinases (DUBs). In the last 10 years, only a handful of novel DUBs have been identified, adding up to a total of around 100 proteases (Sowa *et al*, 2009; Le *et al*, 2019). This demonstrates the plasticity of these enzymes in removing ubiquitin moieties from any substrate. However, in addition to their catalytic domain, they contain other domains which can participate in the promotion of protein/substrate-protein interactions, enabling specificity

at protein substrate level (Citterio, 2015). There are 7 different families of de-ubiquitin enzymes, indicating a high degree of substrate specificity, the type of ubiquitin modifications they can target, and the chemical reaction they perform in order to modify their substrate (Al-Hakim *et al*, 2010; Le *et al*, 2019).

4.1. Ubiquitin signaling in the FA pathway

The FA pathway is tightly regulated by ubiquitylation. Therefore, it is to discuss the role of these modifications and which key steps they regulate. To begin, the ubiquitin ligase Ring Finger protein 8 (RNF8), together with its partner the Ubiquitin Conjugating enzyme E2N (UBC13), is involved in the ubiquitylation of the chromatin that surrounds a DNA lesion. This complex can either regulate a pathway through K63 poly-ubiquitylation or induce proteasomal degradation through K48 poly-ubiquitylation. Through the first modification, RNF8 can induce the recruitment of proteins such as BRCA1 after DSBs (Panier & Durocher, 2009). In addition, it has been shown that, after ICL generation, RNF8 catalyzes K63 poly-ubiquitylation marks on chromatin which are, in turn, recognized by the UBZ domain of FAAP20 (**Figure 5: step 4 – inner circle**) (Bick *et al*, 2017). This protein has been previously described as a member of the Core Complex and its correct binding to ubiquitin will ensure normal activation of the FA pathway and the mono-ubiquitylation of FANCD2 (Yan *et al*, 2012). Depletion of RNF8 results in the abolition of FANCD2 recruitment to foci. Similarly, PALB2 recruitment is lost in the absence of the ubiquitin mark. However, the regulation of PALB2 is independent of that of FANCD2 since it will depend on the Mediator of DNA damage checkpoint protein 1 (MDC1) (Bick *et al*, 2017). MDC1 is an important protein in the repair of DSBs, hence it is involved in the recruitment of PALB2 to the damaged site at a later point than FANCD2.

Activation of the FA pathway is characterized by the ubiquitylation of the ID Complex. This process is performed by the Core Complex, but more specifically by the ubiquitin ligase FANCL. FANCL is characterized as having three main domains, conserved amongst FANCL homologs: the ELF domain for accurate FANCD2 ubiquitylation, the DRWD domain for substrate binding, and the RING domain to interact with UBE2T (Miles *et al*, 2015). The essential proteins for this reaction are: E1, E2 conjugase (UBE2T), FANC-L and, surprisingly, FANCI. Presence of FANCI will enable specificity to the reaction so that the lysine 561 of FANCD2 is modified correctly. Additionally, FANCL also mono-ubiquitylates FANCI on lysine 523 (Garner & Smogorzewska, 2011). It has been established that this step is essential for the pathway and that the mutations/loss of FANCD2 will induce defects in ICL repair (Al-Hakim *et al*, 2010).

Concomitantly, Ub-FANCD2 serves as a scaffold for the recruitment of nucleases such as FAN1 via the UBZ-like domain present in the nuclease (Lachaud *et al*, 2016). The nuclease SLX4 also has a UBZ domain that renders the cells sensitive to crosslinking-inducing agents when mutated, and is associated with FANCD2 (Yamamoto *et al*, 2011; Garner & Smogorzewska, 2011). This modification is reverted by USP1 in order to promote a controlled shutting down of the FA pathway. This DUB works in conjunction with the UAF1. It is, at the same time, regulated at a transcriptional level, showing a peak of expression during S-phase and via polyubiquitylation which will mediate proteasome-dependent degradation when it is no longer needed (Garner & Smogorzewska, 2011).

In addition to de-ubiquitylating FANCL and FANCD2, USP1 acts on PCNA. PCNA has a predominant role in TLS for the activation of plastic polymerases in order to bypass lesions that block the progression of the replication fork during S-phase, including ICLs (Liang *et al*, 2014; Arkinson *et al*, 2018). PCNA is ubiquitylated by the ubiquitin ligase complex RAD18-RAD6 (Simpson *et al*, 2006). This PTM allows for polymerase REV1 to bind through its Ubiquitin Binding Motif (UBM), and, together with Pol ζ , to bind to the DNA and synthesize the new DNA strand (**Figure 5: step 7 – inner circle**) (Geng *et al*, 2010). The RAD18-RAD6-PCNA axis has an additional role in regulating the FA pathway. On the one hand, PCNA can directly bind to FANCL and FANCD2. On the other hand, the RAD18 mono-ubiquitylation on the lysine 164 of PCNA enables FANCL to correctly bind to chromatin and promote its catalytic activity (Geng *et al*, 2010; Howlett *et al*, 2009).

As mentioned before, FAAP20 is also involved in REV1 recruitment. Given this, it is likely that Ub-PCNA recruitment of REV1 is not enough for correct activation of the TLS pathway. REV1 can self-ubiquitylate itself, and this mark is identified by the UBZ domain present in FAAP20, inducing TLS activation (Kim *et al*, 2012a). Interestingly, the FA pathway is able to activate TLS independently of ID complex ubiquitylation. This indicates that the FA pathway may be able to coordinate ICL repair in a PCNA-dependent manner without activation of the HR pathway.

BRCA1 is a large phosphoprotein that contains several BRCT domains in its C-terminal and a RING domain in its N-terminal. BRCA1 specifically binds to an E2 conjugase enzyme, BRCA1 Associated Ring Domain 1 (BARD1), through its RING domain, which has been determined to be an essential interaction in order for BRCA1 to be shuttled into the nucleus and perform its function (Panier & Durocher, 2009). When they are bound together they acquire E3 ubiquitin ligase activity, however, it is unclear if this function has an important role in the DNA damage response since loss of the RING domain also induces loss of interaction with BARD1, abolishing BRCA1-BARD1 transportation into the nucleus. Point

mutants disrupting the RING domain but not the interaction between the two proteins seem not to affect the response to DSBs (Uckelmann *et al*, 2018; Reid *et al*, 2008; Shakya *et al*, 2008).

Multi-site ubiquitylation of RPA is important for restarting HR after replication stress. This PTM induces the removal of RPA from chromatin, exposing the ssDNA to the HR machinery and enabling error-free repair. The E3 ubiquitin ligase RFWD3 is in charge of initiating this function (**Figure 5: step 7 – inner circle**) (Elia *et al*, 2015). Upon ICL damage, it has been shown that RFWD3 ubiquitylates both RPA and RAD51 reducing their DNA binding capability. This enables HR proteins to come to the site of damage and repair the lesion (Inano *et al*, 2017; Feeney *et al*, 2017).

Altogether, it has been shown that ubiquitylation has a major role in signaling repair of DNA lesions, specifically in the regulation of the FA pathway. Interestingly, the presence of UBZ domains is a hallmark of DNA damage proteins. This again shows the relevance of ubiquitin in the accurate activation of DDR pathways in order to eliminate genome instability.

5. Model systems for investigating the Fanconi anemia disease/pathway

The FA pathway is incredibly complex since it is very tightly interconnected with other pathways. Hence, a variety of model systems have been developed in order to give more clarity to the repair of ICLs. I will now discuss the most relevant systems.

5.1. Animal models of FA disease

FA disease, as a monogenic rare disease, serves as an ideal model to understand the DDR against ICLs. The most relevant organisms used to mimic FA are: the zebrafish *Danio rerio*, the worm *C. elegans*, the mouse and, most recently, the pig.

- ***Danio rerio***

The zebrafish has proven to be an excellent model organism for the study of vertebrate biology. The external appearance during embryogenesis allows for the visualization of developmental processes. Additionally, with the development of tools such as antisense morpholino technology, it is possible to perform large scale genetic screens that have revealed phenotypes comparable to human diseases (Dooley & Zon, 2000). The first studies undertaken to understand the role of the FA pathway in zebrafish were made in 2003. *fancd2* was 50% identical to its homolog in humans, conserving two important catalytic sites: serine 222 (ATM phosphorylation after IR) and serine 561 (FANCL ubiquitylated after ICL-induced damage). *fancd2* knock-down in zebrafish embryos resulted in an abnormal phenotype with high levels of p53-induced apoptosis and reduced size compared to WT (Liu *et al*, 2003). These characteristics all correlate with known data on FA patients. Later, it was determined that in embryo and adult tissue the zebrafish has a complete set of the *fanc* genes that are often affected in FA patients (Titus *et al*, 2009).

With advances in genome editing, multiplexed CRISPR-Cas9 knock-out in zebrafish has been possible. 19 FA genes have been depleted: 17 FA genes and 2 Fanconi anemia associated genes. 11/17 FA genes showed sensitivity to DEB and all of them developed to adulthood, demonstrating that they are not essential for early development (Ramanagoudr-Bhojappa *et al*, 2018). None of them showed significant abnormalities except *fancp*, which correlates with the *Fancp* mouse model and FANCP patients. Overall, the zebrafish is a good model for studying FA, more specifically, for the study of defects during gonadogenesis and hypogonadism, known hallmarks of the pathophysiology of FA patients.

- ***Caenorhabditis elegans***

The worm has been used as a model organism since the 1970s, due to its low cost and space constraints. To study DNA repair, *C. elegans* is a highly suitable model since most of the genes present in humans are conserved in the nematode. However, DNA repair studies are focused on the germline since these cells offer optimal visualization of the damage and the dynamics of the repair proteins. In the context of the FA pathway, the only proteins known to be conserved are FANCD2 and FANCI and proteins from the BRCA axis of the pathway. It has been demonstrated that monoubiquitylated FANCD2 in *C. elegans* is part of the response to ICLs, suggesting that proteins with a role equivalent to that of the FA Core Complex might exist (Youds *et al*, 2009).

Several members of the FA pathway have been studied in order to determine their essentiality in *C. elegans* although not all of them recapitulate FA, The most characteristic ones are *fcd2* (FANCD2), and *dog-1* (BRIP1). *Drh3* (FANCM) and *fnci* (FANCI) also show sensitivity to ICLs, assessed through their hatching viability rate after treatment with a damaging agent (Lee *et al*, 2010).

Altogether, *C. elegans* is a good model for the study of DNA damage, however those FA genes that give rise to FA, with the highest prevalence, do not seem to be present in the nematode (Youds *et al*, 2009). Their reduced complexity by comparison with humans does not allow for correct dissection of the FA pathway or correct correlation with FA patients.

- ***Mus musculus***

Mouse models are more accurate than nematode models since phylogenetically they are more closely related to humans. The mouse shares approximately 90% of its genome with humans, which makes it an exceptional tool for the study of human diseases.

Thus far, 13 mouse models can be found in the Mice Genome Informatics database (MGI) associated to FA, covering 6 FA genes: *Fanca*, *Fancc*, *Fancd1*, *Fancd2*, *Usp1* and *Slx4*. Additionally, according to the literature, other FA genes have been knocked-out, hence targeting a wide spectrum of the FA pathway: *Fancg*, *Fancl*, *Fancn*, *Fancm*, *Fanco* and *Fancp* (Bakker *et al*, 2013).

Despite these attempts to develop an accurate FA model in mice, none of these can recapitulate the standard clinical features of an FA patient. Knock-outs in genes such as *Fancd1*, *Fancn* and *Fanco* are lethal in mice, indicating that they have an essential role in development (Parmar *et al*, 2009; Bakker *et al*, 2013). This could correlate with humans, since only hypomorphic mutations have been identified in patients that are defective in

FANCN or *FANCD1*. Nonetheless, a closer look at the clinical features of FA patients reveals correlations with some of the mice models.

Bone marrow failure

The absence of major hematological abnormalities is the biggest disappointment in the field of FA mice models since anemia and BMF are the predominant life-threatening pathologies in FA patients. The counts in peripheral blood are normal in all models. However, *Fanca* mice have thrombocytopenia (Pawlikowska *et al*, 2014), *Fancp* mice have low numbers of white blood cells and platelets and *Fancd1* have a proliferation defect in hematopoietic progenitors (Navarro *et al*, 2006).

Nevertheless, all FA mouse models have defects in the proliferation of HSCs in vitro (Parmar *et al*, 2009). In addition, when mice are subjected to ICL-inducing agents, they show reduced repopulation capacity of the BM, hence allowing for the study of the FA pathway in hematopoietic homeostasis (Bakker *et al*, 2013). Interestingly, BMF only manifests upon external damage, in contrast with humans, suggesting that the metabolism of mice blocks endogenous damage or that the controlled conditions under which mice are housed protects them from stressful environmental cues.

On the other hand, all FA mouse models show gonadal abnormalities that correlate with a reduced number of PGCs and sterility. It is not yet clear why this defect is conserved in all models in contrast to the hematological defects.

Cancer predisposition

Generally, FA patients develop AML and Squamous Cell Carcinoma (SCC) in different organs. These and other cancer types endanger the survival of these individuals. On the contrary, FA mice do not suffer from accelerated tumorigenesis. Tumors have been detected after one year of age, resulting in a low correlation with a DNA damage repair defect (Parmar *et al*, 2009). The mouse models that seem to suffer from advanced tumorigenesis are *Fancd2* and *Fancf*-deficient, nevertheless the growth rate of tumors in these mice is not comparable to humans.

Developmental abnormalities

In general, the different FA models do not present gross developmental abnormalities and only some — such as *Fanca*, *Fancp* and *Fancd2* present mild microcephaly (Parmar *et al*, 2009).

All the symptoms described above are variable depending on the genetic background of the mouse strain, making this FA model even more variable. But this has not discouraged the

scientific community. The fact that these mice are sensitive to ICL-inducing agents, even if they do not show symptoms at basal levels, indicates that there are fundamental differences in metabolism between mice and humans. In fact, concomitant loss of *Fancd2* and *Aldh2*, an aldehyde dehydrogenase responsible for the detoxification of aldehydes, results in a mouse with low life expectancy and very similar pathophysiology to FA patients (Langevin *et al*, 2011). This indicates that mice are more proficient in processing endogenous aldehydes and that their accumulation gives rise to FA physiology.

- ***Sus scrofa domestica***

None of the previous models are able to faithfully recapitulate the pathophysiology of FA. Nevertheless, the success of the cystic fibrosis pig model has prompted scientists in the FA field to develop a pig that recapitulates FA (Rogers *et al*, 2008). The pig has a similar weight and organ distribution to humans, and genomic, transcriptomic and proteomic tools are available, as are effective cloning techniques. The major drawback of this model could, potentially, be cost effectiveness. However, the Fanconi anemia Research Fund has invested over \$400 000 in the William Flemming and Markus Grompe laboratories for this purpose (Fanconi.org). Moreover, the Wilfried Kues laboratory in Germany is also involved in the development of a *FANCA*-deficient pig.

5.2. Induced pluripotent stem cells (iPSCs)

One way of enabling studies that can fully recapitulate FA in the most relevant samples has been to generate immortalized cell lines from patient material. This approach has proved extremely tedious, since FA-deficient HSC are extremely sensitive to endogenous damage resulting in the activation of the p53 pathway and cell death. As an alternative, iPSCs have been derived from FA patients (Chlon *et al*, 2016). However, this is only possible when the depleted FA gene is complemented or *in situ* corrected during reprogramming in order to protect the cells from genomic stress induced by this process (Chlon *et al*, 2016; Bharathan *et al*, 2017; Liu *et al*, 2014). Notwithstanding, the study of differentiation towards HSCs can potentially be useful in elucidating the pathogenesis of BMF.

5.3. Mammalian cells

The use of stable mammalian cells in research is of great importance. The *in vitro* culture system allows for highly controlled conditions which, together with the detailed characterization of many cell lines, enable us to dissect the cause of molecular changes in

cellular models. In the case of FA, and due to the conservation of the DDR in all cells, it has been determined that all FA-deficient cells show a chromosomal instability phenotype (Neveling *et al*, 2009), hence providing an effective tool for the study of the underlying molecular mechanism of FA.

With fast developing genetic technologies, such as small interference(si)/small hairpin(sh) RNA, insertional mutagenesis using gene-trap cassettes and genome editing with CRISPR-Cas9, performing whole-genome screens has become a possibility. For the understanding of the FA pathway, two different interaction types have been identified. On the one hand, synthetic lethal interactions allow us to identify an interaction between two genes which, through their simultaneous depletion, results in cell death. These interactions have become relevant to the treatment of cancer (Aly & Ganesan, 2011). On the other hand, synthetic rescue interactions allow us to identify an interaction between two genes which, through their simultaneous depletion, results in cell fitness. These interactions are relevant to the treatment of monogenic diseases (Larrieu *et al*, 2014).

- **Genetic synthetic lethal approaches**

Due to the relationship between the FA pathway and genome stability, these genes have been identified as tumor suppressor genes and found mutated in non-FA individuals who have cancer. Mutations in tumor suppressor genes or oncogenes transform normal cells into cancer cells with metabolic and growth advantages. This disruption of the cellular homeostasis forces the cells to rely on different molecular pathways, which become the perfect targets for cancer therapy (**Figure 6**).

It is already known that breast and ovarian cancers with mutations in *BRCA1* can be targeted by inhibiting PARP1, a protein involved in an error-prone repair pathway of DSBs. This type of interaction is termed synthetic lethal interaction; similarly, by performing whole genome siRNA screens, ATM has been found to be a lethal interactor of *FANCG* (Kennedy *et al*, 2007). In addition, *RAD52* depletion together with loss of *BRCA1* or *PALB2* also reduces cell fitness (Lok *et al*, 2013).

These screens focus on the depletion of FA-deficient cells and, at the same time, provide us with new information about the FA pathway and its role in DDR.

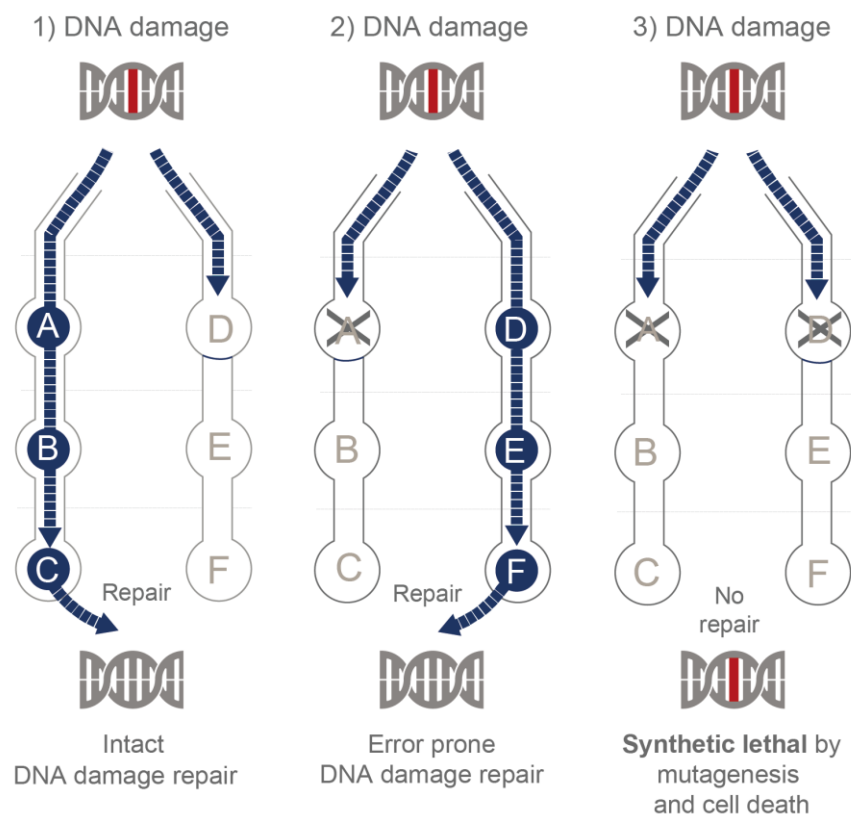


Figure 6. Schematic representation of a synthetic lethal interaction in the context of the DDR. 1) When a lesion occurs in the DNA, a pre-determined pathway is activated in order to repair it; 2) when the preferred repair pathway is defective the lesion can be repaired by an alternative pathway, more error-prone; 3) when there is a synthetic lethal interaction, this will induce cell death of the cells by simultaneously depleting both pathways.

- **Genetic synthetic rescue approaches**

Other type of screens, focus on finding a genetic interaction that, upon depletion, increases cell viability (**Figure 7**). These interactions are termed either as synthetic rescue or gene suppression interactions. One of the goals of these screens is to identify novel resistance mechanisms in cancer cells. However, these screens are also ideal for the identification of targets that can alleviate the symptoms of patients that suffer from rare monogenic diseases. By finding these interactions, it is possible to find a suitable therapeutic substrate that can be targeted either with drugs or small molecules, thus benefiting the patient.

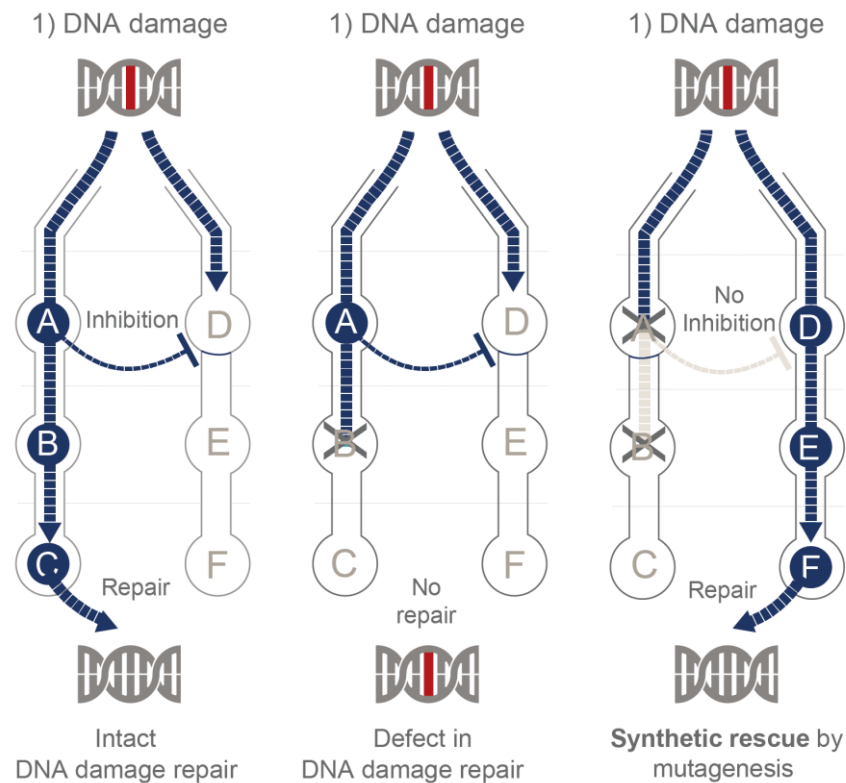


Figure 7. Schematic representation of a synthetic rescue interaction in the context of the DDR. 1) When a lesion occurs in the DNA, a pre-determined pathway is activated in order to repair it; 2) when the preferred repair pathway is defective the lesion is not dealt with giving rise to genome instability and eventually cell death; 3) when there is a synthetic rescue interaction, this will allow for the activation of a complementary pathway that was previously blocked and correct repair of the lesion will take place.

It has been argued that the interactions found in these assays exclusively improve the fitness of cells, suggesting that it is not possible to identify connections that restore defective pathways. Nevertheless, several studies have proven this theory wrong. One of the most striking genetic synthetic rescue interactions was found in a canine model for muscular dystrophy. Here, a dog bred to develop muscular dystrophy carrying a mutation in the *dystrophin* gene but remained healthy. Whole genome sequencing of this dog identified *Jagged1* to be mutated in this animal. Hence, the mutual mutation of *dystrophin* and *Jagged1* enabled a healthy dog (Vieira *et al*, 2015).

When focusing on rescue interaction within the DDR pathways, several interactions have also been identified. Excitingly, *BRCA1*-deficient cells, which are highly genetically unstable, become more stable upon concomitant loss of *53BP1* (Bunting *et al*, 2011). These two proteins compete for the repair of DSBs, however, depletion of both of them restores the balance towards a more error-free repair. Another interaction has been identified between a chemical compound that inhibits NAT10 (N-acetyl-transferase) and *LMNA* loss (Larrieu *et al*, 2014). Loss of *LMNA* gives rise to a monogenic disease that encompasses the laminopathies. At a cellular level they manifest loss of nuclear shape and chromatin

organization. This rescue interaction revealed a suitable target for treating laminopathies and the use of NAT10 inhibitors for this purpose.

Gene suppression interactions have also been found in the FA pathway. They have shown to play a major role in re-channeling ICL repair into a high-fidelity repair pathway. One example is the rescue interaction between *fcd2* and the NHEJ gene *lig-4* in *C. elegans* (Adamo *et al*, 2010a). Similar interactions have been found between *FANCC*-deficient cells and concomitant loss of Ku70. Ku70 is also involved in NHEJ, hence strengthening the role of the FA pathway in counteracting error-prone repair (Pace *et al*, 2010).

6. Mapping synthetic rescue interactions for the FA pathway

Recent discoveries about the existence of genetic suppression interactions between the FA pathway and NHEJ (Adamo *et al*, 2010b; Pace *et al*, 2010) encouraged the Loizou laboratory to set up new strategies to generate a map of synthetic rescue interactions for the FA pathway. Thus far, the interactions identified have been in *C. elegans* and DT40 chicken cells. We aim to broaden the research of genetic suppression interactions by using the human cell line, HAP1. This cell line is an ideal tool for genetic screens, having been derived from the KBM7 chronic myeloid leukemia (CML) cell line with a near-haploid karyotype, since it allows for the efficient deletion of a gene by only knocking out one allele (Kotecki *et al*, 1999; Carette *et al*, 2009). To build a synthetic rescue map for FA, we selected 3 FA genes with a role in the formation of the Core Complex: *FANCA*, *FANCC* and *FANCG*. These genes are also the most prevalent in FA patients (**Figure 2**). We also selected *FANCI* and *FANCD2*, which are essential for the activation of downstream effectors. These genes were then deleted via CRISPR-Cas9 generating 5 FA-deficient cell lines presenting all the hallmarks of FA cells.

Next, we sought to perform high-throughput loss-of-function screens by utilizing gene-trap insertional mutagenesis approaches. The mutagenized FA cells were treated with MMC in order to retrieve those that by additional loss of a second gene would be resistant to damage (**Figure 8**). To identify specificity within the FA pathway we also use WT HAP1 cells in our screens, therefore we could determine which genes, upon deletion, would improve the FA defect.

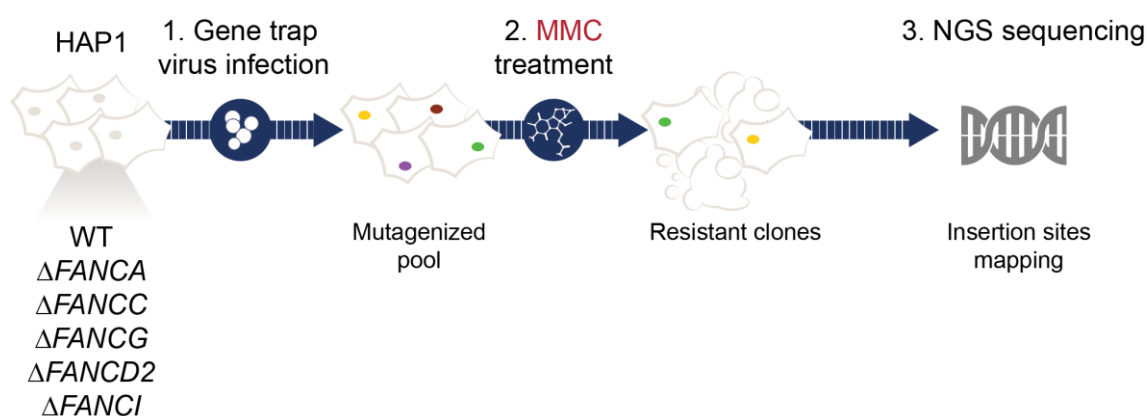


Figure 8. Workflow for the identification of synthetic rescue interactions in FA-deficient cells. 1) FA-deficient cells are infected with the gene trap retrovirus resulting in a mutagenized pool of cells. 2) Exposure to MMC will select for resistant clones which are then 3) subjected to NGS for the identification of the mutated genes.

To our knowledge, we are the first laboratory to perform such systems-level approaches, to systematically identify approaches to alleviate phenotypes associated with diseases caused by defective DNA repair. Hence, this study provides a plethora of information that can only

be obtained by applying these methodologies. We have generated a synthetic rescue interaction map for the FA pathway in human cells. Furthermore, we have characterized the molecular mechanisms by which the Ubiquitin Specific Peptidase 48 (USP48) functions as a novel player in the repair of ICLs. In doing so, we have identified novel potential therapeutic targets for the treatment of FA patients.

7. Aims

- 1) Establish high thorough-put loss-of-function screens to identify suppressors within the FA pathway
- 2) Generate a map of synthetic rescue interactions in the FA pathway
- 3) Molecularly characterize an identified protein, amenable for inhibition, as a suitable potential target for the treatment of FA

CHAPTER 2: RESULTS

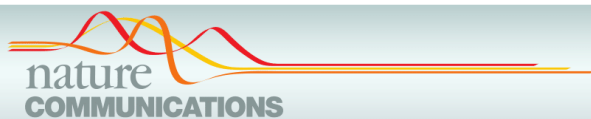
1. Prologue

Here I present the results from my PhD project that were published in *Nature Communications* in June 2018 entitled: “Map of synthetic rescue interactions for the Fanconi anemia pathway identifies USP48”. In this article, we aimed to identify genetic suppressors for FA pathway capable of reverting cellular hypersensitivity to ICLs. To do so, we performed 6 whole-genome loss-of-function screens in five FA-deficient HAP1 cell lines ($\Delta FANCC$, $\Delta FANCA$, $\Delta FANCG$, $\Delta FANCI$ and $\Delta FANCD2$) and WT HAP1 cells. After treatment with MMC, an ICL-inducing agent, we scored those genes that upon depletion would significantly confer resistance to the otherwise hypersensitive FA cells. By taking this high-throughput approach we generated a map of synthetic rescue interactions for the FA pathway. In addition, we characterized the molecular mechanism of our top hit: USP48, a de-ubiquitin enzyme poorly described in the context of the DDR.

We demonstrate that concomitant loss of *USP48* and *FANCC* rescues sensitivity to ICL-inducing agents by allowing the restoration of HR proteins such as BRCA1 and RAD51. Thus, DNA repair is balanced towards more error-free repair as noted by a decrease in SCEs. In addition, we determine that USP48 loss in FA-deficient cells alters the ubiquitylation signaling of the repair pathway with effects on H2A ubiquitylation. Finally, we discussed the possible mechanisms by which USP48 might have a role in ICL repair.

This project was the result of the joint efforts of Georgia Velimezi and myself. The data was analyzed by our collaborators from the Centre of Computational Biology and Bioinformatics, San Diego, USA. Additional experiments strengthening our hypothesis were performed by the Jackson lab, UK and the van Attikum lab, The Netherlands. The paper was written by Georgia Velimezi and myself with input from Joanna I. Loizou and all other authors.

2. Research article



ARTICLE

DOI: [10.1038/s41467-018-04649-z](https://doi.org/10.1038/s41467-018-04649-z)

OPEN

Map of synthetic rescue interactions for the Fanconi anemia DNA repair pathway identifies USP48

Georgia Velimezi¹, Lydia Robinson-Garcia¹, Francisco Muñoz-Martínez², Wouter W. Wiegant³, Joana Ferreira da Silva¹, Michel Owusu¹, Martin Moder¹, Marc Wiedner¹, Sara Brin Rosenthal⁴, Kathleen M. Fisch⁴, Jason Moffat⁵, Jörg Menche¹, Haico van Attikum³, Stephen P. Jackson², Joanna I. Loizou¹

Defects in DNA repair can cause various genetic diseases with severe pathological phenotypes. Fanconi anemia (FA) is a rare disease characterized by bone marrow failure, developmental abnormalities, and increased cancer risk that is caused by defective repair of DNA interstrand crosslinks (ICLs). Here, we identify the deubiquitylating enzyme USP48 as synthetic viable for FA-gene deficiencies by performing genome-wide loss-of-function screens across a panel of human haploid isogenic FA-defective cells (FANCA, FANCC, FANCG, FANCI, FANCD2). Thus, as compared to FA-defective cells alone, FA-deficient cells additionally lacking USP48 are less sensitive to genotoxic stress induced by ICL agents and display enhanced, BRCA1-dependent, clearance of DNA damage. Consequently, USP48 inactivation reduces chromosomal instability of FA-defective cells. Our results highlight a role for USP48 in controlling DNA repair and suggest it as a potential target that could be therapeutically exploited for FA.

¹CeMM Research Center for Molecular Medicine of the Austrian Academy of Sciences, Lazarettgasse 14, AKH BT 25.3, 1090 Vienna, Austria. ²The Gurdon Institute and Department of Biochemistry, University of Cambridge, Tennis Court Road, Cambridge CB2 1QN, UK. ³Department of Human Genetics, Leiden University Medical Center, Leiden, Einthovenweg 20, 2333 ZC Leiden, The Netherlands. ⁴Center for Computational Biology & Bioinformatics, Department of Medicine, University of California, San Diego, 9500 Gilman Drive #0681, La Jolla, CA 92093, USA. ⁵Donnelly Centre and Banting and Best Department of Medical Research, University of Toronto, Toronto, ON M5S 1A8, Canada. These authors contributed equally: Georgia Velimezi, Lydia Robinson-Garcia. Correspondence and requests for materials should be addressed to J.I.L. (email: joizou@cemm.oew.ac.at)

ARTICLE

NATURE COMMUNICATIONS | DOI: 10.1038/s41467-018-04649-z

The human genome is constantly exposed to various sources of DNA damage that can arise from either endogenous or exogenous sources. To deal with this stress, cells possess several highly conserved and effective mechanisms for DNA repair. If these repair mechanisms are defective, due to germline mutations in relevant DNA repair genes, rare diseases with DNA repair deficiencies can arise^{1,2}. One such disease is Fanconi anemia (FA), which is characterized by chromosomal instability, bone marrow failure, and cancer predisposition, for which inadequate treatments are currently available^{3,4}. FA is caused by mutations in genes encoding components of the FA pathway, which mediates repair of DNA interstrand crosslinks (ICLs), highly toxic lesions that block DNA replication and transcription. Consequently, cells that have disruptive mutations in FA genes exhibit increased sensitivity to DNA ICL-inducing agents^{3,4}.

The classical concept of synthetic viability (also termed synthetic rescue or genetic suppression), in combination with the use of advanced and high-throughput methods allows for the development of new approaches to ameliorate defects associated with human genetic diseases^{5–9}. Moreover, the identification of such interactions provides significant insights into the mechanisms underlying molecular processes and crosstalk between cellular pathways. To explore, in an unbiased and systematic manner, genetic synthetic-viable interactions for FA deficiency, we have used human haploid genetic screens—a powerful approach that can identify genetic interactions in human cells^{10–12}. Thus, we have used a previously described gene-trap retrovirus¹⁰ to mutagenize a panel of human cell lines individually carrying mutations in five different FA genes (*FANCA*, *FANCC*, *FANCG*, *FANCI*, and *FANCD2*). As described herein, through this approach, we identify *USP48* as a deubiquitylating enzyme (DUB) whose loss alleviates increased sensitivity and genomic instability of FA-deficient cells following DNA crosslinking damage, while enhancing the recruitment of homologous recombination (HR) markers and histone H2A ubiquitylation.

Results

Map of synthetic rescue interactions in FA cells. In order to mimic the defect observed in FA in a cellular system that is appropriate for further genetic manipulations, we generated CRISPR-Cas9-mediated knockout HAP1 cells with individual mutations in five FA genes: *FANCA*, *FANCC*, *FANCG*, *FANCI*, and *FANCD2*. We selected these genes based on their clinical relevance (*FANCA*, *FANCC*, and *FANCG* account for the majority of mutations in FA patients) but also based on their molecular function, as *FANCA*, *FANCC*, and *FANCG* are part of the core complex, while *FANCI* and *FANCD2* function downstream during ICL repair, in order to broadly cover the FA pathway^{3,4}. The HAP1 cell line is near-haploid, making it ideal for genetic screens using insertion mutagenesis, since disruptive mutations in a single allele will result in a knockout¹⁰. We confirmed the generation of frameshift mutations and loss of protein expression in the knockout cell lines by Sanger sequencing and immunoblotting (Supplementary Fig. 1a, b). In line with a previous report, we noted that loss of *FANCA* affected the protein stability of *FANCG* and vice-versa¹³. We also observed mutual interdependences for *FANCI* and *FANCD2* protein stabilities. The expected hypersensitivity of the FA knockout cells to the DNA crosslinking agent mitomycin C (MMC) was confirmed by cell viability assays (Fig. 1a) and clonogenic survival assays (Supplementary Fig. 1c).

To screen for potential genetic disruptions that alleviate the DNA damage hypersensitivity of FA-defective cells, we inserted, via retroviral delivery, a gene-trap cassette that contains a splice acceptor site into the HAP1 knockout cells. This method has been

previously used successfully in haploid genetic screens^{10–12}. We next treated the mutagenized cells with MMC at a dose that we predetermined as selectively killing the FA-deficient cells, thereby providing a selective pressure to enrich for resistant cells (Fig. 1b). Genomic DNA was then extracted and subjected to next generation sequencing (NGS), allowing for the mapping of both the position and orientation of the gene-trap cassette. As a control, we additionally analyzed a non-selected, untreated mutagenized population of wild-type (WT) HAP1 cells¹⁴.

In order to identify cellular processes and pathways represented by the genes that specifically rescue FA-defective cells but not WT cells, we overlaid the significantly enriched hits onto a manually curated interactome network of physical protein–protein interactions¹⁵. We identified neighboring genes to this initial set using network propagation based on a previously described method¹⁶. Groups of highly interconnected genes were revealed using a modularity maximization clustering algorithm¹⁷, which after functional enrichment analysis of each cluster, showed significant enrichment for biologically-relevant canonical pathways (Fig. 1c; Supplementary Data 1). Clusters including “Ubiquitin-mediated proteolysis” and “Pathways in cancer” demonstrate the high connectivity among the identified genes. Also displayed are the DNA repair genes that were not identified tightly connected in a cluster but rather falling within the above two mentioned clusters (Fig. 1c; Supplementary Data 1).

***USP48* loss alleviates sensitivity of FA cells to ICLs.** We next created a synthetic-viable interaction network from all the identified rescue protein-coding genes (Fig. 2a; Supplementary Data 2). Closer examination of the top 10 individual genes revealed *NQO1* and *USP48* as the most recurrently targeted and significantly enriched genes, based on *fdr*-corrected *p*-values (*q*-values) (Fig. 2b). We, therefore, chose to focus on these for our ensuing analyses. Other enriched genes, notably *LAMTOR1* and *LAMTOR5*, which are members of the LAMTOR complex and promote activation of the mTOR signaling pathway, will be the subject of our ensuing studies. In addition, we note that we have recently reported that inactivation of members of the BLM complex (*BLM*, *TOP3A*, and *RMI1*), which appear among the top shared hits among FA-deficient cell screens, can rescue the survival of FA-deficient cells in response to ICL induction¹⁸.

NQO1 is a quinone reductase that has been shown to contribute to MMC bio-activation in cells, thereby allowing its toxic actions¹⁹. Furthermore, expression levels of *NQO1* in human tumors have been positively correlated to enhanced sensitivity to MMC treatment²⁰. As expected from its function in MMC activation, disruptive insertions within *NQO1* were highly significantly enriched in wild-type (WT) cells as well as FA-deficient cells selected for MMC resistance, indicating a general mode-of-action irrespective of the DNA repair status of the cell line.

More interestingly, mutagenic insertions within *USP48*, a deubiquitylating enzyme (DUB), were found as significantly enriched in resistant populations of all the FA-deficient backgrounds but not in WT cells, potentially indicating a function specifically connected to the DNA repair defect in FA cells. Moreover, mapping of the insertion sites of the gene-trap cassette in *USP48* showed that the majority of insertions were localized upstream in the gene or at a region corresponding to the catalytic domain of *USP48* (Supplementary Fig. 2a), indicative of disruptive mutations resulting in loss of function. We next validated this rescue interaction by generating, via *de novo* CRISPR-Cas9 gene editing, a HAP1 cell line double mutant for *FANCC* and *USP48* (Fig. 3a and Supplementary Fig. 2b). The resulting double mutant, $\Delta USP48 \Delta FANCC$, was more resistant to

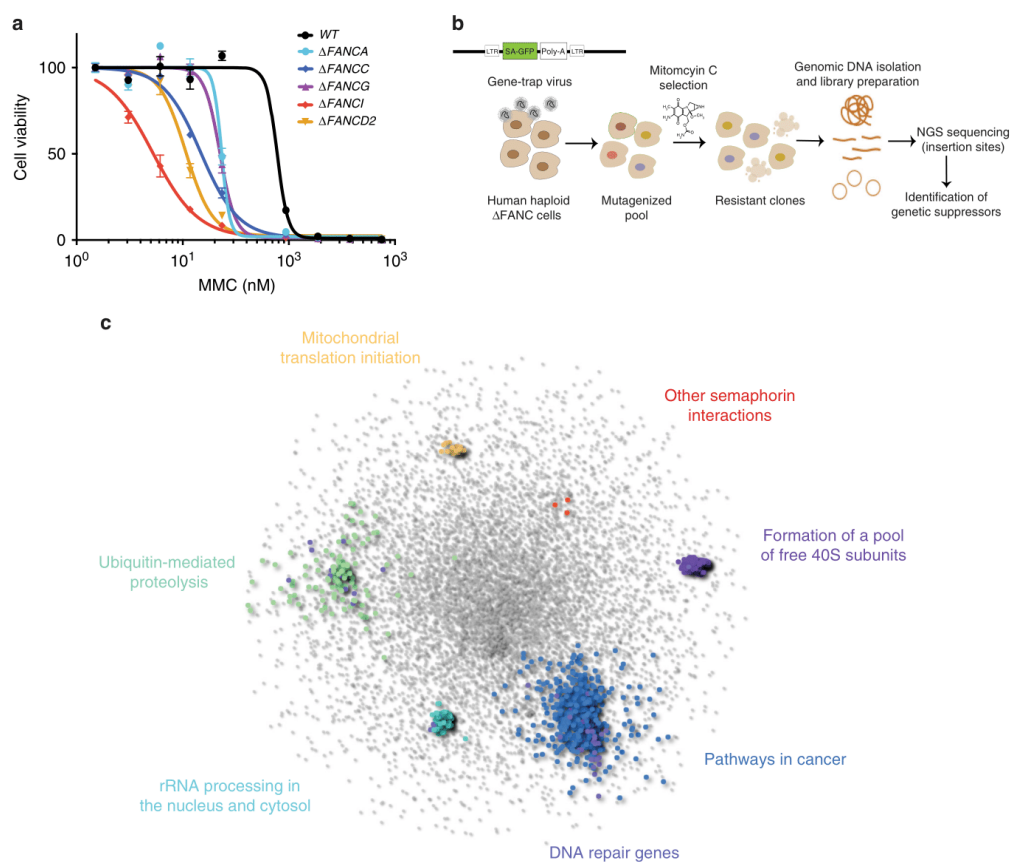


Fig. 1 Genetic screens identify synthetic-viable interactions for FA. **a** Dose-response of FA-defective HAP1 cell lines to MMC exposure. Cells were treated for 3 days and viability was measured by Cell Titer Glo[®]. Error bars indicate S.E.M (standard error of the mean) of triplicates. **b** Workflow for the identification of genetic synthetic-viable interactions for FA-defective human haploid HAP1 cells following MMC exposure by gene-trap-based insertional mutagenesis. **c** Protein-protein interaction network analysis reveals pathways significantly enriched specifically in the FA-deficient cells, in response to MMC

crosslinking agents compared to the Δ FANCC single mutant, as shown by clonogenic survival after treatment with MMC, cisplatin or diepoxybutane (DEB) (Fig. 3b–d). Interestingly, we did not observe the same effect on survival when we compared WT cells to Δ USP48 cells, although a slight but not significant difference was observed, further validating the results of our screens and the specificity of this genetic interaction for FA-deficient cells. Re-introduction of exogenous wild-type USP48, but not the catalytically inactive C98S USP48 mutant, partially reduced ICL resistance of Δ USP48 Δ FANCC cells (Supplementary Fig. 2c, d), thus indicating that lack of USP48 catalytic activity is important for the increased survival of Δ USP48 Δ FANCC cells. Further confirming that the synthetic rescue was indeed dependent on USP48, when we subjected USP48 to short-hairpin RNA (shRNA) depletion (Supplementary Fig. 2e, f) or carried out *USP48* gene inactivation by CRISPR-Cas9 editing by using a different single guide (sg)RNA targeting a different exon (Supplementary Fig. 2g, h) in Δ FANCC cells, we observed similar results. We also tested the effect of USP48 loss on MMC

sensitivity of Δ FANCG and Δ FANCD2 cells using CRISPR-Cas9 editing to target USP48. The pooled populations of FA mutant cells targeted for USP48 displayed reduced USP48 protein (Supplementary Fig. 2g) and increased survival to MMC (Supplementary Fig. 2h), thus confirming the synthetic viability interaction in additional FA backgrounds.

Since monoubiquitylation of components of the FANCI/FANCD2 complex is an important step of ICL repair^{3,4} and considering that USP48 is a DUB, we tested whether USP48 depletion could rescue the FANCI/FANCD2 monoubiquitylation defect of Δ FANCC cells. Western immunoblot assays revealed that lack of MMC-induced FANCI/FANCD2 monoubiquitylation in Δ FANCC cells was not restored upon shRNA-mediated depletion of USP48 (Supplementary Fig. 2i), suggesting that USP48 may affect the repair of ICLs downstream of FANCI/FANCD2. Moreover, USP48 depletion in Δ FANCC cells did not correct the defect that these cells had in recruiting FANCD2 to MMC-induced DNA-damage foci, thereby implying that the mechanism of rescue was independent of FANCD2 (Supplementary Fig. 2j).

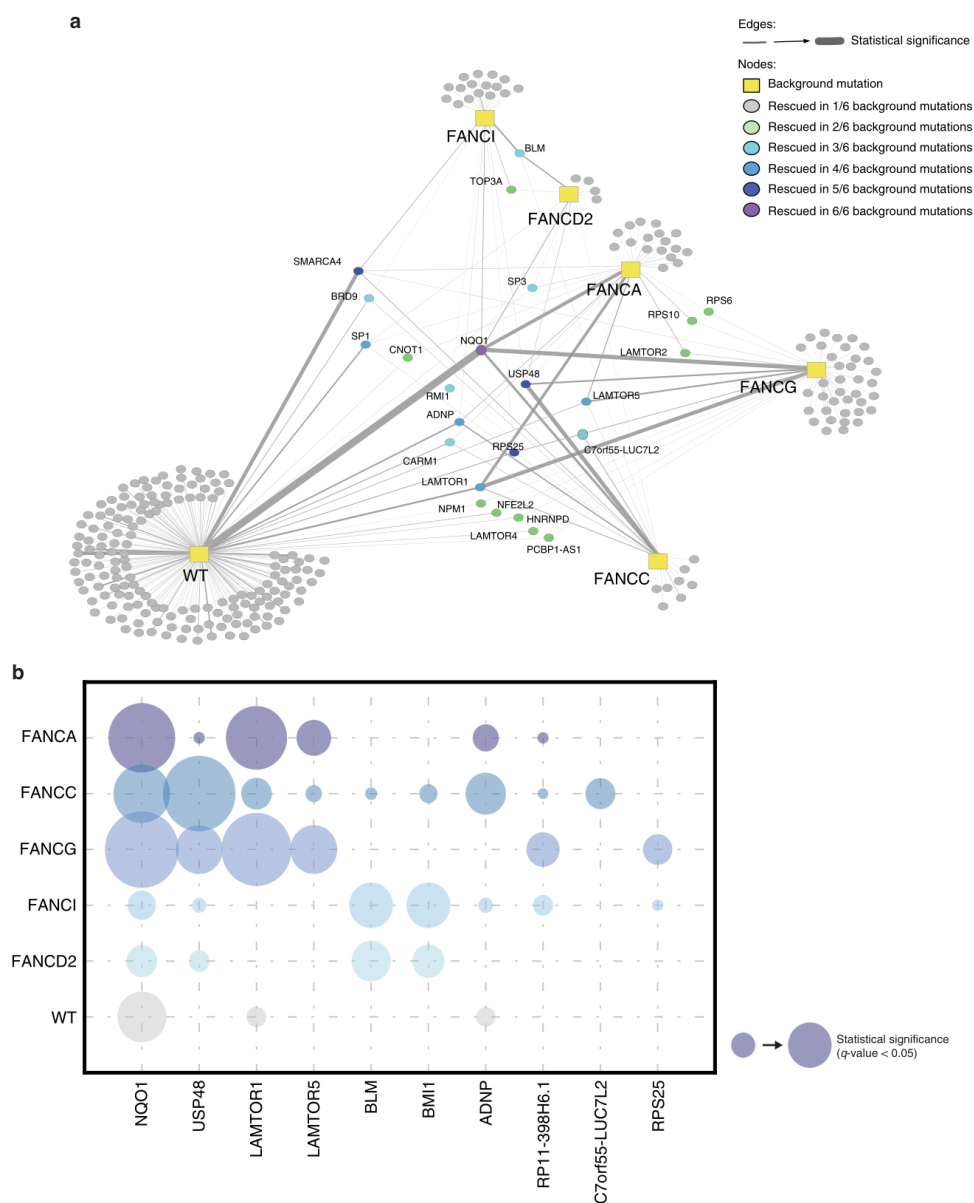


Fig. 2 Synthetic-viable genes for FA cells. **a** Map of the synthetic viability interaction network identified by insertional mutagenesis screens using wild-type (WT) and five FA-deficient HAP1 cell lines after MMC treatment. Links in this network indicate an increased viability of cell lines with a given mutational background (rectangular nodes) when the respective secondary gene (circles) is also knocked out. A total of 23 genes were found to rescue more than one mutational background (color coded with green to purple), including USP48. **b** Bubble plot showing the frequency and statistical significance of the top ten genes identified in the screens depicted in **a**

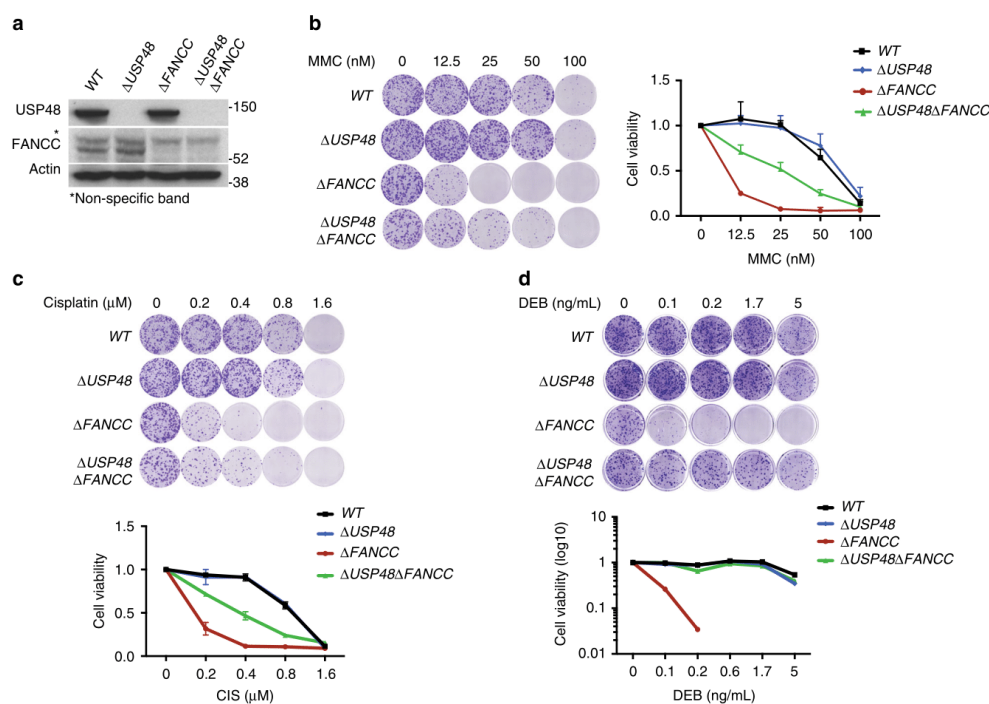


Fig. 3 USP48 loss partially rescues sensitivity of Δ FANCC cells to ICLs. **a** Immunoblot for USP48, FANCC, and actin on the indicated cell lines. Asterisk (*) denotes non-specific band. **b–d** Colony formation and subsequent quantification of the indicated cell lines 7 days after treatment with crosslinking agents (Mitomycin C, MMC; Cisplatin; Diepoxybutane, DEB) at the indicated doses. Error bars show S.D. (standard deviation) from two replicates

USP48 is recruited to sites of DNA damage. In light of our findings, we next investigated the cellular localization of USP48 and whether it is recruited to sites of DNA damage. GFP-tagged USP48 was expressed in WT and Δ FANCC cells with and without MMC treatment. We observed that GFP-USP48, both WT and the catalytically inactive C98S mutant, localized primarily in the nucleus with a pan-nuclear signal (Supplementary Fig. 3). Interestingly, the catalytically inactive C98S mutant, but not WT USP48, formed foci that co-localized with γ H2AX foci (arrows in Supplementary Fig. 3). This suggested that USP48 interacts with a substrate at the site of damage and inhibition of its activity entraps the enzyme, hence leading to the formation of USP48 foci. We next tested if USP48 is specifically recruited to sites of DNA damage created by laser micro-irradiation of FANCC-proficient (U2OS) and FANCC-deficient (VU1131) cells (Supplementary Fig. 4a). Indeed, both WT and C98S USP48 accumulated at sites of laser micro-irradiation within 10 min of DNA-damage induction (then declined after a further 10 min), with the mutant protein accumulating more strongly than the WT protein (Supplementary Fig. 4b, c), again suggesting that mutation of the catalytic domain may prevent release of USP48 from its substrate(s) at DNA-damage sites. Furthermore, we found that USP48 DNA-damage accumulation was more efficient in FANCC-deficient cells than in these cells complemented with FANCC, suggesting that USP48 recruitment may be actively suppressed by FANCC and associated FA proteins (Supplementary Fig. 4d, e). Finally, we tested whether USP48 can specifically localize to ICLs by irradiating cells that had been pre-treated with Trioxalen, a psoralen derivative that forms ICLs upon UV

irradiation (Fig. 4a). Notably, we observed efficient recruitment of mutant USP48 in ICL-containing tracks marked by FANCD2 in a substantial fraction of cells, while we were unable to detect WT USP48 recruitment (Fig. 4b). By contrast, we detected DNA-damage accumulation of both WT and mutant USP48 in a substantial fraction of FANCC-deficient cells, with the mutant protein being detectable in laser tracks in a much larger proportion of the cells than the WT protein (Fig. 4b). Collectively, these data indicated that USP48 is recruited to ICLs and that it appears to do so independently of a functional FA-protein assembly.

USP48 loss promotes repair of MMC-induced damage in FA cells. We next determined whether the effect of USP48 loss on survival of FA-defective cells after treatment with DNA crosslinking agents correlated with less DNA damage induction and/or increased DNA repair. Hence, we analyzed the formation and clearance of γ H2AX foci, a marker for DNA damage lesions, in WT, Δ USP48, Δ FANCC, and Δ USP48 Δ FANCC cells at different time-points after being treated with MMC for 18 h. Although the number of γ H2AX foci were similar in all settings immediately after MMC treatment (0 h after MMC removal), we observed persistence of γ H2AX foci at 48 h after MMC removal in Δ FANCC cells but not in Δ USP48 Δ FANCC cells (Fig. 4c, d). These findings thus suggested that Δ USP48 Δ FANCC cells repair MMC-induced DNA damage more efficiently than Δ FANCC cells. Interestingly, we also observed that Δ USP48 cells displayed increased clearance of γ H2AX foci than WT cells (Fig. 4c, d), suggesting that loss of USP48 improves DNA repair also in ICL-

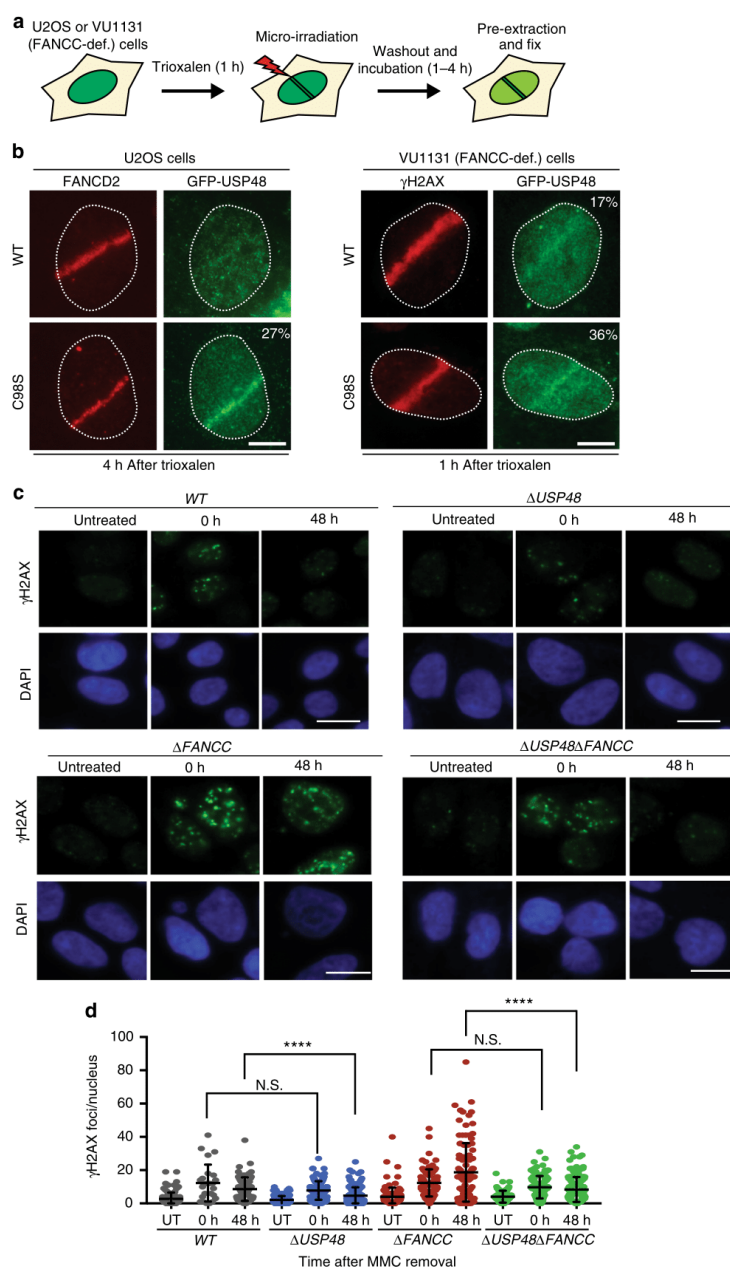


Fig. 4 USP48 is recruited to ICLs and attenuates clearance of γ H2AX foci. **a** Workflow for the recruitment of proteins to ICLs in U2OS and VU1131 cells. **b** Localization of FANCD2 and GFP-USP48 (WT and C98S mutant) to sites of laser micro-irradiation after Trioxalen treatment in U2OS and VU1131 cells. Scale bar = 10 μ m. **c** Representative immunofluorescence images after staining for γ H2AX on WT, Δ USP48, Δ FANCC, and Δ USP48 Δ FANCC cells after treatment with MMC (30 nM) for 18 h and then recovery for the indicated time-points. Scale bar = 10 μ m. **d** Quantification of γ H2AX foci of the indicated cell lines. UT untreated cells. Quantification was performed using the Cell Profiler software. Error bars show mean with S.D. (standard deviation). Statistical significance was determined by Wilcoxon test with $p < 0.05$ as threshold. N.S. not significant; **** = $p < 0.0001$

repair proficient cells, although with a less pronounced phenotypic effect than in a Δ FANCC setting.

USP48 loss enhances BRCA1 and RAD51 localization in FA cells. FA-protein-dependent homologous recombination (HR) plays a crucial role in the repair of ICL lesions during S-phase²¹. To assess the potential impact of USP48 loss on HR in Δ FANCC cells, we examined the DNA damage-induced recruitment of BRCA1, a HR factor²². Analysis of BRCA1 localization into foci at DNA damage sites revealed that Δ USP48 Δ FANCC cells displayed significantly higher numbers of BRCA1 foci at 24 and 48 h after MMC treatment as compared to Δ FANCC cells (Fig. 5a, b). Furthermore, Δ USP48 Δ FANCC cells displayed a higher number of BRCA1 foci in untreated conditions, which could reflect enhanced BRCA1 recruitment following endogenous replication stress²³. We did not, however, observe significant differences in the formation or persistence of BRCA1 foci between WT and Δ USP48 cells (Fig. 5a, b). Since we had found that USP48 can affect the formation or maintenance of BRCA1 foci in Δ FANCC cells, we then addressed whether it also co-localizes with BRCA1 at DNA damage sites. To this end, we investigated the co-localization of BRCA1 with GFP-tagged WT or C98S USP48, after MMC treatment of Δ USP48 Δ FANCC cells. In accord with our results on its co-localization with γ -H2AX (Supplementary Fig. 3), mutant USP48 was observed to co-localize with nuclear foci of BRCA1 (Fig. 5c). Interestingly, in many cases co-localization was not exact with adjacent foci being observed, possibly suggesting competitive activities of the two proteins in DNA repair pathway choice.

BRCA1 is required for loading of RAD51, a protein necessary for pairing of homologous regions and strand exchange during HR^{22,24}. We thus measured, by immunofluorescence staining, DNA damage recruitment of RAD51. At 18 h after MMC treatment, recruitment of RAD51 into foci was significantly higher in U2OS cells simultaneously depleted for both FANCC and USP48 by siRNA treatment, compared to cells depleted for FANCC alone (Fig. 5d and Supplementary Fig. 5a–c), implying that USP48 loss restores HR efficiency at replication forks encountering ICL damage in FA-deficient cells. By contrast, USP48 depletion did not enhance MMC-induced RAD51 focus formation in control cells (Fig. 5d and Supplementary Fig. 5c), suggesting that USP48 may inhibit HR processes specifically in an FA-deficient background. Altogether, these findings suggested that USP48 counteracts BRCA1 and RAD51 recruitment at sites of ICLs, most notably when the FA pathway is deficient, thus preventing efficient HR.

To explore potential effects of USP48 on HR processes, we used the well established Traffic Light Reporter (TLR) system in human U2OS cells^{25,26}. Our results showed that depletion of USP48 reduced HR levels in both WT and FANCC-depleted cell backgrounds when compared to control cells (Supplementary Fig. 5d). While this did not correlate with the increased RAD51 recruitment we observed upon USP48 depletion after induction of DNA ICLs, we note that the direct generation of DNA double-strand breaks by the endonuclease I-SceI in this system renders it quite different from the HR-repair templates generated via ICL processing in S-phase. As an alternative measurement for homology-based repair, we assessed RPA recruitment to chromatin as an indicator of end-resection. We did not observe a major effect of USP48 depletion on RPA chromatinization upon induction of camptothecin (CPT)-induced replication stress, although a marginally significant increase of RPA foci was evident when both USP48 and FANCC were depleted compared to when FANCC was depleted alone (Supplementary Fig. 5e).

USP48 loss rescues ICL sensitivity of FA cells through BRCA1.

Since Δ USP48 Δ FANCC cells exhibited markers of enhanced ICL-dependent HR (as evidenced by BRCA1 and RAD51 foci) compared to Δ FANCC cells, and because USP48 inactivation alleviated the sensitivity of Δ FANCC cells to DNA crosslinking agents, we determined whether this effect on cell survival depended on BRCA1. Indeed, shRNA-mediated depletion of BRCA1 reversed the resistance of Δ USP48 Δ FANCC cells to MMC or cisplatin, as shown by clonogenic survival assays (Fig. 6a, b, marked by green frame), although residual resistance was still observed when compared to BRCA1-depleted Δ FANCC cells (Fig. 6b, marked by red frame), possibly because of incomplete shRNA-mediated depletion resulting in residual BRCA1 activity, or reflecting an additional BRCA1-independent effect of USP48. These results were thus in line with a model in which USP48 functions, at least in part, to counteract BRCA1 activity.

To explore the potential involvement of BRCA1 ubiquitin ligase activity²⁷, we reconstituted BRCA1-depleted Δ USP48 Δ FANCC cells with wild-type BRCA1 (WT) or with a mutant form of BRCA1 carrying a point mutation (I26A), previously shown to affect its ubiquitin ligase activity^{28,29}. Notably, we found that both WT and I26A BRCA1 were able to alleviate the hypersensitivity of BRCA1-depleted cells towards MMC treatment (Supplementary Fig. 5f, g), suggesting that the E3 ubiquitin ligase activity of BRCA1 might not be crucial for the synthetic rescue phenotype observed upon loss of USP48 in a FANCC-deficient background.

Loss of USP48 affects histone H2A ubiquitylation. We next asked what could be the substrate of USP48 in the context of ICL repair. Ubiquitylation of RPA has been recently implicated in the proper recruitment and resolution of RAD51 accumulation at sites of DNA ICL repair, in a manner dependent on the RFW3 ubiquitin ligase^{30,31}. Interestingly, RFW3-deficient cells are hypersensitive to DNA crosslinking agents, thus supporting a model where USP48 might counteract the effect of RFW3 on RPA and RAD51 recruitment. However, we did not observe a significant impact of USP48 siRNA depletion on the levels of ubiquitylation of GFP-tagged RPA70 in U2OS cells treated with camptothecin (Supplementary Fig. 5h, i). Based on these findings, we conclude that it is unlikely that USP48 counteracts RNFWD3/RNF4/PRP19-mediated ubiquitylation of RPA70.

USP48 has been reported to be recruited on chromatin and be associated to modified histones³². Histone ubiquitylation and especially H2A/H2B ubiquitylation is involved in repair of DNA double-strand breaks^{33,34}, and various sites have been identified as ubiquitin substrates that are ubiquitylated by different ubiquitin E3 ligases. We thus decided to investigate whether histone ubiquitylation levels are affected by loss of USP48. To this end, we immunoprecipitated Flag-tagged H2A from WT, Δ USP48, Δ FANCC, and Δ USP48 Δ FANCC cells following MMC treatment and blotted for ubiquitin (Fig. 6c and Supplementary Fig. 5j). Immunoprecipitation of Flag-tagged WT H2A, followed by immunoblotting against protein-conjugated ubiquitin chains using FK2 antibody showed a small but noticeable increase in poly-ubiquitylated forms of H2A in double Δ USP48 Δ FANCC cells compared to Δ FANCC cells, and increase that was further enhanced by MMC treatment (Fig. 6c). Immunoprecipitation of a mutant form of H2A that lacks the ubiquitin target sites K5-9-118-119-125-127-129 (K5-9-118-119-125-127-129R mutant) showed almost no poly-ubiquitylation, implicating at least one of these sites as being affected by USP48 loss (Fig. 6c, residual bands for the immunoprecipitated mutant H2A in the Δ USP48 Δ FANCC background likely correspond to ubiquitylated H2A at RNF168-dependent sites K13-15, which were not targeted for mutation, thus not excluding their contribution in the observed poly-ubiquitylated H2A profile).

ARTICLE

NATURE COMMUNICATIONS | DOI: 10.1038/s41467-018-04649-z

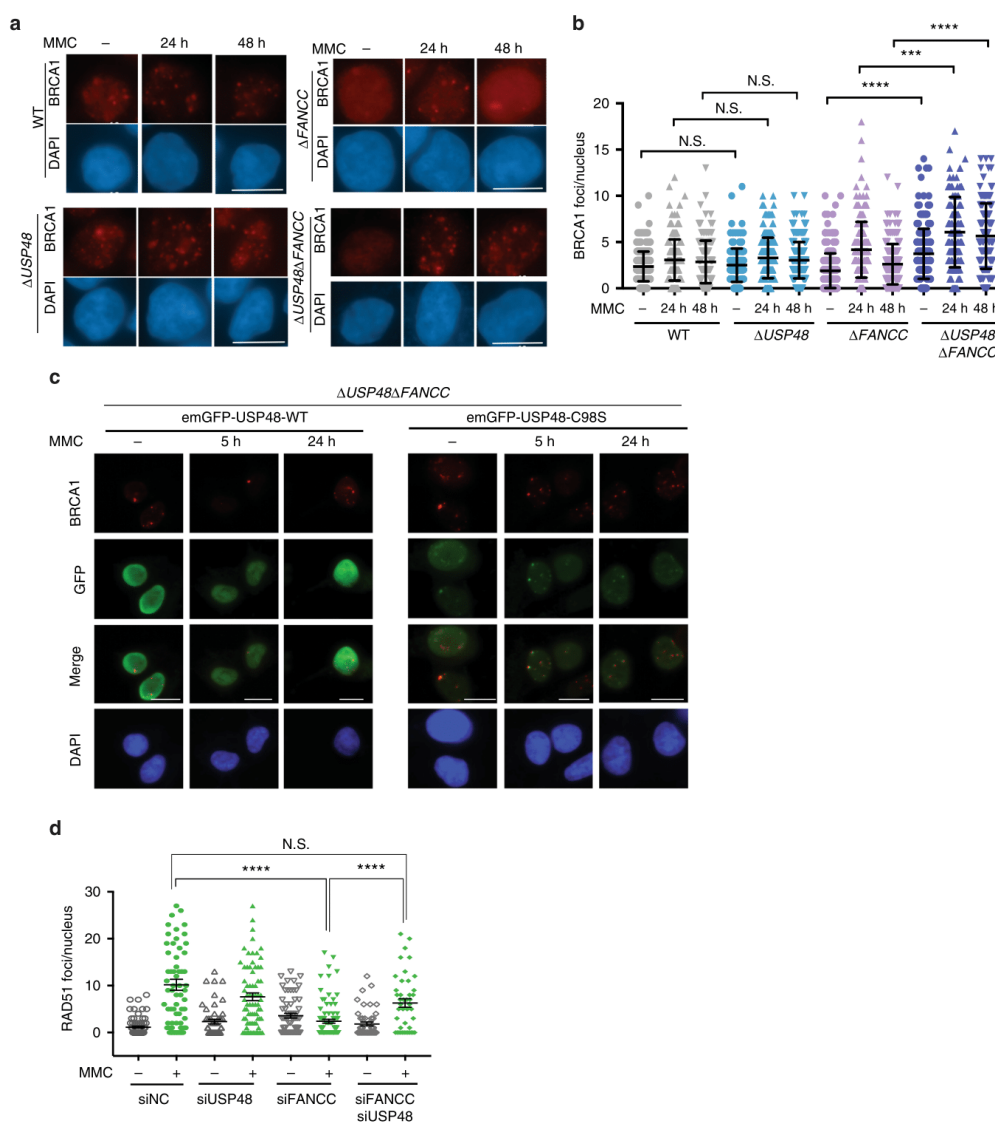


Fig. 5 FA cells lacking USP48 show enhanced recruitment of HR markers. **a** Representative immunofluorescence images of WT, Δ USP48, Δ FANCC, and Δ USP48 Δ FANCC cells after staining for BRCA1 following MMC treatment (25 nM) for the indicated times. Scale bar = 10 μ m. **b** Quantification of BRCA1 foci in WT, Δ USP48, Δ FANCC, and Δ USP48 Δ FANCC cells. Error bars show mean with SD (standard deviation). Statistical significance was determined using the Mann-Whitney test with $p < 0.05$ as a threshold. N.S. not significant; *** = $p < 0.001$; **** = $p < 0.0001$. **c** Immunofluorescence images after staining for BRCA1 and GFP on Δ USP48 Δ FANCC cells after treatment with MMC at the indicated time-points. Cells were transiently transfected with emGFP-USP48-WT and emGFP-USP48-C98S. **d** Quantification of RAD51 foci in WT, *siUSP48*, *siFANCC*, and *siUSP48siFANCC* cells treated with MMC (100 nM) for 18 h. Quantification was performed using the ImageJ software. Error bars show mean \pm S.E.M. (standard error of the mean). Statistical significance was determined using the Mann-Whitney test with $p < 0.05$ as a threshold. N.S. not significant; **** = $p < 0.0001$

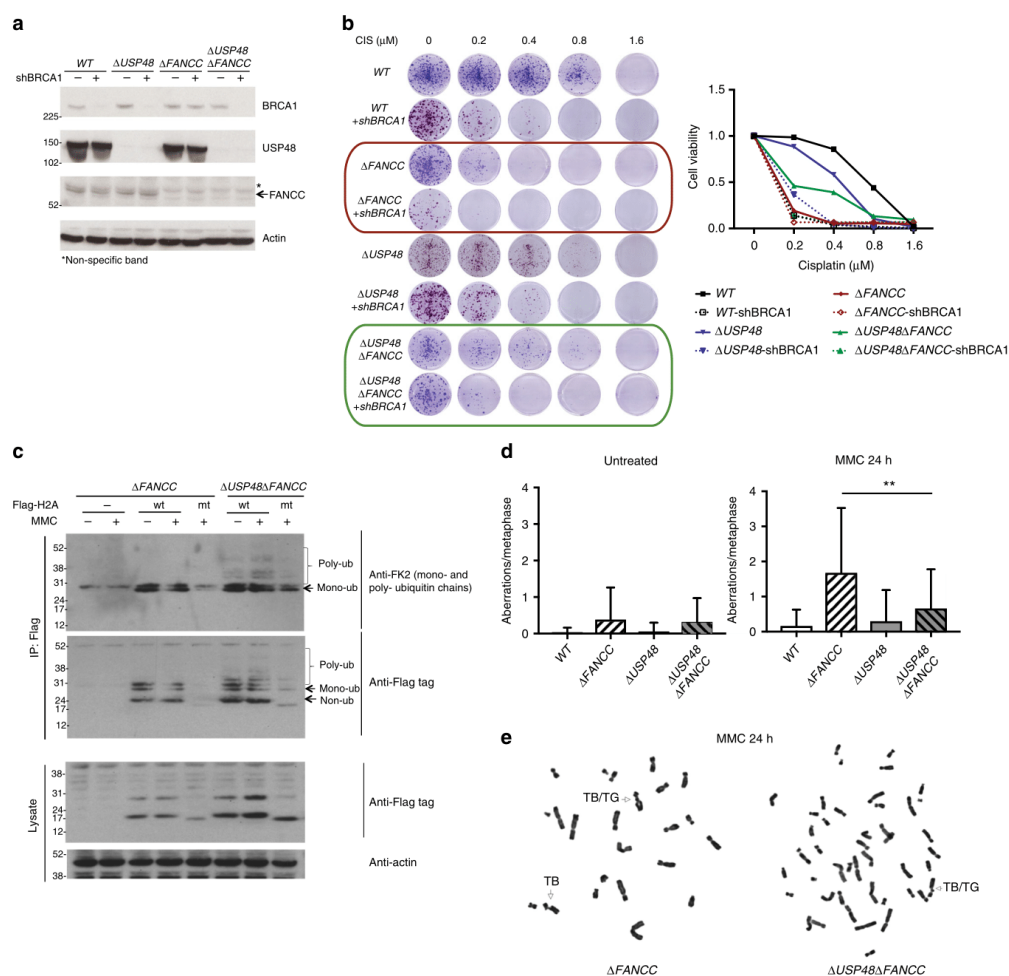


Fig. 6 USP48 acts on H2A and reduces chromosomal aberrations in FA cells. **a** Immunoblot for BRCA1, USP48, FANCC, and actin on the indicated cell lines. Asterisk (*) denotes non-specific band. **b** Colony formation and quantification of cell survival of the indicated cell lines 7 days after treatment with MMC at the indicated doses. **c** Anti-Flag-H2A immunoprecipitation probed against FK2, Flag and actin for the indicated cell lines. Lower bands correspond to monoubiquitylation modifications and higher bands correspond to poly-ubiquitin chains. Cells were transfected with wt = wild-type and mt = mutant (K5-9-118-119-125-127-129R) H2A and then treated with MMC (50 nM) for 4 h. **d-e** Plot of mean number of chromosomal aberrations (**d**) and representative images from metaphase spreads (**e**) of wild-type (WT), ΔFANCC and ΔUSP48ΔFANCC cells after treatment with MMC (25 nM) for 24 h. TB/TG: chromatid break/chromatid gap. Error bars show SD. Statistical significance was determined using the Mann-Whitney test with $p < 0.05$ as a threshold. ** = $p < 0.01$

These data raise the possibility that USP48 might at least in part affect the ICL sensitivity of FANCC-gene deficient via influencing H2A ubiquitylation.

Genomic instability of FA cells is reduced upon USP48 loss. A hallmark of FA-defective cells is increased chromosomal aberrations upon treatment with crosslinking agents^{3,4}, manifested as breaks and radials on mitotic chromosomes. As we had found that USP48 loss enhances HR in ΔFANCC cells, we determined whether it could also alleviate chromosome breaks in ΔFANCC cells. Indeed, analysis of metaphase spreads from cells treated

with MMC showed that chromosomal aberrations were significantly reduced in ΔUSP48ΔFANCC cells compared to ΔFANCC cells, the latter of which exhibited a high number of breaks after MMC treatment compared to WT cells (Fig. 6d; representative images of chromosomal aberrations shown in Fig. 6e). This result thus indicated that absence of USP48 can alleviate the increased genomic instability of FA-defective cells.

Discussion

In the current study, we have taken an unbiased approach to reveal an extended network of synthetic rescue interactions for

ARTICLE

NATURE COMMUNICATIONS | DOI: 10.1038/s41467-018-04649-z

FA deficiency, providing a resource for potential therapeutic targets. Among these, we have selected and validated a synthetic-interaction between the deubiquitylating enzyme USP48 and FA genes. We have shown that USP48 loss specifically improves the survival of FA-defective cells to DNA crosslinking agents, and that this is associated with enhanced recruitment of the HR proteins BRCA1 and RAD51 to DNA damage sites and reduced chromosomal instability. This implies that USP48 counteracts BRCA1 activity or indirectly prevents conditions permissive for HR.

Our data indicate an early role for USP48 at sites of DNA damage, as shown by its rapid recruitment at irradiated sites, likely targeting substrates at or flanking sites of DNA lesions. Interestingly, we have found that recruitment and retention of USP48 at ICLs appears to be negatively modulated by its catalytic activity and by the presence of FA proteins, suggesting that FA-protein assembly at DNA damage sites serves to likely counteract USP48 recruitment and activity at sites of DNA ICLs to promote HR and genome integrity. Our findings thus support a role for USP48 in regulating the balance between different repair pathways at the site of damage.

While our manuscript was under review, a new study was published showing that USP48 is recruited to sites of double-strand breaks and that its depletion leads to increased RAD51 recruitment and enhanced BRCA1-mediated DNA end-resection³⁵. Although not in the context of interstrand crosslink repair, these results are complementary and similar to what we observed, and further highlight that USP48 plays a role(s) in DNA repair. Notably, the authors in this study showed the activity of USP48 counteracts BRCA1-mediated ubiquitylation of H2A K127/129 and thereby preventing chromatin remodeling and resection during double-strand break repair after IR and camptothecin treatment³⁵. Significantly, however, our studies in USP48-depleted FA-gene-deficient cells have indicated that both wild-type and I26A BRCA1 were able to alleviate the hypersensitivity of BRCA1-depleted FA-gene deficient, USP48-depleted cells towards MMC treatment. This suggests that the effect of BRCA1 under this setting is unlikely to operate via effects on reversing BRCA1-mediated ubiquitylation of histone H2A or other proteins. However, since the role of E3 ubiquitin ligase activity of BRCA1 is a subject of debate^{28,29,36}, more experiments are needed to better understand its involvement or not in the mechanism of the genetic interaction between USP48 and FA genes during crosslink repair. It is important to note that our data do not exclude the contribution of other H2A sites in the mechanism by which USP48 loss counteracts the ICL hypersensitivity of FA cells. Since crosstalk between histone marks has also been reported³⁷, another possible mechanism is that USP48 regulates ubiquitylation of multiple H2A sites by trimming poly-ubiquitin chains, thus performing a balancing act between different DNA repair pathways in combination with the activity of E3 ubiquitin ligases such as RNF168 or others.

An important step in ICL repair is unhooking of the DNA lesion, which happens with the contribution of various nucleases, including FAN1, MUS81-EME1, XPF-ERCC1, SLX1, and the scaffold protein SLX4, all thought to assemble into a large structure-specific endonuclease complex²¹. Importantly, SLX4 and FAN1 both contain UBZ domains that recognize ubiquitin and play important roles in their recruitment and function that is also dependent, at least partially, on FA proteins, especially monoubiquitylated FANCD2/FANCI^{38–41}. Our data demonstrate that loss of USP48 does not restore FANCI/FANCD2 monoubiquitylation or FANCD2 recruitment at ICLs, but if USP48 targets one or more sites on H2A that can be recognized by these nucleases, then loss of USP48 might bypass the requirement of

the FA proteins and allow the recruitment of FAN1 or SLX4 and subsequent unhooking of the ICL in an FA-deficient background.

Recently, USP48 has also been shown to promote the stability of Mdm2 that in turn results in enhanced degradation of p53⁴², which has been associated to FA cell death⁴³. However, HAP1 cells, which have used in various parts of our study, have a p53 mutation, which likely affects p53 normal function, as we have shown in a previous study¹⁸ but also as implied by the fact that p53 is not retrieved as a significant suppressor-hit from any of our screens. Moreover, we have shown similar effects upon USP48 depletion in U2OS cells, which possess wild-type p53. We thus, conclude that the function of USP48 in the context of ICL repair and synthetic rescue in an FA-deficient background is unlikely to be through its effects on p53.

Importantly, the results of the present study show that loss of USP48 improves DNA repair and prevents genomic instability of FA-defective cells, thus highlighting the potential of developing USP48 inhibitory molecules as novel therapeutic approaches that could potentially alleviate the phenotypes of FA patients. In this regard, it will be of interest to employ existing FA mouse models to investigate whether loss or inhibition of USP48 could alleviate disease phenotypes.

Methods

Cell lines and culture conditions. Human HAP1 cells were obtained from Horizon Discovery, they were grown in Iscove's Modified Dulbecco's Medium (IMDM) from GIBCO, containing L-Glutamine and 25 mM HEPES and supplemented with 10% fetal bovine serum (FBS) and 1% Penicillin/Streptomycin (P/S). HEK293T cells were obtained from the CRUK Cell Facility, they were used for virus production, expanded in Dulbecco's modified Eagle medium (DMEM) and supplemented with 10% FBS. U2OS cells were originally obtained from ATCC cell repository, they were cultured in DMEM (Sigma-Aldrich), supplemented with 10% FBS. Human mCherry-Geminin-expressing U2OS⁴⁴, FANCC-deficient VU1131 and complemented VU1131 cells (a gift from Josephine Dorsman, VU Medical Center Amsterdam) were cultured in DMEM, supplemented with antibiotics and 10% fetal calf serum. VU1131 cells were grown with G418 (300 µg/mL). All cells were grown at 37 °C in a 3% oxygen and 5% CO₂ atmosphere. All cell lines used in this publication were tested negative for mycoplasma contamination using the MycoAlert™ Mycoplasma Detection Kit. They were all authenticated by the specified providers and, furthermore, they are not listed as commonly misidentified by ICLAC.

CRISPR-Cas9-mediated gene editing. ΔUSP48 HAP1 cells were purchased from Horizon Genomics (clone HZGH000915c012). CRISPR-Cas9 knockouts of FANCA, FANCC, FANCG, and FANCI were generated in collaboration with Horizon Genomics. Sequences for gRNAs were designed by Horizon Genomics or with the use of <http://crispr.mit.edu/> and <https://www.deskgen.com/landing/>, respectively. Sequences of gRNAs used were:

FANCA: 5'-CGGGATGGTTCCTCTAGCG-3';
FANCC: 5'-GCCAACAGTTGACCAATTGT-3';
FANCG: 5'-GAATACCGGCTCGTTTCGAC-3';
FANCI: 5'-GTATCCAGTTGGTGAATCG-3';
USP48^{ex1}: 5'-TCGAGACCCGTTACCCGATC-3';
USP48^{ex6}: 5'-GCTTAGACTCTCTGCCACAC-3'

Sanger sequencing. Genomic DNA was extracted using the Qiagen Biotech DirectPCR Lysis Reagent (Cell) according to the manufacturer's protocol. Genomic regions around the gRNA-targeted sequences were amplified using the following primer pairs:

FANCA-For: 5'-ATACTGAGCAAACCTCTAACAGGGAA-3';
FANCA-Rev: 5'-GGCATTTTAAACAGCAAGTCTTTGG-3';
FANCC-For: 5'-CAAACCTACACACATACATGGAC-3';
FANCC-Rev: 5'-ACTAAACAAGAAGCATTCACGTTCC-3';
FANCG-For: 5'-GTTGTCACAGGATCAATCCTTTT-3';
FANCG-Rev: 5'-TTCACCTTCTCTAAGTCGGCTT-3';
FANCI-For: 5'-CTTTTCAAAGCCCTTAACCATTCG-3';
FANCI-Rev: 5'-CCCTCAACAATTAACAACCCCTCAA-3';
USP48-For: 5'-GATGGGAACCCAAACCTCTCTAAAG-3';
USP48-Rev: 5'-CTCGGGAGGCGTTCTCTGG-3'

The following sequencing primers were used:
FANCA: 5'-GGCATTTTAAACAGCAAGTCTTTGG-3';
FANCC: 5'-ACTAAACAAGAAGCATTCACGTTCC-3';
FANCG: 5'-GTTGTCACAGGATCAATCCTTTT-3';
FANCI: 5'-CTTTTCAAAGCCCTTAACCATTCG-3';

USP48: 5'-GATGGGAACCCAACTTCCTAAAG-3'.

PCR amplification conditions were as follows: heat lid 110 °C; 94 °C 2 min; loop 35 × (94 °C 30 s; 55 °C 30 s; 68 °C 1 min) 68 °C 7 min. Frameshift mutations were identified using Nucleotide BLAST against the reference genome GCF_000001405.33.

Plasmids. GFP-WT and GFP-C98S mutant USP48 constructs were generated via Gateway cloning. WT and C98S mutant USP48 cDNA sequences were amplified by PCR using primers complementary to attB sites and partially to cDNA sequence and cloned into pDONR221 vector. Following reaction with L recombinease (Invitrogen, Thermo Fisher Sci) WT and C98S mutant USP48 cDNA sequences were cloned into the pCDNA6.2/N-EmGFP-DEST destination vector (Invitrogen, Thermo Fisher Sci). Correct sequence and in-frame N-terminal expression of the GFP tag was confirmed by Sanger sequencing. A mammalian expression plasmid encoding 3 × HA-Ubiquitin was previously generated together with the laboratories of Yossi Shiloh (Sackler School of Medicine, University of Tel Aviv) and Moshe Oren (Weizmann Institute of Science). pCDNA3.1-Flag-H2A (Addgene plasmid # 63560) and pCDNA3.1-Flag-H2A K5-9-118-119-125-127-129R (Addgene plasmid # 63565) were a gift from Titia Sixma³⁴. pEGFP1-C1-BRCA1 and pCIN4-Flag-BARD1 plasmids were a kind gift from Jiri Lukas (Novo Nordisk Foundation Center for Protein Research, University of Copenhagen). To generate the I26A mutant construct, the Q5[®] site-directed mutagenesis kit (NEB) was used according to the manufacturer's instructions. The mutagenesis primers were designed using the NEBaseChanger[™] Tool (<http://nebasechanger.neb.com/>). The following primer sequences were used:

BRCA1 I26A For: 5'-AGAGTGTCCCGcCTGTCTGGAG-3',
BRCA1 I26A Rev: 5'-AAGATTTTCTGCATAGCATTAATG-3'

Plasmid transfection. Transfection of pCDNA6.2/N-emGFP USP48 WT and C98S vectors was carried out using Xfect transfection reagent (Takara, Clontech) according to manufacturer's protocol. Briefly, HAP1 cells at 60% confluency in six-wells plates were transfected with 8 µg of plasmid in antibiotics-free medium containing 10% FBS. The next day, cells were trypsinized and seeded for colony formation or immunofluorescence assays.

BRCA1 siRNA transfection. Transfection of HAP1 cells with siBRCA1 and non-targeting control siRNA was done using Dharmafect-1 (Dharmacon) reagent according to manufacturer's instructions. For expression of BRCA1 constructs, Effectene transfection reagent (Qiagen) was used the next day following siRNA transfection according to manufacturer's protocol.

siRNA sequences targeting 3'UTR of BRCA1 were synthesized by Dharmacon:
siBRCA1 3'UTR-1: GCUCCUCACUCUUCAGU
siBRCA1 3'UTR-2: AAGCUCUCUCACUCUUCAGU

BRCA1 knock-down by shRNA. HAP1 cells were infected with the virus-containing supernatant in the presence of polybrene (final concentration 8 µg/mL), diluted 1:3. Infected cells were selected using puromycin (2 µg/mL; Sigma-Aldrich) for 48 h.

DsiRNAs. Pre-designed dicer-substrate short interfering 27-mer RNAs (DsiRNAs) targeting USP48 (design ID hs.Ri.USP48.13.1 and hs.Ri.USP48.13.2), FANCC (design ID hs.Ri.FANCC.13.1 and hs.Ri.FANCC.13.2) or RBBP8/CtIP (design ID hs.Ri.RBBP8.13.1) were from Integrated DNA Technologies. Cells were transfected with 5 nmol DsiRNAs using Lipofectamine RNAiMAX (Thermo Fisher Scientific) according to the manufacturer's instructions.

Quantitative reverse transcription PCR (RT-PCR). Cells were harvested from which RNA was isolated using Trizol extraction (following the manufacturer's instructions). RNA was treated with 1 µL DNase (Sigma) and then reverse transcribed with the SuperScript III Reverse Transcriptase protocol (Invitrogen) to obtain cDNA. An amount of 1 µg of cDNA template was used for the qRT-PCR using SYBR Green qPCR Mastermix (Qiagen). Analysis was performed out in triplicates using expression of GAPDH for normalization of data. The PCR was performed on a 7900HT Fast Real-Time PCR System (Applied Biosystems). The following primers were used:

BRCA1: 5'-TCAACTCCAGACAGATGGGAC-3'; 5'-GGCTGTGGGGTTTCTCAGAT-3'; GAPDH: 5'-CGAGCCACATCGCTCAGACA-3'; 5'-GGGCCCAATACGACCAAT-3'.

Dose-response curves. Dose-response curve for mitomycin C (MMC), was performed in 96-well plates by seeding 1000 cells per well, the day before treatment. The following day, compounds were added at twofold serial dilutions. Four days after treatment with compounds, cell viability was measured using CellTiter-Glo (Promega).

Colony formation assays. Cells were seeded in six-well plates the day before exposure to compounds (1000 cells/well). The next day compounds were added at the indicated concentrations. Three days after, compound-containing medium was

changed with fresh compound-free medium. Cells were left in culture until visible colonies appeared (7–10 days). Colonies were then fixed in 3.7% formaldehyde in phosphate-buffered saline (PBS) for 1 h, washed in PBS and stained with 0.1% crystal violet solution in PBS supplemented with 10% ethanol for 1 h, followed by washing twice with H₂O. For quantification, crystal violet was extracted using 50% EtOH, and absorbance was measured at 595 nm.

Laser micro-irradiation. U2OS cells were grown on 18 mm coverslips and sensitized with 6 µM Trioxalen for 1 h, or 10 µM 5'-bromo-2-deoxyuridine (BrdU) for 24 h as described⁴⁴. The cells were placed in a Chamlide TC-A live-cell imaging chamber that was mounted on the stage of a Leica DM IRBE widefield microscope stand (Leica, Wetzlar, Germany) integrated with a pulsed nitrogen laser (Micro-point Ablation Laser System; Photonic Instruments, Inc., Belfast, Ireland). The pulsed nitrogen laser (16 Hz, 364 nm) was directly coupled to the epifluorescence path of the microscope and focused through a Leica 40 × HCX PLAN APO 1.25–0.75 oil-immersion objective. The growth medium was replaced by CO₂-independent Leibovitz's L15 medium supplemented with 10% FCS and penicillin–streptomycin and cells were kept at 37 °C. The laser output power was set to 75 to generate strictly localized sub-nuclear DNA damage. Cell were micro-irradiated (two iterations per pixel) within 35 min using Andor IQ software. Following micro-irradiation, cells were incubated for the indicated time-points at 37 °C in Leibovitz's L15 and subsequently fixed with 4% formaldehyde before immunostaining.

Immunofluorescence. BRCA1, γH2AX, and GFP staining: Cells were seeded on coverslips in 24 well plates, at a density of 2 × 10⁴ cells/mL. For BRCA1 staining, soluble proteins were pre-extracted with 0.2% Triton X-100 for 1 minute at room temperature. Cells were then fixed in 4% PFA and permeabilized with 0.2% Triton X-100. After blocking in 10% FCS in PBS for 1 h at room temperature, cells were incubated with primary antibodies overnight and with secondary AlexaFluor antibodies for 1 h at room temperature. DNA was stained with DAPI.

RAD51 and FANCD2 staining: Cells were washed with PBS containing 0.1% Tween20 (PBST), fixed 20 min with 2% paraformaldehyde (w/v) in PBS and blocked in PBST containing 5% bovine serum albumin (BSA) (w/v). Primary antibody incubation with anti-Rad51 (H-92) antibody (Santa Cruz, sc-8349) diluted 1:100 or anti-FANCD2 antibody (Santa Cruz, sc-20022) diluted 1:100 in 5% BSA PBST was performed at 4 °C overnight. After washing with PBST, cells were incubated with AlexaFluor 488-conjugated secondary antibody (Molecular Probes, A11034) diluted 1:1000 in 5% BSA PBST and counterstained with DAPI (2 µg/mL). After washing in PBST the cells were mounted using Vectashield (Vector Labs).

Labeling of laser micro-irradiated cells: Cells were pre-extracted with 0.25% Triton-X-100 (Serva, Heidelberg, Germany) in cytoskeletal (CSK) buffer (10 mM Hepes-KOH, 300 mM Sucrose, 100 mM NaCl, 3 mM MgCl₂, pH 7.4) on ice for 1 or 2 min and subsequently fixed with 2% formaldehyde in PBS for 20 min at room temperature. Cells were blocked for 15 min in PBS with 0.5% BSA and 0.15% glycine (PBS+). Antibody steps and washes were in PBS-. The primary antibodies were incubated overnight at 4 °C. Detection was done using goat anti-mouse or goat anti-rabbit Ig coupled to Alexa 488, 546 or 647 (1:1000; Invitrogen Molecular probes). Samples were incubated with 0.1 µg/mL DAPI and mounted in Polymount.

Microscopy of immunofluorescence. γH2AX imaging: Images were taken with a Leica DMI 6000B microscope with an HBO lamp with a 100-W mercury short arc UV-bulb light source and six filter cubes, with only three cubes necessary to produce excitations at wavelengths of 360, 488, and 555 nm. Images were captured at each wavelength sequentially with a Plan apochromat HCX 100 × /1.4 oil objective at a resolution of 1392 × 1040 pixels.

BRCA1 imaging: Images were captured on a AxioImager M2, with three lasers giving excitation at 360, 555 and 488 nm wavelengths. Images at each wavelength were collected sequentially at a resolution of approximately 1024 × 1024 pixels, with a Plan apochromat 100 × /1.4 oil objective.

RAD51 and FANCD2 imaging: Images were captured on a FluoView 1000 confocal microscope (Olympus) through a 100 × UPlanSApo/1.4 Oil objective. Images were collected sequentially at each wavelength (405 nm and 488 nm) at the same resolution as above.

Imaging of laser micro-irradiated cells: Images of fixed samples were acquired on a Zeiss AxioImager M2 or D2 widefield fluorescence microscope equipped with 40 ×, 63 × and 100 × PLAN APO (1.4 NA) oil-immersion objectives (Zeiss) and an HXP 120 metal-halide lamp used for excitation. Fluorescent probes were detected using the following filters: DAPI (excitation filter: 350/50 nm, dichroic mirror: 400 nm, emission filter: 460/50 nm), GFP/Alexa 488 (excitation filter: 470/40 nm, dichroic mirror: 495 nm, emission filter: 525/50 nm), mCherry (excitation filter: 560/40 nm, dichroic mirror: 585 nm, emission filter: 630/75 nm), Alexa 555 (excitation filter: 545/25 nm, dichroic mirror: 565 nm, emission filter: 605/70 nm), Alexa 647 (excitation filter: 640/30 nm, dichroic mirror: 660 nm, emission filter: 690/50 nm). Images were recorded using ZEN 2012 software.

ARTICLE

NATURE COMMUNICATIONS | DOI: 10.1038/s41467-018-04649-z

Quantification and analysis of immunofluorescence. BRCA1 and γ H2AX analysis: Quantification of foci (number and intensity) was performed using Cell Profiler software.

RAD51 and FANCD2 foci analysis: Quantification of Rad51 foci was performed in ImageJ using a macro developed by Dr. Richard Butler at the Gurdon Institute Imaging Facility (University of Cambridge), which is essentially a version of the FindFoci plugin specifically optimized for Rad51 and FANCD2 foci quantification and the immunofluorescence conditions detailed above.

Local irradiated areas: Images recorded after micro-irradiation of cells were analyzed using ImageJ software. The average pixel intensity of laser tracks was measured within the locally irradiated area (I_{damage}), in the nucleoplasm outside the locally irradiated area ($I_{\text{nucleoplasm}}$) and in a region not containing cells in the same field of view ($I_{\text{background}}$). The relative level of accumulation expressed relative to the protein level in the nucleoplasm was calculated as follows: $(I_{\text{damage}} - I_{\text{background}}) / (I_{\text{nucleoplasm}} - I_{\text{background}}) - 1$ for GFP signals and $(I_{\text{damage}} - I_{\text{background}}) / (I_{\text{nucleoplasm}} - I_{\text{background}}) - 1$ for γ H2AX signals. The average reflects the quantification of between 50–150 cells from 2–4 independent experiments.

Immunoblotting and antibodies. Cell extracts were prepared in RIPA lysis buffer (NEB) supplemented with protease inhibitors (Sigma) and phosphatase inhibitors (Sigma, NEB). Immunoblots were performed using standard procedures. Protein samples were separated by sodium dodecyl sulfate–polyacrylamide gel electrophoresis (SDS–PAGE) (4–12% gradient gels; Invitrogen) and subsequently transferred onto nitrocellulose membranes. Details of primary antibodies used for western blotting (WB) and immunofluorescence (IF) are described in Supplementary Table 1. Secondary antibodies were used at 1:5000 (HRP-conjugated goat anti-mouse, rabbit or goat IgG from Jackson Immunochemicals) for WB and 1:600 or 1:1000 for IF (AlexaFluorophores).

H2A immunoprecipitation. HAP1 cells were transfected in 15 cm dishes with FLAG-H2A constructs using X-fect transfection reagent (Clontech) and 40 h later treated with mitomycin C for 4 h. Cell extracts were prepared in nuclear/chromatin extraction HEPES buffer (HEPES 20 mM pH 7.9, NaCl 420 mM, glycerol 25%, EGTA 1 mM, EDTA 1 mM, DTT 0.1 mM) supplemented with NaF 50 mM, Na_2VO_4 1 mM, PMSF 1 mM, NEM 20 mM, protease inhibitor cocktail (Sigma-Aldrich) and Benzonase endonuclease 25 U/mL (Merck-Millipore). After lysis, extracts were sonicated and protein was quantified by Bradford. One milligram of lysate was used for immunoprecipitation after dialysis with HEPES buffer to a final salt concentration of 150 mM NaCl and then incubated with FLAG M2 Magnetic Beads (Sigma-Aldrich) overnight at 4 °C. Beads were washed in wash buffer (HEPES 50 mM, NaCl 150 mM, EDTA 5 mM, NP-40 substitute 0.2% three times) and bound proteins were eluted in 2 \times Laemmli Sample Buffer for 20 min with gentle agitation. Eluates were loaded on SDS–PAGE gels for western blot.

RPA70 immunoprecipitation. To test whether RPA70 is de-ubiquitinated in an USP48-dependent manner, we co-expressed HA-ubiquitin in either GFP-expressing or GFP-RPA70-expressing U2OS cells (kind gift from John Rouse at University of Dundee), transfected with pre-design DsiRNAs targeting USP48 (from Integrated DNA Technologies) using Lipofectamine RNAiMAX according to the manufacturers' instructions. Seventy-two hours post-transfection cells were treated or mock-treated with camptothecin (TOP1 inhibitor) 1 μ M for 1 h. Next, we prepared cell extracts and assessed GFP immunoprecipitates for HA-ubiquitin and FK2 staining by immunoblotting as described in Schmidt et al.²⁹ Briefly, U2OS cells expressing GFP or RPA70-GFP were transfected in 10 cm dishes with negative-control or USP48-targeting DsiRNAs using Lipofectamine RNAiMAX (Thermo Fisher Scientific) the night before. The following day cells were transfected with a mammalian expression plasmid encoding 3 \times HA-Ubiquitin using TransIT-LT1 transfection reagent (Mirus Bio LLC), and 48 h later treated with camptothecin plus 10 μ M MGI32 proteasome inhibitor for 1 h. Cell extracts were prepared by scraping cells from PBS-washed plates into ice-cold lysis buffer (20 mM Tris-HCl pH 7.5, 40 mM NaCl, 2 mM MgCl₂, 10% glycerol, and 0.5% NP-40) containing EDTA-free protease inhibitor cocktail (Roche) and benzonase (10 μ l/mL lysis buffer, Novagen 70664-3). After increasing the salt concentration to ~250 mM NaCl, extracts were rotated for 10–15 min at room temperature, subsequently diluted 1:2 with lysis buffer (without benzonase) and the extracts cleared by centrifugation at 16,000 \times g for 45 min at 4 °C. Immunoprecipitation reactions were rotated overnight at 4 °C using GFP-Trap-A beads (ChromoTek, 10 μ l per mg protein) followed by five washes with immunoprecipitation buffer (lysis buffer without benzonase containing a final concentration of ~250 mM NaCl). Proteins were eluted from the GFP-Trap-A beads in a 5–10-min incubation step at 95 °C in 1.5 \times SDS sample buffer and loaded on SDS–PAGE gels for western blot.

TLR assay. A minimum of 10,000 doubly-transfected (IFP+ and BFP+) cells were scored for each condition in four independent experiments, three of which performed in duplicate using either of two different DsiRNAs targeting USP48 or FANCC²⁶. Analyses were conducted using FlowJo (TreeStar). For each DsiRNA treatment, results were normalized (including the negative-control DsiRNA) to cells treated with RNAiMAX only, resulting in relative homologous recombination (HR) and mutagenic end-joining (mutEJ) percentages for each DsiRNA treatment.

Finally, the HR values for each condition were normalized to the total amount of cells in S and G2 phases obtained by flow-cytometry analysis of a subset of DAPI-stained cells transfected only with DsiRNAs and grown in parallel at the same cell density.

RPA70-GFP chromatinization. Cells were mock-treated or treated for 1 h with 1 μ M camptothecin to induce replication fork collapse, and then processed as described in detail in Forment and Jackson⁴⁵. RPA70-GFP+ cells were co-stained with DAPI and analyzed by flow-cytometry using a BD LSRFortessa™ cell analyzer (BD Biosciences).

Metaphase spreads. Cells were seeded in 10 cm dishes and treated with MMC for the indicated times. Colcemid (KaryoMAX™, Gibco, Thermo Fisher Scientific) was added at a final concentration of 500 ng/mL 3 h before harvesting. Cells were trypsinized and incubated in KCl at 0.075 M (KaryoMAX™, Gibco, Thermo Fisher Scientific) for 6 min. After centrifugation, cells were resuspended in fixation solution (methanol:acetic acid at 3:1) and incubated for 15 min at room temperature. Centrifugation and re-suspension in fresh fixation solution was repeated two times. Metaphase spreads, slide preparation and measurement of chromosomal aberrations was performed at Karyologic Inc (North Carolina, USA). All analysis was performed in a blinded manner. Fifty metaphases were scored for each condition, providing a total count of the overall chromosome counts, and the total of the different types of aberrations (chromatid gaps, chromosome gaps, chromatid breaks, chromosome breaks, double minutes, tri-radial, quadri-radial, complex rearrangement, pulverized, and polyploid).

Genome-wide insertional mutagenesis. Gene-trap virus was produced in HEK293T using Lipofectamine 2000 Transfection reagent (Invitrogen, Thermo Fisher Scientific)¹¹. Δ FANCA, Δ FANCC, Δ FANCG, Δ FANCI, and Δ FANCD2 HAP1 cells were transduced with concentrated retrovirus containing the gene-trap cassette¹¹. After integration of the GFP-expressing gene-trap cassette, cells were analyzed by flow-cytometry to measure efficiency of infection and populations with more than 70% GFP-expressing cells were used for treatment with MMC. The control non-selected WT-HAP1 population was generated in Blomen et al.¹⁴. One-hundred million cells from the mutagenized pools were seeded in 15 cm dishes at a density of 6 million cells per dish. The following day, MMC was added at a concentration that selectively killed FA-deficient cells, leaving only around 5–10% of cells surviving (46 nM for Δ FANCA, Δ FANCC, and Δ FANCG, 40 nM for Δ FANCI and Δ FANCD2). Cells were left to grow for 10 days after which cells were trypsinized and frozen at -80 °C. For preparation of the gene-trapped DNA libraries, genomic DNA was extracted from 30 million cells using the QIAamp DNA mini kit (Qiagen), subjected to digestion with MseI (NEB) and NlaIII enzymes (NEB) and subsequently ligated by T4 DNA ligase (NEB). Digested and ligated fragments were used as templates for inverse PCR with primers targeting the LTR regions of the gene-trap cassette. After amplification and purification of the fragments, the DNA sample was prepared for next generation sequencing (Illumina HiSeq 2000, 50 base pair single-read) by the CeMM Biomedical Sequencing Facility (BSF). For the control non-selected WT-HAP1 sample, samples from Blomen et al.¹⁴ were used.

Statistical analysis. Gene-trap screen: Bioinformatics analysis of the next generation sequencing data was done in R as described¹⁸. Insertions were considered mutagenic or disruptive to the gene if they occurred within exons irrespective of their orientation to the corresponding gene or if they were located within introns in sense orientation. Insertions in antisense direction in respect to the gene orientation were considered silent. All mutagenic insertions were summarized independently for each gene. For each gene a one-sided Fisher's exact-test was applied to estimate a significant enrichment of insertions over an unselected control data set.

Immunofluorescence analysis: Statistical analysis of the immunofluorescence data was performed using Prism software. We performed Student T-test analysis to determine statistical significances between independent samples, this test requires the assumption of a normal distribution of the groups. When it is not possible to assume a normal distribution, we have performed the Mann–Whitney test.

Metaphase spreads analysis: Statistical analysis was performed using Prism software. We performed a Mann–Whitney test. The significance was indicated as: **** = $p < 0.0001$, *** = $p < 0.001$, ** = $p < 0.01$, * = $p < 0.05$, N.S. = not significant.

Network analysis. Background network construction: Network analysis methods were employed to explore the functional context of the genes identified in the FA screens (individual, all combined, and those unique to the screens not found in WT). The background interactome used was that compiled by Menche et al.¹⁵ and contains physical protein–protein interactions that were manually curated from seven different databases, including regulatory interactions (TRANSFAC), Yeast two-hybrid screens (IntAct, MINT), literature curated interactions (IntAct, MINT, BIOGRID, HPRD), metabolic enzyme-coupled interactions (KEGG, BIGG), protein complexes (CORUM), kinase network (PhosphositePlus), and signaling interactions¹⁶. A gene list from the FA screens (individual, all combined and those unique to the screens not found in WT) was used to seed the network.

Network propagation: To identify the local interactome neighborhoods of the genes identified in the FA screen, we implemented the network propagation method previously published¹⁵. Briefly, the method simulates how heat would diffuse, with loss, through the network by traversing the edges, starting from an initially hot set of “seed” nodes. At each step, one unit of heat is added to the seed nodes and is then spread to its neighbors. A constant fraction of heat is then removed from each node, so that total heat is conserved in the system. The amount of heat per node eventually converges to a stable value, which can then be used as a measure of its integrated distance to the set of seed nodes. For example, a node connected to several seed nodes would have a higher final heat value than a node that is located far from the seeds.

Identify network neighborhood of seed genes and clustering: The network propagation method described above finds genes, which are close to the set of seed genes in network space. We sort the genes in the network by their network propagation score, and extract genes in the top N ($N = 1000$ here) of the sorted list to define the network neighborhood. This results in a subgraph, which we cluster into groups of highly interconnected genes, using a modularity maximization clustering algorithm¹⁷. Functional enrichment analysis of the genes in each cluster was performed using the ToppFun function of ToppGene⁴⁷ and the ORA function as published⁴⁸.

Data availability. All data generated or analyzed during this study is included in this published article and its Supplementary Information or from the authors upon reasonable request.

Received: 21 August 2017 Accepted: 14 May 2018

Published online: 11 June 2018

References

- Hoeijmakers, J. H. Genome maintenance mechanisms for preventing cancer. *Nature* **411**, 366–374 (2001).
- Jackson, S. P. & Bartek, J. The DNA-damage response in human biology and disease. *Nature* **461**, 1071–1078 (2009).
- Kottemann, M. C. & Smogorzewska, A. Fanconi anaemia and the repair of Watson and Crick DNA crosslinks. *Nature* **493**, 356–363 (2013).
- Joenje, H. & Patel, K. J. The emerging genetic and molecular basis of Fanconi anaemia. *Nat. Rev. Genet.* **2**, 446–457 (2001).
- Larrieu, D., Britton, S., Demir, M., Rodriguez, R. & Jackson, S. P. Chemical inhibition of NAT10 corrects defects of laminopathic cells. *Science* **344**, 527–532 (2014).
- Balmus G. et al. Targeting of NAT10 enhances healthspan in a mouse model of human accelerated aging syndrome. *Nat. Commun.* **9**, 1700 (2018).
- Bouwman, P. et al. 53BP1 loss rescues BRCA1 deficiency and is associated with triple-negative and BRCA-mutated breast cancers. *Nat. Struct. Mol. Biol.* **17**, 688–695 (2010).
- Chen, R. et al. Analysis of 589,306 genomes identifies individuals resilient to severe Mendelian childhood diseases. *Nat. Biotechnol.* **34**, 531–538 (2016).
- Vieira, N. M. et al. Jagged 1 rescues the duchenne muscular dystrophy phenotype. *Cell* **163**, 1204–1213 (2015).
- Carette, J. E. et al. Haploid genetic screens in human cells identify host factors used by pathogens. *Science* **326**, 1231–1235 (2009).
- Carette, J. E. et al. Global gene disruption in human cells to assign genes to phenotypes by deep sequencing. *Nat. Biotechnol.* **29**, 542–546 (2011a).
- Carette, J. E. et al. Ebola virus entry requires the cholesterol transporter Niemann-Pick C1. *Nature* **477**, 340–343 (2011b).
- García-Higuera, I. I., Kuang, Y., Denham, J. & D’Andrea, A. D. The fanconi anemia proteins FANCA and FANCG stabilize each other and promote the nuclear accumulation of the Fanconi anemia complex. *Blood* **96**, 3224–3230 (2000).
- Blomen, V. A. et al. Gene essentiality and synthetic lethality in haploid human cells. *Science* **350**, 1092–1096 (2015).
- Menche, J. et al. Disease networks. Uncovering disease-disease relationships through the incomplete interactome. *Science* **347**, 1257601 (2015).
- Vanunu, O., Magger, O., Ruppini, E., Shlomi, T. & Sharan, R. Associating genes and protein complexes with disease via network propagation. *PLoS Comput. Biol.* **6**, e1000641 (2010).
- Blondel V. D., Guillaume J., Lambiotte R., Lefebvre E. Fast unfolding of communities in large networks. *J. Stat. Mech.* P10008 (2008).
- Moder, M. et al. Parallel genome-wide screens identify synthetic viable interactions between the BLM helicase complex and Fanconi anemia. *Nat. Commun.* **8**, 1238 (2017).
- Siegel, D., Yan, C. & Ross, D. NAD(P)H:quinone oxidoreductase 1 (NQO1) in the sensitivity and resistance to antitumor quinones. *Biochem. Pharmacol.* **83**, 1033–1040 (2012).
- Mikami, K. et al. DT-diaphorase as a critical determinant of sensitivity to mitomycin C in human colon and gastric carcinoma cell lines. *Cancer Res.* **56**, 2823–2826 (1996).
- Michl, J., Zimmer, J. & Tarsounas, M. Interplay between Fanconi anemia and homologous recombination pathways in genome integrity. *EMBO J.* **35**, 909–923 (2016).
- Moynahan, M. E., Chiu, J. W., Koller, B. H. & Jasin, M. Brca1 controls homology-directed DNA repair. *Mol. Cell* **4**, 511–518 (1999).
- Pathania, S. et al. BRCA1 haploinsufficiency for replication stress suppression in primary cells. *Nat. Commun.* **5**, 5496 (2014).
- Scully, R. et al. Association of BRCA1 with Rad51 in mitotic and meiotic cells. *Cell* **88**, 265–275 (1997).
- Certo, M. T. et al. Tracking genome engineering outcome at individual DNA breakpoints. *Nat. Methods* **8**, 671–676 (2011).
- Schmidt, C. K. et al. Systematic E2 screening reveals a UBE2D-RNF138-CtIP axis promoting DNA repair. *Nat. Cell Biol.* **17**, 1458–1470 (2015).
- Hashizume, R. et al. The RING heterodimer BRCA1-BARD1 is a ubiquitin ligase inactivated by a breast cancer-derived mutation. *J. Biol. Chem.* **276**, 14537–14540 (2001).
- Yu, X., Fu, S., Lai, M., Baer, R. & Chen, J. BRCA1 ubiquitinates its phosphorylation-dependent binding partner CtIP. *Genes Dev.* **20**, 1721–1726 (2006).
- Reid, L. J. et al. E3 ligase activity of BRCA1 is not essential for mammalian cell viability or homology-directed repair of double-strand DNA breaks. *Proc. Natl Acad. Sci. USA* **105**, 20876–20881 (2008).
- Inano, S. et al. RFW3-mediated ubiquitination promotes timely removal of both RPA and RAD51 from DNA damage sites to facilitate homologous recombination. *Mol. Cell* **66**, 622–634 (2017).
- Feeney, L. et al. RPA-mediated recruitment of the E3 ligase RFW3 is vital for interstrand crosslink repair and human health. *Mol. Cell* **66**, 610–621 (2017).
- Ji, X. et al. Chromatin proteomic profiling reveals novel proteins associated with histone-marked genomic regions. *Proc. Natl Acad. Sci. USA* **112**, 3841 (2015).
- Uckelmann, M. & Sixma, T. K. Histone ubiquitination in the DNA damage response. *DNA Repair. (Amst.)* **56**, 92–101 (2017).
- Mattiroli, F. et al. RNF168 ubiquitinates K13-15 on H2A/H2AX to drive DNA damage signaling. *Cell* **150**, 1182–1195 (2012).
- Uckelmann, M. et al. USP48 restrains resection by site-specific cleavage of the BRCA1 ubiquitin mark from H2A. *Nat. Commun.* **9**, 229 (2018).
- Wu, W., Koike, A., Takeshita, T. & Ohta, T. The ubiquitin E3 ligase activity of BRCA1 and its biological functions. *Cell Div.* **3**, 1 (2008).
- van Attikum, H. & Gasser, S. M. Crosstalk between histone modifications during the DNA damage response. *Trends Cell Biol.* **19**, 207–217 (2009).
- Yamamoto, K. N. et al. Involvement of SLX4 in interstrand cross-link repair is regulated by the Fanconi anemia pathway. *Proc. Natl Acad. Sci. USA* **108**, 6492–6496 (2011).
- Lachaud, C. et al. Distinct functional roles for the two SLX4 ubiquitin-binding UBZ domains mutated in Fanconi anemia. *J. Cell Sci.* **127**, 2811–2817 (2014).
- MacKay, C. et al. Identification of KIAA1018/FAN1, a DNA repair nuclease recruited to DNA damage by monoubiquitinated FANCD2. *Cell* **142**, 65–76 (2010).
- Smogorzewska, A. et al. A genetic screen identifies FAN1, a Fanconi anemia-associated nuclease necessary for DNA interstrand crosslink repair. *Mol. Cell* **39**, 36–47 (2010).
- Cetkovská, K., Sustová, H. & Uldrijan, S. Ubiquitin-specific peptidase 48 regulates Mdm2 protein levels independent of its deubiquitinase activity. *Sci. Rep.* **7**, 43180 (2017).
- Ceccaldi, R. et al. Bone marrow failure in Fanconi anemia is triggered by an exacerbated p53/p21 DNA damage response that impairs hematopoietic stem and progenitor cells. *Cell Stem Cell* **11**, 36–49 (2012).
- Luijsterburg, M. S. et al. PARP1 links CHD2-mediated chromatin expansion and H3.3 deposition to DNA repair by non-homologous end-joining. *Mol. Cell* **61**, 547–562 (2016).
- Forment, J. V. & Jackson, S. P. A flow cytometry-based method to simplify the analysis and quantification of protein association to chromatin in mammalian cells. *Nat. Protoc.* **10**, 1297–1307 (2015).
- Arunachalam, V. et al. A directed protein interaction network for investigating intracellular signal transduction. *Sci. Signal.* **4**, rs8 (2011).
- Chen J., Bardes E. E., Aronow B. J., Jegga A. G. ToppGene suite for gene list enrichment analysis and candidate gene prioritization. *Nucl. Acids Res.* **37**, W305–W311 (2009).
- Wang, J. et al. WebGestalt 2017: a more comprehensive, powerful, flexible and interactive gene set enrichment analysis toolkit. *Nucl. Acids Res.* **45**, W130–W137 (2017).

Acknowledgements

The Δ FANCD2 HAP1 cells were kindly provided by Prof Ketan J. Patel (LMB, Cambridge, UK). The shRNA constructs for BRCA1 were a kind gift from Prof Sebastian

ARTICLE

NATURE COMMUNICATIONS | DOI: 10.1038/s41467-018-04649-z

Nijman (Ludwig Cancer Research, Oxford, UK). The EGFP-BRCA1 construct was a kind gift from Prof. Jiri Lukas (Novo Nordisk Foundation Center for Protein Research, University of Copenhagen). Dr. Josephine Dorsman (VU Medical Center, Amsterdam) kindly provided VU1131 and complemented VU1131 cells. We thank Dr. Thijn Brummelkamp (NKI, The Netherlands) for providing protocols and the WT-HAP1 insertional mutagenesis data. Ms. Fiorella Schischlik and Dr. Michael Schuster assisted with the analysis of the NGS data. All NGS was performed by the Biomedical Sequencing Facility, CeMM, Austria. G.V. was a recipient of an EMBO Fellowship (ALTF 730-2014) and is supported by an FWF grant to J.L.L. (Project number: FWF29555). M.O. is supported by an FWF grant to J.L.L. (Project number: 29763). L.R.-G. is funded by a Boehringer Ingelheim Fonds Ph.D. fellowship. The Loizou lab was funded by a Marie Curie CIG to J.L.L. (Project number: 321602-NonCanATM). CeMM is funded by the Austrian Academy of Sciences. K.M.F. and S.B.R. were partially supported by the National Institutes of Health, Grant UL1TR001442 of CTSA. The lab of H.v.A. is funded by an ERC Consolidator grant. Research in the S.P.J. laboratory is funded by Cancer Research UK (program grant C6/A18796) and a Wellcome Trust Investigator Award 206388/Z/17/Z). Institute core infrastructure funding is provided by Cancer Research UK (C6946/A24843) and the Wellcome Trust (WT203144).

Author contributions

G.V. designed the experiments with help from L.R.G. G.V. and L.R.G. performed experiments, interpreted results, and prepared figures. G.V. wrote the manuscript with help from L.R.G. F.M.-M., and W.W.W. M.O. and M.M. performed experiments, analyzed data, and interpreted results. J.F.da.S. analyzed data. M.W. performed experiments. J.Mo. provided reagents. S.B.R., K.M.F., and J.M. analyzed data and contributed to writing the manuscript. H.v.A. and S.P.J. interpreted results and contributed to writing the manuscript. J.L.L. designed experiments, interpreted results, and wrote the manuscript.

Additional information

Supplementary Information accompanies this paper at <https://doi.org/10.1038/s41467-018-04649-z>.

Competing interests: The authors declare no competing interests.

Reprints and permission information is available online at <http://npg.nature.com/reprintsandpermissions/>

Publisher's note: Springer Nature remains neutral with regard to jurisdictional claims in published maps and institutional affiliations.



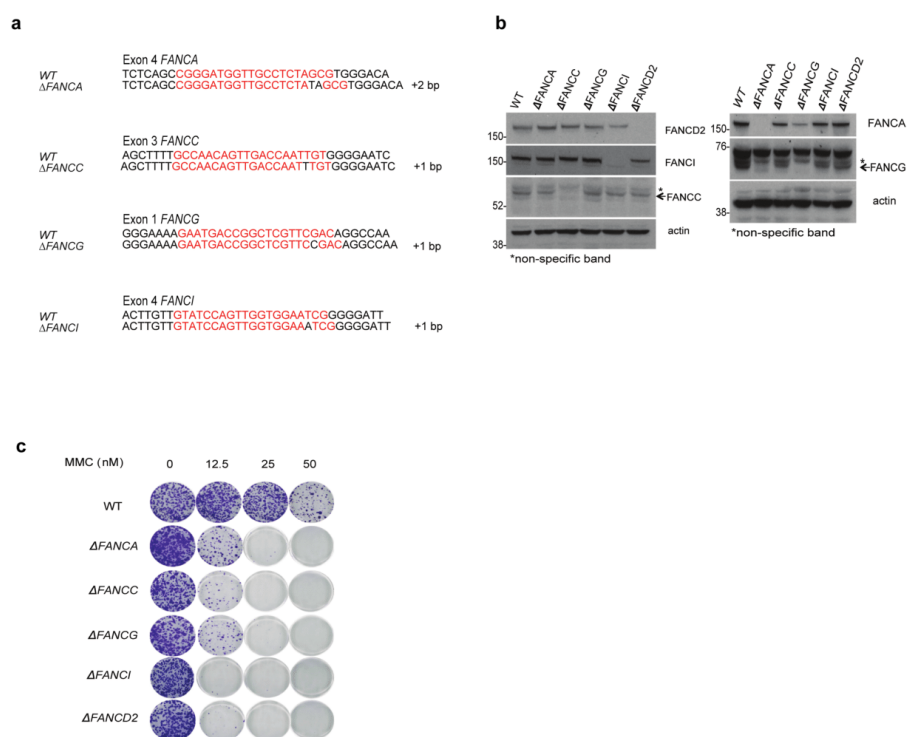
Open Access This article is licensed under a Creative Commons Attribution 4.0 International License, which permits use, sharing, adaptation, distribution and reproduction in any medium or format, as long as you give appropriate credit to the original author(s) and the source, provide a link to the Creative Commons license, and indicate if changes were made. The images or other third party material in this article are included in the article's Creative Commons license, unless indicated otherwise in a credit line to the material. If material is not included in the article's Creative Commons license and your intended use is not permitted by statutory regulation or exceeds the permitted use, you will need to obtain permission directly from the copyright holder. To view a copy of this license, visit <http://creativecommons.org/licenses/by/4.0/>.

© The Author(s) 2018

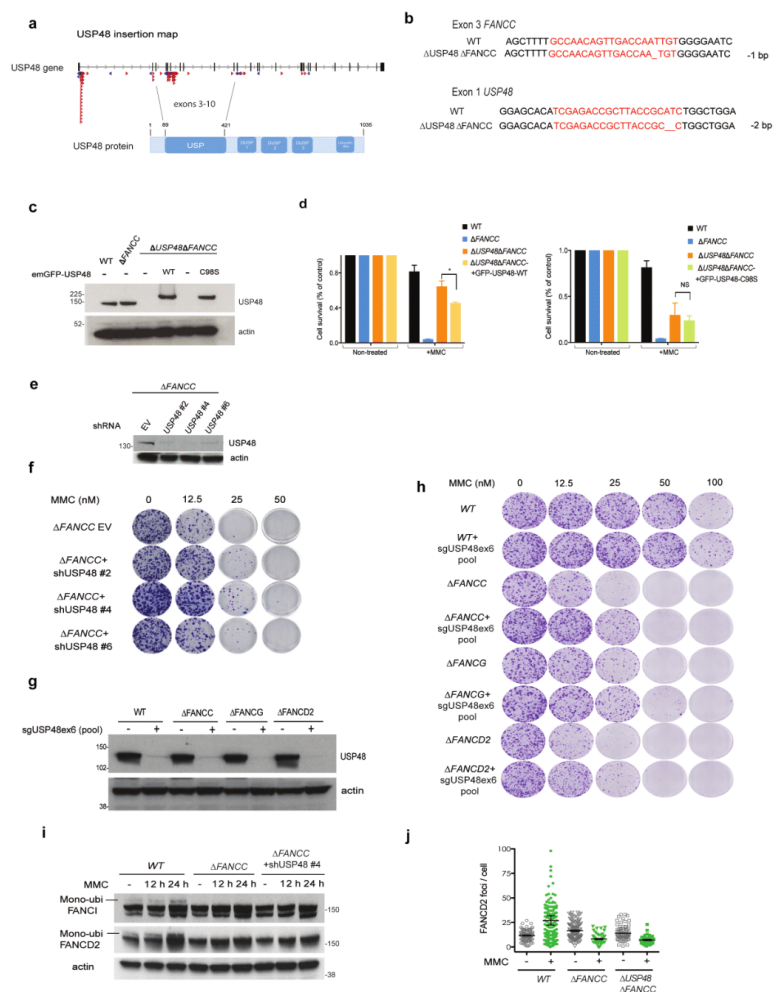
2.1. Supplementary Information

Antibody	Species	Company	Catalog number	Technique	Dilution
FANCC-8F3	Mouse	Merck-Millipore	MABC524	WB	1:250
FANCG	Rabbit	Novus	NB100-2566	WB	1:2000
FANCA	Rabbit	Bethyl	301-980A-T	WB	1:1000
FANCD2	Rabbit	Abcam	ab108928	WB	1:2000
FANCD2	Mouse	Santa Cruz Biotech	sc-20022	IF	1:100
FANCI	Rabbit	Bethyl Labs	A301-254	WB	1:1000
USP48	Rabbit	Bethyl Labs	A301-190	WB	1:4000
β -Actin	Rabbit	Sigma	A5060	WB	1:5000
BRCA1 D-9	Mouse	Santa Cruz Biotech	sc-6954	IF	1:500
RPA32	Mouse	Abcam	ab2175	WB / FACS	1:5000 / 1:500
Rad51	Rabbit	Santa Cruz Biotech	sc-8349	IF	1:100
GFP	Rabbit	ThermoFisher Scientific	A-6455	IF	1:800
GFP	Mouse	Roche Applied Science	11814460001	WB	1:1000
HA-tag	Mouse	Covant Research Products	MMS-101R	WB	1:500
Flag M2	Mouse	Sigma-Aldrich	F1804	WB	1:2000
FK2	Mouse	Enzo Life Sciences Ltd	BML-PW8810	WB	1:1000
γ H2AX S139 JBW301	Mouse	Merck-Millipore	05-636	IF	1:1000

Supplementary Table 1. Antibody list indicating Catalog number, technique and conditions used. WB: Western Blot assay, IF: immunofluorescence assay, FACS: Fluorescence-activated cell sorting assay.

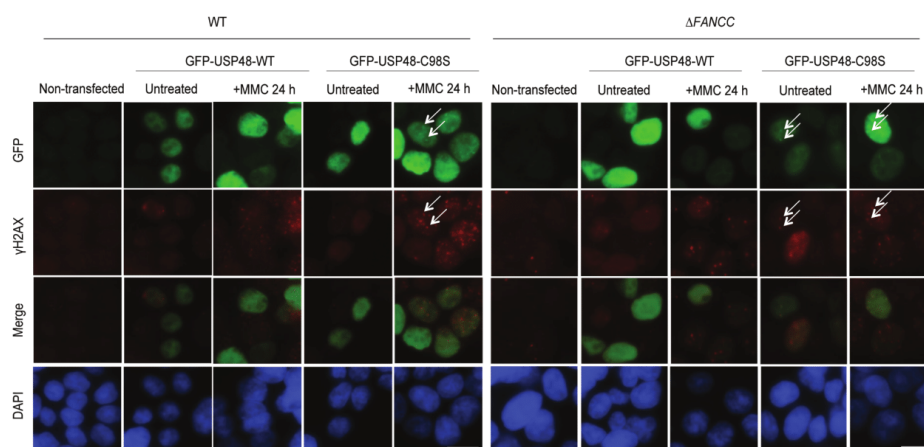


Supplementary Figure 1. CRISPR-Cas9 mediated generation of HAP1 FA-defective cells. (a) CRISPR-Cas9-mediated mutation of FA genes in HAP1 cells. Red sequences in wild-type (WT) correspond to the guide RNAs (gRNAs) used. (b) Immunoblot for FANCA, FANCC, FANCG, FANCI, FANCD2 and actin. Asterisk (*) denotes non-specific band. (c) Colony formation of the FA-defective HAP1 cell lines 7 days after treatment with MMC at the indicated doses.

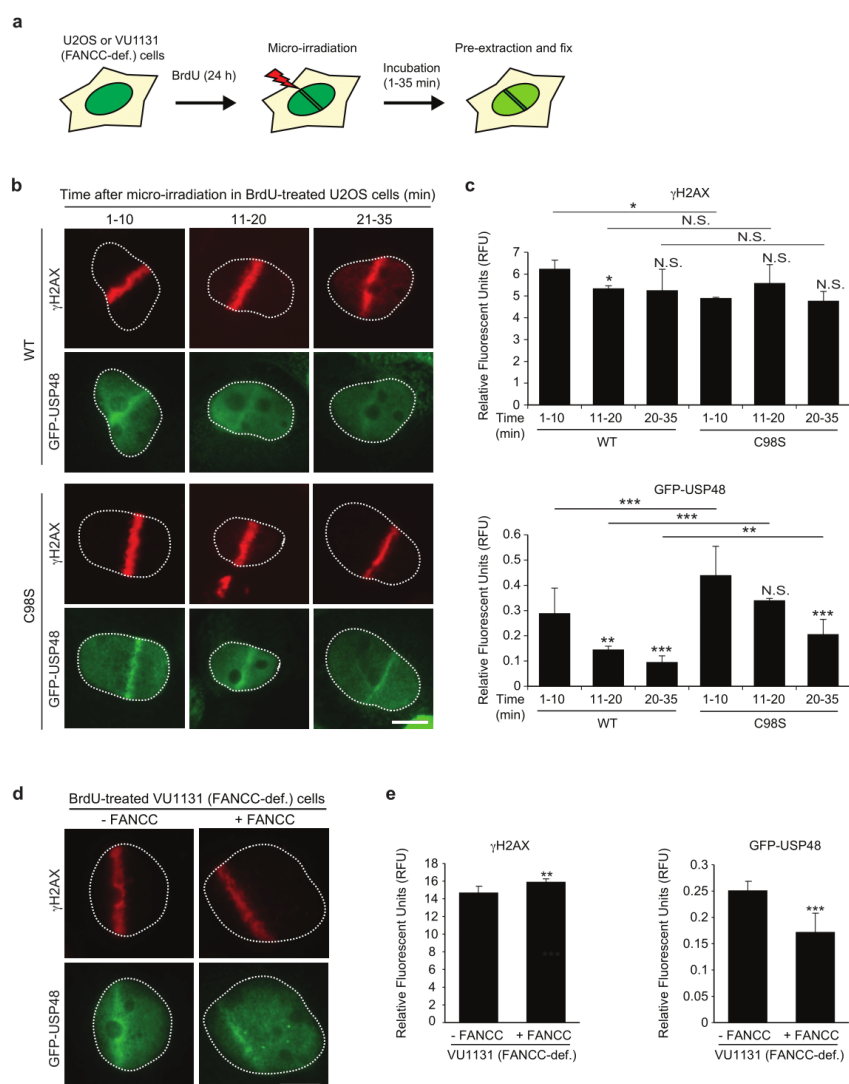


Supplementary Figure 2. Validation of suppression interaction between FA and USP48. (a) Gene-trap insertions within the *USP48* gene enriched in Δ FANCC cells treated with MMC. Red arrows indicate mutagenic insertions in the sense orientation while blue arrows indicate insertions in the antisense orientation (inactivating only in exonic regions). Schematic representation of the USP48 protein shows that the exonic region of exons 3 to 10 corresponds to the USP catalytic domain of the protein (source: Uniprot, Q86UV5 (UBP48_HUMAN)). (b) CRISPR-Cas9-mediated mutation of FANCC and *USP48* in HAP1 cells. Red sequences in wild-type (WT) correspond to the gRNAs. Δ *USP48* cells were purchased from Horizon Genomics. (c) Immunoblot for USP48 and actin. Higher band on the USP48 blot corresponds to the fused protein emGFP-USP48 WT/C98S. (d) Quantification of

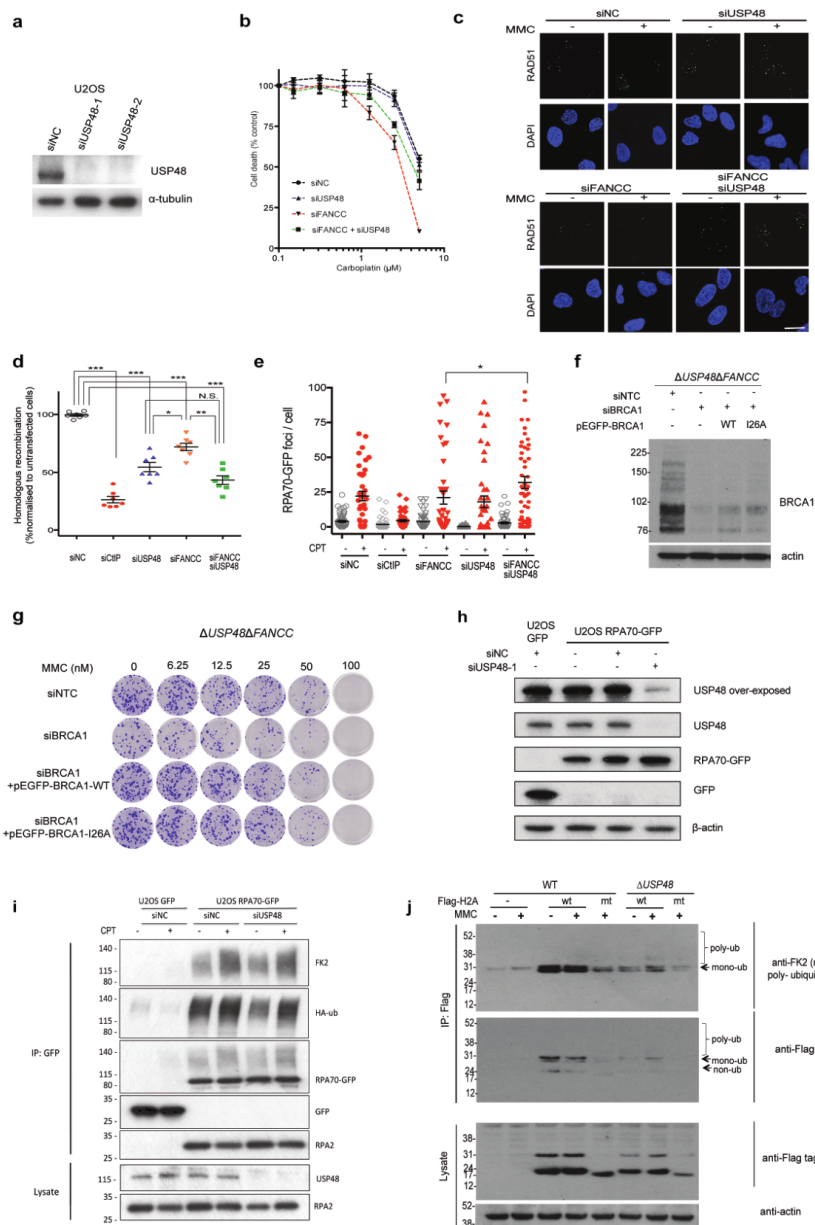
viability of cells with reconstituted USP48 WT or USP48 catalytic inactive (C98S mutant), after treatment with MMC (25nM) for 6 days. Statistical significance was determined using a multiple t-test with $p < 0.05$ as a threshold. $*=p < 0.05$. Error bars indicate SD (standard deviation) of two replicates (e) Immunoblot for USP48 and actin. (f) Colony formation of $\Delta FANCC$ cells with or without *USP48* knockdown by shRNA 7 days after treatment with MMC at the indicated doses. (g) Immunoblot for USP48 and actin in FA deficient cells: $\Delta FANCC$, $\Delta FANCG$ and $\Delta FANCD2$. (h) Colony formation of $\Delta FANCC$, $\Delta FANCG$ and $\Delta FANCD2$ cells with or without sgUSP48ex6 and CRISPR-Cas9 expression 7 days after treatment with MMC at the indicated doses. Sg=Single-guide RNA. (i) Immunoblot for FANCD2, FANCI and actin. Upper band corresponds to mono-ubiquitylated form of FANCD2 or FANCI. (j) Quantification of FANCD2 foci for the indicated cell lines was performed following MMC treatment (50nM) for 5 hours, similarly to the Rad51 foci quantification described in materials and methods.



Supplementary Figure 3. GFP-USP48 is localized in the nucleus. Immunofluorescence images depicting the nuclear localization of GFP-USP48 WT and GFP-USP48-C98S after transfection in WT and Δ FANCC cells and the induction of γ H2AX foci before and after MMC treatment (30nM) for 24 hours. Arrows indicate the colocalisation of GFP-USP48-C98S into foci with γ H2AX. Scale bar=10 μ m.



Supplementary Figure 4. USP48 is recruited to sites of DNA damage. (a) Workflow for the induction of DNA breaks and immunofluorescence in U2OS and VU1131 cells. (b-c) Images (b) and quantification (c) of γ H2AX and GFP-tagged USP48 (WT and C98S mutant) localization to sites of laser micro-irradiation after BrdU sensitization in U2OS. N.S.=not significant; *= p <0.05; **= p <0.01; ***= p <0.001 (d-e) Images (d) and quantification (e) of γ H2AX and GFP-tagged USP48 (WT and C98S mutant) localization to sites of laser micro-irradiation after BrdU sensitization in FANCC-deficient (VU1131) cells and FANCC-proficient (FANCC-complemented VU1131) cells. N.S.=not significant; **= p <0.01; ***= p <0.001. Scale bar=10 μ m.



Supplementary Figure 5. Role of USP48 in the DNA damage response. Knockdown efficiency (a) and evaluation of sensitivity (b) of siNC (negative control), siUSP48, siFANCC and siUSP48siFANCC U2OS cells following Carboplatin exposure at the different doses. (c) Representative

immunofluorescence images after staining for RAD51 on WT, *siUSP48*, *siFANCC* and *siUSP48siFANCC* U2OS cells treated with MMC (100nM) for 18 hours. Scale bar=10 μ m (d) Quantification of HR repair after DSB induction with IScE-I enzyme, using the Traffic Light Reporter System developed in U2OS cells. N.S.=not significant; *= p <0.05; **= p <0.01; ***= p <0.001. (e) Quantification of RPA70-GFP foci for the indicated cell lines after treatment with Camptothecin (CPT; 1 μ M) for 1h by the FACS-based RPA chromatinization assay as described in materials and methods. *= p <0.05. (f) Immunoblot for BRCA1 and actin. (g) Colony formation assay of Δ USP48 Δ FANCC cells with siRNA BRCA1 mediated knockdown and reconstitution of BRCA1 WT and BRCA1 ubiquitin ligase mutant (I26A) 7 days after treatment with MMC at the indicated doses. (h) Anti-GFP immunoprecipitation probed against USP48, RPA70-GFP, GFP and actin to determine knock-down efficiency. (i) anti-GFP immunoprecipitation blot probed against FK2, HA-ub, RPA70-GFP, GFP and RPA2; lysate blotted against USP48 and RPA2. (j) Anti-Flag H2A immunoprecipitation probed against FK2, Flag and actin for the indicated cell lines. Lower bands correspond to mono-ubiquitination modifications and higher bands correspond to poly-ubiquitin chains. Cells were transfected with wt=wild-type and mt=mutant (K5-9-118-119-125-127-129R) H2A and then treated with MMC (50nM) for 4 hours.

CHAPTER 3: DISCUSSION

1. HAP1 as an ideal tool for genetic screens

To identify synthetic rescue interactions, we chose the HAP1 cell line since it is an ideal tool for genetic screens. The near-haploid karyotype of HAP1 enables the efficient deletion of a gene by knocking out just one allele (Kotecki *et al*, 1999; Carette *et al*, 2009).

In order to employ the HAP1 cell line as a genetic tool, we must understand which intrinsic mutations the parental cell has. HAP1 cells have been found to carry the BCR-ABL fusion the same way as KBM7 cells. However, their proliferation does not depend on this mutation (Owusu *et al*, 2019). In addition, a point mutation has been identified in the *TP53* gene (Essletzbichler *et al*, 2014). Due to the fact that p53 has been shown to be involved in the induction of cell death in FA cells, we would have expected it to be one of the top candidates in our gene-trap screens. However, this was not the case, which indicates that p53 is not fully functional in these cells. Further studies on p53 functionality were previously reported in the Loizou laboratory and have confirmed this hypothesis (Moder *et al*, 2017). However, to rule out any contributions from p53 activity, we have validated our findings in the osteosarcoma cell line U2OS, which is known to be p53 WT (Allan & Fried, 1999). Therefore, we have successfully advanced our studies by making use of this cell line and the technology aforementioned.

2. How does USP48 function in the FA pathway?

USP48 was first identified in 2004 as a gene residing in the PARK6 locus and identified as related to the autosomal recessive Parkinson disease (Lockhart *et al*, 2004). Since then, high-throughput approaches have been performed to further understand the role of DUBs but very little has been discovered on the function of USP48 and its interactors (Sowa *et al*, 2009). USP48, also termed USP31, is ubiquitously expressed in the different organs of the human body (The Human Protein Atlas). USP48 has been found to be present in cytoplasm as well as the nucleus and it has recently been determined that the ⁹³⁸RHRK⁹⁴¹ domain allows for nuclear localization signal of USP48 (Liu *et al*, 2018). However, of the 8 different isoforms described in Uniprot, this domain remains unaltered in only 2 of them.

To date, we have determined that USP48 is involved in ICL repair although its role only appears to become relevant after the depletion of the FA pathway. We have preliminary data indicating that the catalytic site of USP48 does play a role in alleviating the hypersensitivity of FA-deficient cells to ICLs, since recruitment of the DUB to damage sites is enhanced in

cells expressing the C98S point mutation (catalytic site) (**Manuscript: Figure 4a-b**). To support this finding, we decided to generate endogenous point mutants in the FA-deficient HAP1 cells (**Figure 9**). Although we successfully reproduced the rescue phenotype in the point mutant cells, the rescue was not as strong as in fully *USP48*-deleted cells. This suggests that other regions of the protein might also be involved. It has previously been reported that the catalytic domain of *USP48* is also important for substrate binding (Ghanem *et al*, 2019).

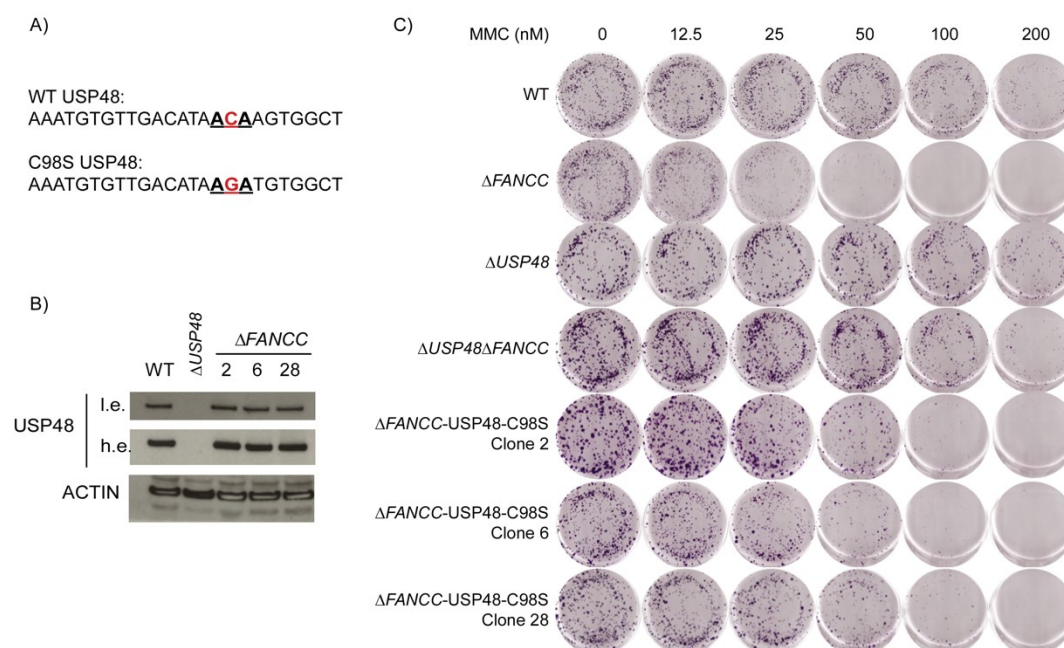


Figure 9. USP48 catalytic dead clones in FA-deficient cells rescues MMC-induced sensitivity. A) Indicates the nucleotide change performed in order to generate endogenous catalytic dead USP48. B) Western Blot assay showing that USP48 expression is not altered upon point mutation generation in three independent clones: 2, 6 and 28. i.e.: low exposure, h.e.: high exposure C) Clonogenics assay of three independent USP48 catalytic dead clones in FA-deficient cells after treatment with MMC, at the indicated doses, for 7 days.

In order to understand the molecular basis of the interaction between USP48 and the FA pathways we need to review what is so far known about this DUB.

2.1. The role of USP48 in the NF- κ B pathway

Thus far, the most notable function associated with USP48 is its relationship with the NF- κ B pathway. The NF- κ B transcription factor consists of a family of 6 subunits: RELA, RELB, cREL, p105/p50 and p100/p52; these can form different types of complexes (hetero or homo-dimeric) in order to activate or repress transcription (Ghanem *et al*, 2019). This family has an important role in a wide range of cellular responses, such as immunity, inflammation, cell differentiation and proliferation. A set of proteins known as κ B inhibitors ($I\kappa$ Bs) are

responsible for regulating this pathway by binding to the NF- κ B complexes and blocking their function (Schweitzer & Naumann, 2015; Ghanem *et al*, 2019; Tzimas *et al*, 2006). Once this pathway has been activated, shutting it down is tightly regulated by different mechanisms: (1) *de novo* synthesis of I κ Bs stabilized in the nucleus by DUBs that reduce the pool of Ub-proteasomal marks, (2) disruption of the DNA binding via PTMs (acetylation/deacetylation) and (3) ubiquitylation of RELA for proteasomal degradation. USP48 has been shown to regulate the stability of RELA by trimming K48-Ub modifications (Schweitzer & Naumann, 2015). This nuclear regulation of the NF- κ B pathway is an active area of research since it provides another level of control within the nucleus that directly affects transcription.

The aforementioned connection between USP48 and the NF- κ B has been determined when cells are stimulated by an inflammatory cytokine, TNF- α . However, it is not yet known if this connection also holds true after DNA damage. Depending on the type of DNA damage, the NF- κ B pathway is activated by different routes. It has been shown that after DNA damage, ATM plays a major role in the activation of the NF- κ B pathway by phosphorylating different IKK components. This interaction has mainly been studied on the induction of DSBs or SSBs, but not specifically after treatment with ICL-inducing agents. It is well known that NF- κ B has a very important role in apoptosis, more specifically the RELA subunit which has antiapoptotic functions. Dysregulation of RELA gives way to the expression of antiapoptotic genes resulting in cell transformation and cancer. We hypothesized that USP48 might function via the NF- κ B pathway in this context and would activate antiapoptotic pathways. To assess this, we checked for nuclear translocation of RELA in cells deleted for both *USP48* and *FANCC* (**Figure 10B**). However, we observed no induction of the translocation indicating that the role of USP48 in the NF- κ B pathway is not involved in this rescue phenotype.

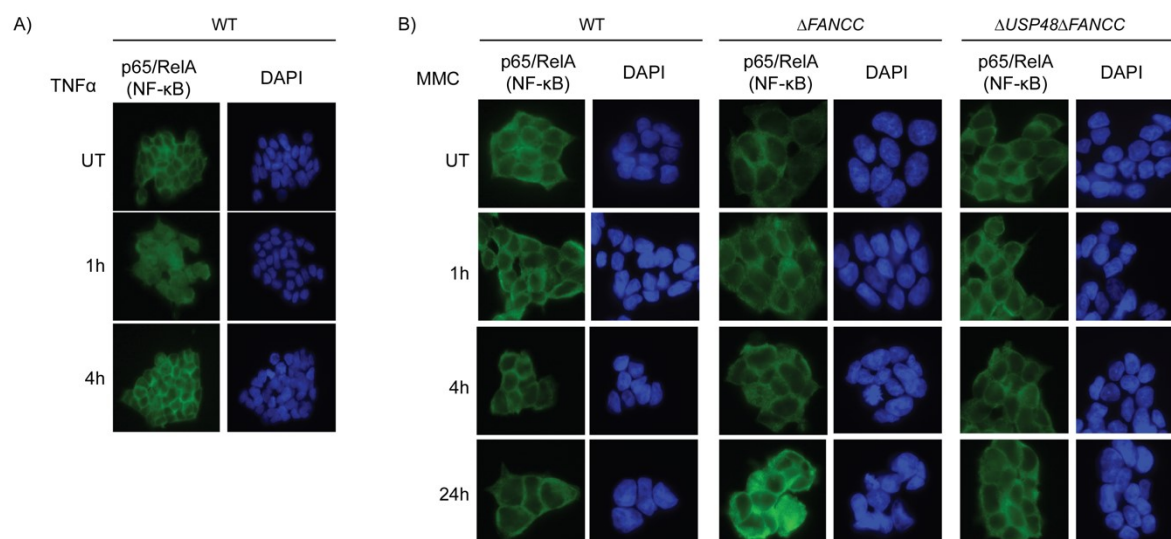


Figure 10. USP48 does not promote p65/RELA nuclear translocation after MMC treatment. A) Immunofluorescence images after staining for p65/RELA and DAPI for WT HAP1 cells treated with TNF α (20ng/mL) at different timepoints, showing p65/RELA nuclear localization. B) Immunofluorescence images after staining for p65/RELA and DAPI in the following HAP1 cell lines: WT, Δ FANCC and Δ USP48 Δ FANCC after treatment with MMC at different timepoints (experiment performed by Georgia Velimezi, Loizou lab). DAPI: 4',6-diamidino-2-phenylindole.

2.2. The role of USP48 in p53 regulation

The p53 pathway, like the NF- κ B pathway, has a major role in the induction of cell cycle arrest and apoptosis in cells that are suffering from stress. Mutations in the *TP53* gene appear in at least 50% of all cancers and are regarded as one of the main tumor suppressor/oncogenic genes to cause cell transformation and tumor development (Cole *et al*, 2017; Kasthuber & Lowe, 2017). p53 functions as a sequence specific transcriptional regulator of a great number of genes. Activation or repression of these genes is dependent on the protein levels of p53 which will be very tightly regulated by a variety of modulators.

The best-characterized negative modulator of p53 is an E3 ubiquitin ligase named MDM2. MDM2 controls the protein levels of p53 via three different pathways: (1) adding poly-ubiquitin marks for proteasomal degradation, (2) adding a mono-ubiquitin mark signaling for nuclear export of p53, and (3) blocking p53 transcription by direct binding (Wu & Prives, 2018). Interestingly, recent studies have associated USP48 as a regulator of MDM2, promoting its stabilization and allowing for p53 inhibition (Cetkovská *et al*, 2017). By doing so, loss of USP48 could promote extensive cell death upon stress. However, in our studies we have not observed any increase in cell death, as depicted in the clonogenic assays where WT and Δ USP48 cells show similar confluency (**Manuscript: Figure 3b-d**). In

addition, we have also determined that loss of *USP48* in FA-deficient cells restores the DDR by reducing the levels of phosphorylated H2A.X (γ H2A.X), a well described mark for unrepaired damage, and promoting the recruitment of HR repair proteins, such as BRCA1 and RAD51 (**Manuscript: Figure 4c-d and Figure 5a**). Nevertheless, to completely exclude the possibility that USP48 is acting via MDM2 stabilization it would be necessary to perform specific assays to assess for cell death, i.e. to determine the levels of DNA damage induced by apoptosis by employing Terminal Deoxynucleotidyl Transferase dUTP Nick End Labeling (TUNEL) in Fluorescence activated cell sorting (FACS).

2.3. The role of USP48 in chromatin regulation

Thus far, the roles of USP48 in regulating RELA within the NF- κ B and stabilizing MDM2, highlight the importance of the activity of USP48 inside the nuclear compartment. Previous reports have also shown that USP48 might interact with histone marks associated with repression of gene transcription (Ji *et al*, 2015). Taking this together, and the fact that depletion of *BRCA1* in the Δ *USP48* Δ *FANCC* cells could restore their sensitivity (**Manuscript: Figure 6a-b**), we decided to investigate the role of USP48 on chromatin; more specifically, we focused on changes on histone H2A.

H2A and its variant H2A.X are known to undergo a variety of PTMs to enable correct signaling of the DDR. As previously mentioned, phosphorylation on lysine 139 of H2A.X by either ATM or ATR, depending on the type of lesions, will signal the recruitment of repair proteins (Rogakou *et al*, 1998; Ward & Chen, 2001). In addition, H2A can be ubiquitylated by three different ubiquitin ligases: RNF168 (lysines: K13-15), RING1B in the polycomb repressive complex 1 (PRC1) (lysine: K119) and BRCA1-BARD1 (lysines: K125-127). Each modification has a specific function within the DDR: for example, K13-15 modified by RNF168 promote DSB repair by NHEJ; K119-Ub is known to induce transcription silencing to avoid transcription of unrepaired genes; and BRCA1-BARD1 modification has been proposed to promote DSB repair by HR (Uckelmann & Sixma, 2017). In our experiments we determined that loss of *USP48* in FA-deficient cells increases the levels of ubiquitin on H2A (**Manuscript: Figure 6c**). As a negative control, we used a construct which had the following lysine residues mutated on H2A: K5-9-118-119-125-127-129R. Mutation of these residues, but not K13-15, showed significant reduction of the ubiquitin levels of H2A suggesting that the lysines targeted by either BRCA1-BARD1 or RING1B must be the target of USP48. To follow up on this finding, we performed chromatin immune precipitation (ChIP) of USP48. We aimed to determine if any region of the genome would show specific binding

to USP48 after treatment with MMC; however, we were not able to identify any gene to be bound to USP48 (**Figure 11**).

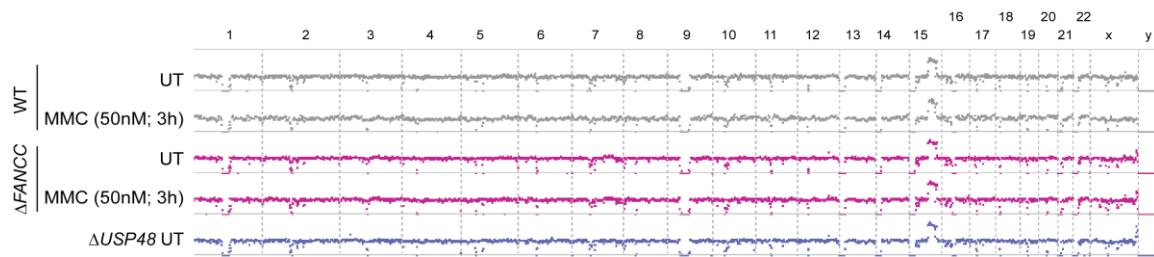


Figure 11. USP48 does not bind specifically to any region of the chromatin. Whole genome tracks retrieved after chromatin sonication and incubation with antibody against USP48 in the following HAP1 genetic backgrounds: WT, Δ FANCC and Δ USP48. The cells were treated with MMC (50nM) for 3h.

This outcome could be explained in a number of ways:

A) USP48 does not directly bind to chromatin

Possibly, USP48 does not directly interact with H2A or any other region of the DNA. However, it could interact with other proteins which, due to proteasomal degradation or loss of stability after deletion of *USP48*, cannot reduce the levels of ubiquitin of H2A. These degradation/signaling networks do exist in the context of the DDR and have as their main player a DUB. One example is USP7, which has been implicated in the de-ubiquitylation of several DNA repair proteins: RNF168, MDM2/p53 and UHRF1 (Zhu *et al*, 2015; Zhang *et al*, 2015; Sheng *et al*, 2006).

B) The experimental set-up is not ideal

As we demonstrated in the paper, USP48-WT constructs were recruited to the laser-induced ICLs at much lower levels than USP48-C98S constructs. Exclusively targeting WT USP48 may prevent us from observing the specific binding of the DUB due to the high speed at which the activity takes place. Also, we harvested the samples after 3h treatment with MMC but this timepoint might need to be optimized to gain better insight. Additionally, the ChIP assay has been performed by targeting endogenous USP48 with an antibody that binds the amino acids in the C-terminal of the protein. Even though we used Δ USP48 as a negative control, the antibody may not be sufficiently specific and, therefore, might introduce a high background that does not allow us to observe specific binding. To avoid this, it would be ideal to endogenously tag USP48.

Since this approach did not reveal any relevant information, we then decided to look in the literature for tools to determine which lysine is specifically targeted by USP48. On the one hand, we asked if the ligase activity of BRCA1 was involved. As we have shown in our

manuscript, loss of BRCA1 re-sensitizes the cells, although this is independent of its ligase activity (**Manuscript: Figure 6a-b, Supp. Figure 5g**). On the other hand, we identified a well-known antibody targeting ubiquitylated K119 in H2A. Strikingly, we observed that a second band appeared on H2A-K119 in all backgrounds deleted for *USP48* (**Figure 12**). To date, it has not been reported that K119 can be poly-ubiquitylated. Nevertheless, this does agree with previous reports that indicate that USP48 has a preference towards trimming poly-ubiquitylated substrates (Tzimas *et al*, 2006; Uckelmann *et al*, 2018). We did not observe differences in the ubiquitin levels of untreated samples, suggesting that this mark might not be related to the rescue phenotype and/or might have an additional function in transcription. It is important to note that the study of H2A ubiquitylation is extremely complicated, since there is a relatively high background of histone ubiquitylation, estimated at around 10-15% of all H2A.

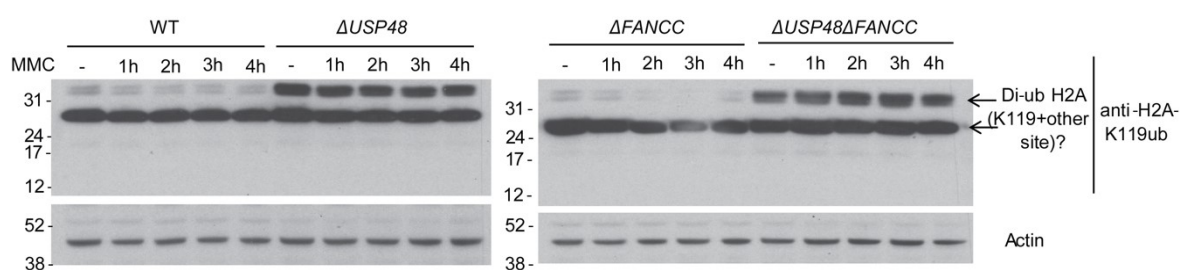


Figure 12. Loss of USP48 uncovers a novel ubiquitin moiety on H2A. Western Blot for ubiquitylated lysine 119 on H2A for the following genetic backgrounds: WT, Δ FANCC, Δ USP48 and Δ USP48 Δ FANCC, after treatment with MMC (50nM) at the indicated timepoints.

2.4. At which step in the FA pathway does USP48 exert its function?

In addition to identifying the substrate of USP48, it is of great importance to determine at which step in the repair pathway it functions. Due to the fact that depletion of USP48 could rescue all 5 FA backgrounds and, concomitantly, does not restore FANCI and FANCD2 mono-ubiquitylation (**Manuscript: Supp. Figure 2i**), one hypothesis would be that it functions downstream of the FA genes. Mono-ubiquitylation of the ID complex is vital for progression of the FA pathway, although despite the absence of this mark, error-free repair is still taking place. This could be due to the appearance of a novel ubiquitin mark upon loss of USP48. This new ubiquitin mark could be essential for the binding of downstream nucleases such as FAN1 that, as mentioned before, uses a UBZ domain to bind to Ub-FANCD2 and exert its function. In order to address this question, we took the approach of depleting *FAN1* using shRNA in all genetic backgrounds: WT, Δ USP48, Δ FANCC and Δ USP48 Δ FANCC. We assumed that, if the rescue interaction depended on restoration of

FAN1 recruitment, we would identify a sensitization of $\Delta USP48\Delta FANCC$ cells. Strikingly, we were not able to reduce the expression levels of FAN1 in *USP48*-deficient cells, showing defects in cell proliferation (**Figure 13**). This finding reveals a synthetic lethal interaction between FAN1 and USP48, suggesting that FAN1 nuclease activity plays a major role in dealing with replication stress and endogenous damage when USP48 is absent. It would be important to further study the activity of FAN1 after MMC treatment, i.e. to determine if it is recruited to foci in $\Delta USP48\Delta FANCC$, assess the sensitivity of $\Delta USP48\Delta FANCC$, by using siRNA or the degradation tag (dTAG) system targeting FAN1, after MMC treatment. The dTAG system allows for fast degradation of a specific (essential) gene by using an all-chemical solution (Nabet *et al*, 2018). Additionally, it would be necessary to determine if this interaction can be reproduced when depleting other nucleases, thus determining if this effect is specific to FAN1.

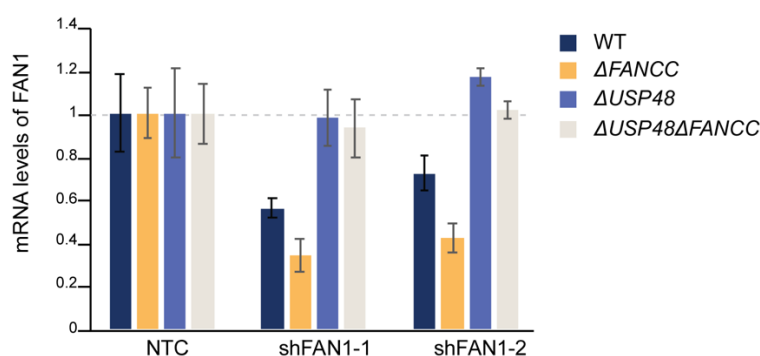


Figure 13. FAN1 depletion is not possible in a *USP48*-deficient background. Expression of *FAN1* after shRNA knock-down measured by quantitative reverse transcription PCR (qRT-PCR) in the following genetic backgrounds: WT, $\Delta FANCC$, $\Delta USP48$ and $\Delta USP48\Delta FANCC$; compared to cells infected with a Non-Targeting control (NTC) (experiment performed by Amandine Moretton, Loizou lab).

Based on the CRISPR screens performed in Wang *et al*, 2019, where they performed whole-genome loss-of-function screens in combination with ATR inhibition, using a small molecule inhibitor known as AZD6738, USP48 was identified as synthetic lethal with ATR in the Human Embryonic Kidney 293 cell line (HEK293). This prompted us to assess the role of ATR in $\Delta USP48$ HAP1 cells, where we were able to confirm synthetic lethality between ATR and USP48 (**Figure 14A**). we next assessed whether these cells displayed aberrant cell cycle regulation due to defects in ATR activity. ATR has a role in protecting cells from replication stress and allowing for correct cell cycle progression, replication and DNA repair. In order to allow for correct repair, ATR is activated during the S phase to regulate the firing of replication origins and the repair of stalled replication forks to maintain faithful DNA replication. If *USP48* loss affects ATR activity, we would observe increase proliferation rates

in basal conditions compared to WT cells, this would lead to alterations in cell cycle progression. We therefore addressed these two points and we observed that neither the proliferation rates of $\Delta USP48$ nor the cell cycle profile showed any differences compared to WT cells (**Figure 14B-C**). Based on this, the synthetic lethal interaction must rise from a common pathway in which both ATR and USP48 are involved. It is not yet clear if this interaction is relevant for the repair of ICLs, and hence additional experiments need to be undertaken to understand if, after ICL-induced damage, the observed phenotype is exacerbated or not. This result would infer in the joint role of USP48 and ATR in ICL repair.

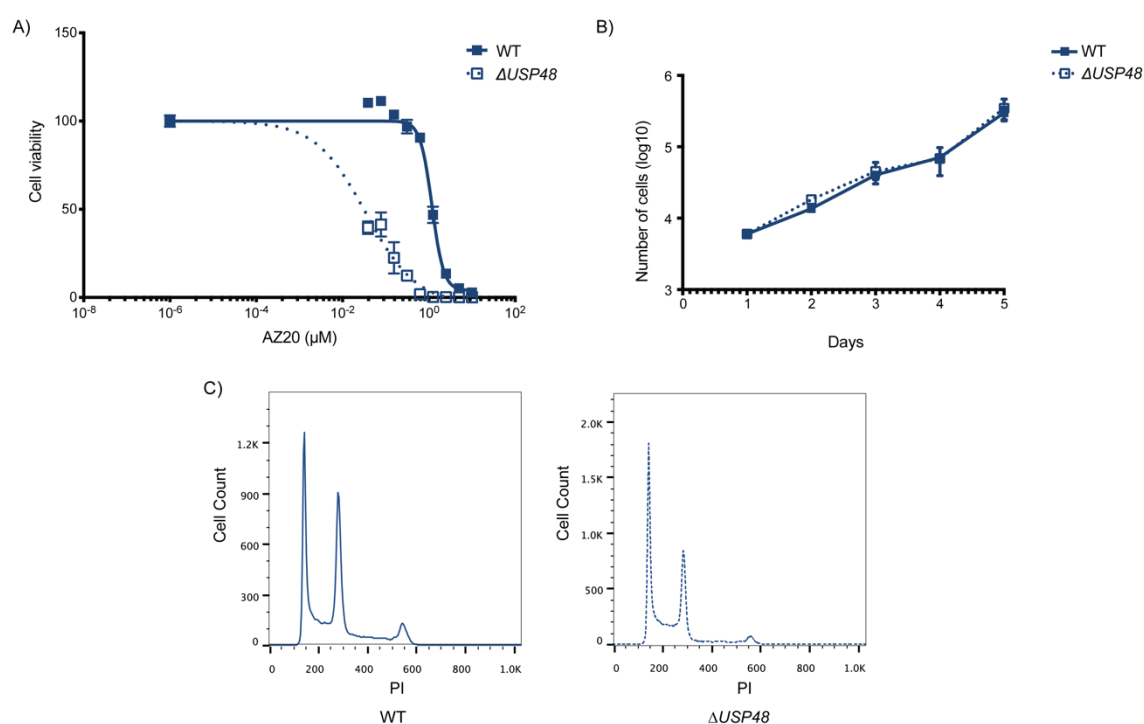


Figure 14. *USP48*-deficient cells do not have a de-regulation in cell cycle progression but are sensitive to ATR inhibition. A) Dose-response of *USP48*-deficient cells after exposure to AZ20 (ATR inhibitor). Cells were treated for 3 days and their viability was measured with Cell Titer Glo[®]. Error bars show S.E.M. (standard error of the mean) of 3 replicates B) Proliferation curve showing the growth rate of WT versus *USP48*-deficient cells in basal conditions. Error bars show S.D. (standard deviation) of 3 replicates. C) Cell cycle profile assay after staining with PI WT and *USP48*-deficient cells in basal conditions. PI: Propidium Iodide.

3. Consequences of the discovery of USP48

3.1. In the context of the FA pathway

Novel players in the FA pathway have been identified at an exponential rate in the past two decades thanks to the development and advancement of new technologies such as NGS. However, their exact role and how they are regulated following ICL generation remain still a mystery. The main reason for this lies in the complex network of interactions between the different repair pathways that constitute the FA pathway. Consequently, we have generated a map of synthetic rescue interactions. With this information we aim to extend the current knowledge of the FA pathway.

The identification of USP48 as a genetic suppressor of FA-deficient cells adds a new component to the ICL repair pathway. Interestingly, we have been able to place USP48 downstream of the Core Complex and the ID Complex, since it is able to rescue the sensitivity of cells deficient in members of both complexes. Furthermore, we have determined that USP48 is connected to other members of the FA pathway such as: H2A (as a possible substrate), FAN1 (as a possible binder of Ub) and ATR (as a signaling interactor). However, this information is not yet enough to understand the role of this DUB. We have suggested that USP48 may play a role in NHEJ, since we have observed that the mutant version of this DUB co-localizes with BRCA1 after MMC exposure (**Manuscript: Figure 5c**). The appearance of this pattern has been previously reported in relation to BRCA1 and 53BP1, when both proteins are competing for the repair of a DSB (Densham *et al*, 2016). This suggests that USP48 has a more predominant role in ICL repair when FA proteins are absent. Resulting in error-prone repair and giving way to an increase in genome instability and cell death. Furthermore, it has been reported elsewhere that USP48 restrains HR by blocking DNA end resection after DSBs (Uckelmann *et al*, 2018). However, we have not observed significantly increased resection after exposure to ICL-inducing agents (**Manuscript: Supp. Figure 5e**). Thus, the role of USP48 within the NHEJ pathway might differ depending on the type of lesions occurring in the DNA. With the accumulating evidence connecting USP48 to chromatin and the exciting finding of another Ub moiety on H2A-K119, we have also hypothesized a role for USP48 in transcription activation after ICL generation and repair. USP48 has been found to bind to histone marks which are important in the activation of gene transcription (Ji *et al*, 2015). The loss of FA proteins could result in the transcription of genes that have not been correctly repaired, inducing genome instability. Concomitant loss of USP48 could, in turn, block the activation of transcription safe-guarding the genome.

These results offer a starting point for further understanding the role of this poorly described DUB. Moreover, we have uncovered a novel player in ICL repair and increased the basic mechanistic knowledge of the FA pathway.

3.2. In the context of FA disease

FA patients are mainly subjected to supportive care as a consequence of the lack of curative treatment. In this project, we aimed to identify suitable potential targets, amenable to inhibition, which would correct for FA deficiency. That said, prioritizing USP48 was based on the importance of ubiquitin modifications in regulating the FA pathway and the fact that USP48 is an enzyme with a conserved catalytic site that is ideal for drug targeting. However, it has been previously reported that USP48 has a role in regulating Gli1 stability in glioblastoma (Zhou *et al*, 2017). Gli1 belongs to the Hedgehog pathway, which is important for the proliferation and development of embryonic stem (ES) cells. The possibility that USP48 might also have a role in a healthy state, would indicate that it is essential for ES cell development. In fact, no known *Usp48* knock-out mice have been described (according to the Mouse Genome Informatics database). Only heterozygous mice of 50 days of age have been generated by the Knockout Mouse Project (KOMP), showing efficient reduction of *Usp48* levels in the spinal cord and brain tissues. Additionally, our collaborators (Ahringer lab, The Gurdon Institute, UK) have observed that *usp48* loss in *C. elegans* induces sterility (data not shown). Consequently, one might think that targeting a gene with a role in development is not ideal for the treatment of FA patients. However, as an example, *Gli1*-deficient mouse are viable in adulthood with no apparent phenotype (Park *et al*, 2000; Bai *et al*, 2002) and *GLI1* deletion in cellular models is also viable (Horizon Discovery). Additionally, it is known that the HH pathway becomes quiescent during adulthood, being mainly active, at low levels, for the maintenance of progenitor cells in the brain. Considering this, USP48 could be targeted locally (in the bone marrow) in individuals after embryonic development.

Targeting DUBs has increasingly become more attractive although developing drugs to target them is challenging. The first obstacle is the conserved catalytic domain within each family which complicates the production of small molecules with high selectivity. Additionally, the enzymatic activity of DUBs is also regulated through allosteric regulators and can be more selective through the binding of ubiquitin chains (Harrigan *et al*, 2018). Thus far, small molecules have been developed to target 8 DUBs, all at a pre-clinical stage of development. This is encouraging for the discovery of a small molecule targeting USP48. Nevertheless, the performance of high throughput screens to identify drugs targeting USP48 will have to be based on prior knowledge of the enzyme's activity. Should a molecule be developed that

successfully inhibits USP48, it will be seen as a drug that can mitigate the development or evolution of the pathophysiology of FA patients. The USP48 inhibitor could potentially delay the appearance of BMF in those patients that do not suffer from this condition in the initial stages. Furthermore, in those patients with early onset BMF, the use of the inhibitor could reduce the side effects of the HSCT and avoid the later occurrence of cancers. Thus far, FA patients are not diagnosed prior to birth. If this were the case, one option would be treatment at the embryo stage. However, having discussed the possibility of USP48 being involved in ES cell development this would not be advisable.

4. Conclusions

We have demonstrated that loss-of-function screens in the context of rare diseases are a suitable tool for the identification of genes that, upon deletion/inhibition, improve the condition of disease-model cell lines and potentially identify suitable targets for treatment. Furthermore, we have generated a synthetic rescue interaction map of the FA pathway, as a resource to further our understanding of this repair pathway. Moreover, we have demonstrated that loss of USP48, a deubiquitylating enzyme, in FA-deficient cells alleviates the cellular hallmarks of the FA phenotype by restoring error-free repair. Therefore, our study has identified USP48 as a novel player in the repair of ICLs and has increased our mechanistic understanding of the FA pathway.

CHAPTER 4: MATERIALS & METHODS**1. Materials****Table 3.** List of materials employed in the experiments described in the Discussion section (additional materials used for these experiments have been previously described in the Manuscript).

CRISPR-Cas9 mediated point mutant	<i>USP48</i> C98S gRNA	5'-AAATGTGTTGACATAACAAGTGG-3'
	C98S donor template	5'-CATTTGTGGGCCTGACTAATCTTGGAGCCA CATCTTATGTCAACACATTTCTTCAAGTGTGGTTT-3'
	C98S locus PCR primers	Fw: 5'-CCGTCTCCCAGCATGTAGTC-3' Rv: 5'-TGGTTGTTTAAAGGAAAATGGGT-3'
Immunofluorescence	NF- κ B p65	1:500 dilution (ab16502, Abcam)
	TNF α	20ng/mL (ab9642, Abcam)
ChIP	Formaldehyde	16% (w/v) methanol free (28908, Thermo Fisher)
	RNase A	DNase-frei 500mg (10204183, Fisher Scientific)
	PNK	Polynucleotide Kinase, 500u (M0201S T4, New England Biolabs)
	NEBNext Ultra II DNA Library Prep Kit for Illumina	E7645S (New England Biolabs)
H2A ubiquitin levels	H2A K119Ub	1:1000 dilution (D27C4, Cell Signaling)
FAN1 synthetic lethality	sh-FAN1-1	5'-GGCCCCAGGAAGAAGAAATTG-3'
	sh-FAN1-2	5'-CTACAGACAGAATCTGAGTTGC-3'
ATR inhibition	AZ20	SML1328 (Sigma Aldrich)
Proliferation assay	Trypan Blue solution	T8154 (Sigma Aldrich)
Cell cycle	PI	81845-25MG (Sigma Aldrich)

2. Methods

2.1. CRISPR-Cas9 mediated point mutation

C98S USP48 endogenous point mutant clones were generated by CRISPR-Cas9 mediated Homologous Directed Repair (HDR). HDR was carried out by transiently transfecting three plasmids, each containing: Cas9 enzyme, Blasticidin resistance cassette, guide RNA (gRNA) targeting the site of interest; and a single stranded donor template with the C→G mutation (ratio: 1:1:1:2, respectively) (**Table 3**). Transfection was done using the Xfect transfection reagent (Takara, Clontech) according to manufacturer's protocol. Briefly, cells at 60% confluency in 6 well plates were transfected with a final concentration of 7.5µg of DNA. The next day cells were selected with Blasticidin (20ug/mL final concentration). Selected cells were then seeded in limiting dilutions in order to retrieve single clones. Genotype of the clones was performed by PCR with GoTaq® polymerase (Promega) following the manufacturer's protocol.

2.2. Immunofluorescence

Cells were seeded on coverslips in a 24 well plate at a density of 2×10^4 cells/mL. after treatment with MMC or $TNF\alpha$, cells were fixed in 4% paraformaldehyde (PFA) for 15 minutes at room temperature and washed with phosphate-buffered saline (PBS). After blocking in 10% fetal calf serum (FCS) in PBS for 1 hour at room temperature, cells were incubated with primary antibody overnight at 4 degrees and with AlexaFluor 488-conjugated secondary antibody for 1 hour at room temperature. Samples were incubated with 0.1 µg/mL DAPI for DNA staining and mounted in Polymount.

2.3. Chromatin Immune Precipitation

Cells at 80% confluency in 15cm dishes were fixed with 1% formaldehyde (methanol-free) for 10 minutes at room temperature. This reaction was quenched with glycine at 0.125M for 5 minutes on ice. Chromatin extraction was performed in 4 incubation/centrifugation cycles using 4 different buffers (**L1**: 50 mM HEPES KOH, pH 7.5, 140 mM NaCl, 1 mM EDTA pH 8.0, 10% glycerol, 0.5 % NP-40, 0.25 % Triton-X 100; **L2**: 200 mM NaCl, 1 mM EDTA pH 8.0, 0.5 mM EGTA pH 8.0, 10 mM Tris pH 8.0; **L3**: 1 mM EDTA pH 8.0, 0.5 mM EGTA pH 8.0, 10 mM Tris pH 8.0, 100 mM NaCl, 0.1% Na-deoxycholate, 0.17 mM N-Lauroyl sarcosine; **Shearing buffer**: 10 mM Tris-HCl, pH 7.8 (or pH 8), 1 mM EDTA, pH 8.0, 0.1 % SDS). For sonication, cells were resuspended in **Harsh Shearing buffer** (10 mM Tris-HCl,

pH 7.8 (or 8.0), 2 mM EDTA pH 8, 0.25 % SDS) and subjected to one 20 minutes cycle of bursting in Covaris 220 sonicator. The supernatant was combined and diluted in **Equilibration buffer** (10 mM Tris-HCl, pH 8.0, 223 mM NaCl, 1.66 % Triton X-100, 0.166 % DOC, 1 mM EDTA, pH 8). The sample was then incubated with an antibody against USP48 overnight, followed by a decrosslinking step (RNase treatment 30 minutes at 37 degrees; PNK treatment 2.5 hours at 55 degrees and overnight at 65 degrees). Next, the USP48 DNA-bound fraction was extracted by Phenol (:Chloroform:Isoamyl) Alcohol and prepared for sequencing. For the last step the NEBNext Ultra II DNA Library Prep Kit for Illumina was used according to the manufacturer's protocol. All buffers prior to DNA extraction contained protease inhibitors (Sigma Aldrich), phosphatase inhibitors (Sigma, NEB) and deubiquitylase inhibitors (Sigma Aldrich).

2.4. H2A ubiquitin levels

Cells were seeded at a density of 2×10^5 cells/mL. The next day, the cells were exposed to MMC (50nM) and harvested at the indicated timepoints. All cell extracts were prepared in RIPA lysis buffer (NEB) containing protease inhibitors (Sigma Aldrich), phosphatase inhibitors (Sigma, NEB) and deubiquitylase inhibitors (Sigma Aldrich). Immunoblot was performed following the standard procedure. Proteins were separated in sodium dodecyl sulfate–polyacrylamide gel electrophoresis (SDS-PAGE) (4-12% gradient gels, Invitrogen). Then transferred to a nitrocellulose membrane. The antibody against H2A-K119Ub was used at the indicated dilution (**Table 3**).

2.5. FAN1 synthetic lethality

HAP1 cells at a confluency of 70-80% were infected with virus containing supernatant in the presence of polybrene (final concentration 8 μ g/mL), at a 1:3 dilution. Then, cells were selected with puromycin (2 μ g/mL; Sigma-Aldrich) for 48 h. After selection, RNA was extraction using Trizol (following the manufacturer's protocol). RNA was incubated with DNase (Sigma) and reverse transcribed with SuperScript III Reverse Transcriptase protocol (Invitrogen). The resulting cDNA was used for qRT-PCR employing SYBR Green qPCR Mastermix (Qiagen).

2.6. ATR inhibition

Cells were seeded at a density 1 500 cells/mL in a 96 well plate. 24 hours later they were subjected to the ATR inhibitor AZ20 at different concentrations (**Table 3**), each dose was performed in triplicates. After 3 days of treatment, the viability of the cells was assessed by using Cell Titer Glo[®].

2.7. Proliferation assay

Cells were seeded at a density of 5 000 cells/mL in a 24 well plate. 24 hours later cells were harvested and counted using Trypan Blue solution (**Table 3**). This procedure was repeated for 5 days, each timepoint was registered for 5 replicates.

2.8. Cell cycle

Cells were harvested at equal density for all samples. After washing two times with ice cold PBS the cells were fixed with 70% ethanol (cold). Then, cells were kept overnight at minus 20 degrees. The next day, the ethanol was removed with PBS and the cells were stained with PI (**Table 3**). The cells were then analyzed by FACS to assessed their cell cycle profile.

REFERENCES

- A. M & L. Z (2013) DNA damage sensing by the ATM and ATR kinases. *Cold Spring Harb. Perspect. Biol.* **5**: 1–17
- Abdullah UB, McGouran JF, Brolih S, Ptchelkine D, El-Sagheer AH, Brown T & McHugh PJ (2017) RPA activates the XPF-ERCC1 endonuclease to initiate processing of DNA interstrand crosslinks. *EMBO J.* **36**: 2017-2060
- Adamo A, Collis SJ, Adelman CA, Silva N, Horejsi Z, Ward JD, Martinez-Perez E, Boulton SJ & La Volpe A (2010a) Preventing Nonhomologous End Joining Suppresses DNA Repair Defects of Fanconi Anemia. *Mol. Cell* **39**: 25–35
- Adamo A, Collis SJ, Adelman CA, Silva N, Horejsi Z, Ward JD, Martinez-Perez E, Boulton SJ & La Volpe A (2010b) Preventing Nonhomologous End Joining Suppresses DNA Repair Defects of Fanconi Anemia. *Mol. Cell* **39**: 25–35
- Al-Hakim A, Escribano-Diaz C, Landry M-C, O'Donnell L, Panier S, Szilard RK & Durocher D (2010) The ubiquitous role of ubiquitin in the DNA damage response. *DNA Repair (Amst)*. **9**: 1229–1240
- Allan LA & Fried M (1999) p53-dependent apoptosis or growth arrest induced by different forms of radiation in U2OS radiation in U2OS cells : p21 WAF1 / CIP1 repression in UV induced apoptosis. *Oncogene* **18**: 5403–5412
- Alter BP (2003) Cancer in Fanconi anemia, 1927-2001. *Cancer* **97**: 425–440
- Aly A & Ganesan S (2011) Review BRCA1, PARP, and 53BP1 : conditional synthetic lethality and synthetic viability. *J. Mol. Cell Biol.* **3**: 66–74
- Andreassen PR, D'Andrea AD & Taniguchi T (2004) ATR couples FANCD2 monoubiquitination to the DNA-damage response. *Genes Dev.* **18**: 1958–1963
- Arkinson C, Chaugule VK, Toth R & Walden H (2018) Specificity for deubiquitination of monoubiquitinated FANCD2 is driven by the N-terminus of USP1. *Life Sci. Alliance* **1**: e201800162
- Arleen D. Auerbach (2010) FA and its diagnosis. *Mutat. Res.* **668**: 4–10
- Ashley AK, Shrivastav M, Nie J, Amerin C, Troksa K, Glanzer JG, Liu S, Opiyo SO, Dimitrova DD, Le P, Sishc B, Bailey SM, Oakley GG & Nickoloff JA (2014) DNA-PK phosphorylation of RPA32 Ser4/Ser8 regulates replication stress checkpoint activation, fork restart, homologous recombination and mitotic catastrophe. *DNA Repair (Amst)*. **21**: 131–139

- Bai CB, Auerbach W, Lee JS, Stephen D & Joyner AL (2002) Gli2, but not Gli1, is required for initial Shh signaling and ectopic activation of the Shh pathway. *Development* **129**: 4753–61
- Bakker ST, de Winter JP & Riele H t. (2013) Learning from a paradox: recent insights into Fanconi anaemia through studying mouse models. *Dis. Model. Mech.* **6**: 40–47
- Bharathan SP, Nandy K, Palani D, Janet A NB, Natarajan K, George B, Srivastava A & Velayudhan SR (2017) Generation of an induced pluripotent stem cell line that mimics the disease phenotypes from a patient with Fanconi anemia by conditional complementation. *Stem Cell Res.* **20**: 54–57
- Bick G, Zhang F, Meetei AR & Andreassen PR (2017) Coordination of the recruitment of the FANCD2 and PALB2 Fanconi anemia proteins by an ubiquitin signaling network. *Chromosoma* **126**: 417–430
- Biswas K, Das R, Alter BP, Kuznetsov SG, Stauffer S, North SL, Burkett S, Brody LC, Meyer S, Byrd RA & Sharan SK (2011) A comprehensive functional characterization of BRCA2 variants associated with Fanconi anemia using mouse ES cell-based assay. *Blood* **118**: 2430–2442
- Bogliolo M & Surrallés J (2015) Fanconi anemia: A model disease for studies on human genetics and advanced therapeutics. *Curr. Opin. Genet. Dev.* **33**: 32–40
- Budzowska M, Graham TG, Soback A, Waga S & Walter JC (2015) Regulation of the Rev1-pol complex during bypass of a DNA interstrand cross-link. *EMBO J.* **34**: 1971–1985
- Bunting SF, Callén E, Wong N, Chen H, Polato F, Gunn A, Bothmer A, Feldhahn N, Fernandez-capetillo O, Cao L, Xu X, Deng C, Finkel T, Nussenzweig M & Stark JM (2011) 53BP1 inhibits homologous recombination in Brca1-deficient cells by blocking resection of DNA breaks. *Cell* **141**: 243–254
- Carette JE, Guimaraes CP, Varadarajan M, Park AS, Wuethrich I, Godarova A, Kotecki M, Cochran BH, Spooner E, Ploegh HL & Brummelkamp TR (2009) Haploid genetic screens in human cells identify host factors used by pathogens. *Science* **326**: 1231–1235
- Ceccaldi R, Parmar K, Mouly E, Delord M, Kim JM, Regairaz M, Pla M, Vasquez N, Zhang QS, Pondarre C, Peffault De Latour R, Gluckman E, Cavazzana-Calvo M, Leblanc T, Larghero J, Grompe M, Soci?? G, D'Andrea AD & Soulier J (2012) Bone marrow failure in fanconi anemia is triggered by an exacerbated p53/p21 DNA damage response that impairs hematopoietic stem and progenitor cells. *Cell Stem Cell* **11**: 36–49

- Cetkovská K, Šustová H & Uldrijan S (2017) Ubiquitin-specific peptidase 48 regulates Mdm2 protein levels independent of its deubiquitinase activity. *Scientific Reports* **7**: 1–9
- Chen R & Wold MS (2014) Replication protein A: Single-stranded DNA's first responder: Dynamic DNA-interactions allow replication protein A to direct single-strand DNA intermediates into different pathways for synthesis or repair Prospects & Overviews R. Chen and M. S. Wold. *BioEssays* **36**: 1156–1161
- Chlon TM, Ruiz-Torres S, Maag L, Mayhew CN, Wikenheiser-Brokamp KA, Davies SM, Mehta P, Myers KC, Wells JM & Wells SI (2016) Overcoming Pluripotent Stem Cell Dependence on the Repair of Endogenous DNA Damage. *Stem Cell Reports* **6**: 44–54
- Ciccio A & Elledge SJ (2010) Review The DNA Damage Response : Making It Safe to Play with Knives. *Mol. Cell Rev.* **40**: 179–204
- Ciccio A, Ling C, Coulthard R, Yan Z, Xue Y, Meetei AR, Laghmani EH, Joenje H, McDonald N, de Winter JP, Wang W & West SC (2007) Identification of FAAP24, a Fanconi Anemia Core Complex Protein that Interacts with FANCM. *Mol. Cell* **25**: 331–343
- Citterio E (2015) Fine-tuning the ubiquitin code at DNA double-strand breaks: Deubiquitinating enzymes at work. *Front. Genet.* **6**: 1–16
- Clauson C, Schärer OD & Niedernhofer L (2013) Advances in understanding the complex mechanisms of DNA interstrand cross-link repair. *Cold Spring Harb. Perspect. Biol.* **5**: a012732
- Cole AJ, Zhu Y, Dwight T, Yu B, Dickson KA, Gard GB, Maidens J, Valmadre S, Gill AJ, Clifton-Bligh R & Marsh DJ (2017) Comprehensive analyses of somatic TP53 mutation in tumors with variable mutant allele frequency. *Sci. Data* **4**: 1–8
- Collins NB, Wilson JB, Bush T, Thomashevski A, Roberts KJ, Jones NJ & Kupfer GM (2009) ATR-dependent phosphorylation of FANCA on serine 1449 after DNA damage is important for FA pathway function. *Blood* **113**: 2181–2190
- Collis SJ, Barber LJ, Clark AJ, Martin JS, Ward JD & Boulton SJ (2007) HCLK2 is essential for the mammalian S-phase checkpoint and impacts on Chk1 stability. *Nat. Cell Biol.* **9**: 391–401
- Dantuma NP & van Attikum H (2016) Spatiotemporal regulation of posttranslational modifications in the DNA damage response. *EMBO J.* **35**: 6–23
- Deans AJ & West SC (2009) FANCM Connects the Genome Instability Disorders Bloom's Syndrome and Fanconi Anemia. *Mol. Cell* **36**: 943–953

- Deans AJ & West SC (2011) DNA interstrand crosslink repair and cancer. *Nat. Rev. Cancer* **11**: 467–480
- Densham RM, Garvin AJ, Stone HR, Strachan J, Baldock RA, Daza-Martin M, Fletcher A, Blair-Reid S, Beesley J, Johal B, Pearl LH, Neely R, Keep NH, Watts FZ & Morris JR (2016) Human BRCA1–BARD1 ubiquitin ligase activity counteracts chromatin barriers to DNA resection. *Nat. Struct. Mol. Biol.* **23**: 647–655
- Dong H, Nebert DW, Bruford EA, Thompson DC, Joenje H & Vasiliou V (2015) Update of the human and mouse fanconi anemia genes. *Hum. Genomics* **9**: 1–10
- Dooley K & Zon LI (2000) Zebrafish: A model system for the study of human disease. *Curr. Opin. Genet. Dev.* **10**: 252–256
- Dufour C (2017) How I manage patients with Fanconi anaemia. *Br. J. Haematol.* **178**: 32–47
- Elia AEH, Wang DC, Willis NA, Boardman AP, Hajdu I, Adeyemi RO, Lowry E, Gygi SP, Scully R & Elledge SJ (2015) RFD3-Dependent Ubiquitination of RPA Regulates Repair at Stalled Replication Forks. *Mol. Cell* **60**: 280–293
- Enoiu M, Jiricny J & Schärer OD (2012) Repair of cisplatin-induced DNA interstrand crosslinks by a replication-independent pathway involving transcription-coupled repair and translesion synthesis. *Nucleic Acids Res.* **40**: 8953–8964
- Essletzbichler P, Konopka T, Santoro F, Chen D, Gapp B V., Kralovics R, Brummelkamp TR, Nijman SMB & Bürckstümmer T (2014) Megabase-scale deletion using CRISPR/Cas9 to generate a fully haploid human cell line. *Genome Res.* **24**: 2059–2065
- Feeney L, Muñoz IM, Lachaud C, Toth R, Appleton PL, Schindler D & Rouse J (2017) RPA-Mediated Recruitment of the E3 Ligase RFD3 Is Vital for Interstrand Crosslink Repair and Human Health. *Mol. Cell* **66**: 610-621.e4
- Ferrarotto R, MacHado K, Mak MP, Shah N, Takahashi TK, Costa FP, Overman MJ, Kopetz S & Hoff PM (2012) A multicenter, multinational analysis of mitomycin C in refractory metastatic colorectal cancer. *Eur. J. Cancer* **48**: 820–826
- Freire BL, Homma TK, Funari MFA, Lerario AM, Leal AM, Velloso EDRP, Malaquias AC & Jorge AAL (2018) Homozygous loss of function BRCA1 variant causing a Fanconi-anemia-like phenotype, a clinical report and review of previous patients. *Eur. J. Med. Genet.* **61**: 130–133
- Garaycochea JI, Crossan GP, Langevin F, Daly M, Arends MJ & Patel KJ (2012) Genotoxic consequences of endogenous aldehydes on mouse haematopoietic stem cell function.

Nat. Lett. **489**: 571–575

Garaycoechea JI, Crossan GP, Langevin F, Mulderrig L, Louzada S, Yang F, Guilbaud G, Park N, Roerink S, Nik-Zainal S, Stratton MR & Patel KJ (2018) Alcohol and endogenous aldehydes damage chromosomes and mutate stem cells. *Nature* **553**: 171–177

Garaycoechea JI & Patel KJ (2013) Why does the bone marrow fail in Fanconi anemia? *Blood. Rev.* **123**: 26–34

García-Rubio ML, Pérez-Calero C, Barroso SI, Tumini E, Herrera-Moyano E, Rosado I V. & Aguilera A (2015) The Fanconi Anemia Pathway Protects Genome Integrity from R-loops. *PLoS Genet.* **11**: 1–17

Garner E & Smogorzewska A (2011) Ubiquitylation and the Fanconi anemia pathway. *FEBS Lett.* **585**: 2853–2860

Geng L, Huntoon CJ & Karnitz LM (2010) RAD18-mediated ubiquitination of PCNA activates the Fanconi anemia DNA repair network. *J. Cell Biol.* **191**: 249–257

Ghanem A, Schweitzer K & Naumann M (2019) Catalytic domain of deubiquitinylase USP48 directs interaction with Rel homology domain of nuclear factor kappaB transcription factor RelA. *Mol. Biol. Rep.* **46**: 1369–1375

Gluckman E (2015) Improving survival for Fanconi anemia patients. *Blood* **125**: 3676

Hanada K, Budzowska M, Davies SL, Van Drunen E, Onizawa H, Beverloo HB, Maas A, Essers J, Hickson ID & Kanaar R (2007) The structure-specific endonuclease Mus81 contributes to replication restart by generating double-strand DNA breaks. *Nat. Struct. Mol. Biol.* **14**: 1096–1104

Hanada K, Budzowska M, Modesti M, Maas A, Wyman C, Essers J & Kanaar R (2006) The structure-specific endonuclease Mus81-Eme1 promotes conversion of interstrand DNA crosslinks into double-strands breaks. *EMBO J.* **25**: 4921–4932

Hanawalt PC (2016) Historical perspective on the DNA damage response. *DNA repair (Amst)*. **36**: 2–7

Harrigan JA, Jacq X, Martin NM & Jackson SP (2018) Deubiquitylating enzymes and drug discovery: Emerging opportunities. *Nat. Rev. Drug Discov.* **17**: 57–77

Hashimoto S, Anai H & Hanada K (2016) Mechanisms of interstrand DNA crosslink repair and human disorders. *Genes Environ.* **38**: 1–8

Hiom K (2005) DNA Repair: How to PIKK a Partner. *Curr. Biol.* **15**: 473–475

- Ho T V. & Schärer OD (2010) Translesion DNA synthesis polymerases in DNA interstrand crosslink repair. *Environ. Mol. Mutagen.* **51**: 552–566
- Hoeijmakers JHJ (2009) DNA damage, aging, and cancer. *N. Engl. J. Med.* **361**: 1475–85
- Howlett NG, Harney JA, Rego MA, Kolling IV FW & Glover TW (2009) Functional interaction between the fanconi anemia D2 protein and proliferating cell nuclear antigen (PCNA) via a conserved putative PCNA interaction motif. *J. Biol. Chem.* **284**: 28935–28942
- Huang Y, Leung JWC, Lowery M, Matsushita N, Wang Y, Shen X, Huang D, Takata M, Chen J & Li L (2014) Modularized Functions of the Fanconi Anemia Core Complex. *Cell Rep.* **7**: 1849–1857
- Inano S, Sato K, Katsuki Y, Kobayashi W, Tanaka H, Nakajima K, Nakada S, Miyoshi H, Knies K, Takaori-Kondo A, Schindler D, Ishiai M, Kurumizaka H & Takata M (2017) RFWD3-Mediated Ubiquitination Promotes Timely Removal of Both RPA and RAD51 from DNA Damage Sites to Facilitate Homologous Recombination. *Mol. Cell* **66**: 622-634.e8
- Jeggo PA, Pearl LH & Carr AM (2016) DNA repair, genome stability and cancer: a historical perspective. *Nat. Rev. Cancer* **16**: 35–42
- Ji X, Dadon DB, Abraham BJ, Lee TI, Jaenisch R, Bradner JE & Young RA (2015) Chromatin proteomic profiling reveals novel proteins associated with histone-marked genomic regions. *Proc. Natl. Acad. Sci.* **112**: 3841–3846
- Joenje H & Patel KJ (2001) The emerging genetic and molecular basis of Fanconi anemia. *Nat. Rev. Genet.* **2**: 446–457
- Joo W, Xu G, Persky NS, Smogorzewska A, Rudge DG, Buzovetsky O, Elledge SJ & Pavletich NP (2011) Structure of the FANCI-FANCD2 complex: Insights into the Fanconi anemia DNA repair pathway. *Science (80-)*. **333**: 312–316
- Kastenhuber ER & Lowe SW (2017) Putting p53 in Context. *Cell* **170**: 1062–1078
- Kennedy RD, Chen CC, Stuckert P, Archila EM, De La Vega MA, Moreau LA, Shimamura A & D'Andrea AD (2007) Fanconi anemia pathway-deficient tumor cells are hypersensitive to inhibition of ataxia telangiectasia mutated. *J. Clin. Invest.* **117**: 1440–1449
- Kennedy RD & D'Andrea AD (2005) The Fanconi Anemia/BRCA pathway: New faces in the crowd. *Genes Dev.* **19**: 2925–2940
- Kim H, Yang K, Dejsuphong D & D'Andrea AD (2012a) Regulation of Rev1 by the Fanconi

- anemia core complex. *Nat. Struct. Mol. Biol.* **19**: 164–170
- Kim Y, Lach FP, Desetty R, Hanenberg H, Auerbach AD & Smogorzewska A (2011) Mutations of the SLX4 gene in Fanconi anemia. *Nat. Genet.* **43**: 142–146
- Kim Y, Spitz GS, Veturi U, Lach FP, Auerbach AD & Smogorzewska A (2012b) Regulation of multiple DNA repair pathways by the Fanconi anemia protein SLX4. *Blood* **121**: 54–63
- Klein Douwel D, Boonen RACM, Long DT, Szybowska AA, Räschle M, Walter JC & Knipscheer P (2014) XPF-ERCC1 Acts in Unhooking DNA Interstrand Crosslinks in Cooperation with FANCD2 and FANCP/SLX4. *Mol. Cell* **54**: 460–471
- Klein Douwel D, Hoogenboom WS, Boonen RA & Knipscheer P (2017) Recruitment and positioning determine the specific role of the XPF-ERCC1 endonuclease in interstrand crosslink repair. *EMBO J.* **36**: 2034–2046
- Knies K, Schuster B, Ameziane N, Rooimans M, Bettecken T, de Winter J & Schindler D (2012) Genotyping of Fanconi Anemia Patients by Whole Exome Sequencing: Advantages and Challenges. *PLoS One* **7**: 1–10
- Knies K, Takata M & Schindler D (2017) Biallelic mutations in the ubiquitin ligase RFWD3 cause Fanconi anemia The Journal of Clinical Investigation. *J Clin Invest* **127**: 3013–3027
- Knipscheer P, Raschle M, Smogorzewska A, Enoiu M, Ho T V., Scharer OD, Elledge SJ & Walter JC (2009) The Fanconi Anemia Pathway Promotes Replication-Dependent DNA Interstrand Cross-Link Repair. *Science (80-.)*. **326**: 1698–1701
- Kotecki M, Reddy PS & Cochran BH (1999) Isolation and characterization of a near-haploid human cell line. *Exp. Cell Res.* **252**: 273–280
- Kottemann MC & Smogorzewska A (2013) Fanconi anaemia and the repair of Watson and Crick DNA crosslinks. *Nature* **493**: 356–363
- Krausz C, Riera-Escamilla A, Chianese C, Moreno-Mendoza D, Ars E, Rajmil O, Pujol R, Bogliolo M, Blanco I, Rodríguez I, Badell I, Ruiz-Castañé E & Surrallés J (2019) From exome analysis in idiopathic azoospermia to the identification of a high-risk subgroup for occult Fanconi anemia. *Genet. Med.* **21**: 189–194
- Kuraoka I, Kobertz WR, Ariza RR, Biggerstaff M, Essigmann JM & Wood RD (2000) Repair of an Interstrand DNA Cross-link Initiated by ERCC1-XPF Repair/Recombination Nuclease. *J. Biol. Chem.* **275**: 26632–26636

- Lachaud C, Moreno A, Marchesi F, Toth R, Blow JJ & Rouse J (2016) Ubiquitinated Fancd2 recruits Fan1 to stalled replication forks to prevent genome instability. *Science (80-.)*. **5634**: 1–8
- Langevin F, Crossan GP, Rosado I V., Arends MJ & Patel KJ (2011) Fancd2 counteracts the toxic effects of naturally produced aldehydes in mice. *Nature* **475**: 53–59
- Larrieu D, Britton S, Demir M, Rodriguez R & Jackson SP (2014) Chemical Inhibition of NAT10 Corrects Defects of Laminopathic Cells. *Science (80-.)*. **344**: 527
- Le J, Perez E, Nemzow L & Gong F (2019) Role of deubiquitinases in DNA damage response. *DNA Repair (Amst)*. **76**: 89–98
- Lee KY, Chung KY & Koo HS (2010) The involvement of FANCM, FANCI, and checkpoint proteins in the interstrand DNA crosslink repair pathway is conserved in *C. elegans*. *DNA Repair (Amst)*. **9**: 374–382
- Lee Y-S, Gregory MT & Yang W (2014) Human Pol purified with accessory subunits is active in translesion DNA synthesis and complements Pol in cisplatin bypass. *Proc. Natl. Acad. Sci.* **111**: 2954–2959
- Liang Q, Dexheimer TS, Zhang P, Rosenthal AS, Villamil MA, You C, Zhang Q, Chen J, Ott CA, Sun H, Luci DK, Yuan B, Simeonov A, Jadhav A, Xiao H, Wang Y, Maloney DJ & Zhuang Z (2014) A selective USP1-UAF1 inhibitor links deubiquitination to DNA damage responses. *Nat. Chem. Biol.* **10**: 298–304
- Liu GH, Suzuki K, Li M, Qu J, Montserrat N, Tarantino C, Gu Y, Yi F, Xu X, Zhang W, Ruiz S, Plongthongkum N, Zhang K, Masuda S, Nivet E, Tsunekawa Y, Soligalla RD, Goebel A, Aizawa E, Kim NY, et al (2014) Modelling Fanconi anemia pathogenesis and therapeutics using integration-free patient-derived iPSCs. *Nat. Commun.* **5**: 1–17
- Liu T, Ghosal G, Yuan J, Chen J & Huang J (2010) FAN1 Acts with FANCI-FANCD2 to Promote DNA Interstrand Cross-Link Repair. *Science (80-.)*. **329**: 693–696
- Liu TX, Howlett NG, Deng M, Langenau DM, Hsu K, Rhodes J, Kanki JP, D'Andrea AD & Look AT (2003) Knockdown of zebrafish Fancd2 causes developmental abnormalities via p53-dependent apoptosis. *Dev. Cell* **5**: 903–914
- Liu YL, Yan J, Zheng J & Tian QB (2018) 938RHRK941 is responsible for Ubiquitin specific protease 48 nuclear translocation which can stabilize NF- κ B (p65) in the nucleus. *Gene* **669**: 77–81
- Lobitz S & Velleuer E (2006) Guido Fanconi (1892-1979): A jack of all trades. *Nat. Rev.*

Cancer **6**: 893–898

Lockhart PJ, Hulihan M, Lincoln S, Hussey J, Skipper L, Bisceglia G, Wilkes K & Farrer MJ (2004) Identification of the human ubiquitin specific protease 31 (USP31) gene: structure, sequence and expression analysis. *DNA Seq.* **15**: 9–14

Lok BH, Carley AC, Tchang B & Powell SN (2013) RAD52 inactivation is synthetically lethal with deficiencies in BRCA1 and PALB2 in addition to BRCA2 through RAD51-mediated homologous recombination. *Oncogene* **32**: 3552–3558

Long DT, Joukov V, Budzowska M & Walter JC (2014) BRCA1 promotes unloading of the CMG Helicase from a stalled DNA replication fork. *Mol. Cell* **56**: 174–185

Luo Y, Hartford SA, Zeng R, Southard TL, Shima N & Schimenti JC (2014) Hypersensitivity of Primordial Germ Cells to Compromised Replication-Associated DNA Repair Involves ATM-p53-p21 Signaling. *PLoS Genet.* **10**: e1004471

MacKay C, Déclais AC, Lundin C, Agostinho A, Deans AJ, MacArtney TJ, Hofmann K, Gartner A, West SC, Helleday T, Lilley DMJ & Rouse J (2010) Identification of KIAA1018/FAN1, a DNA Repair Nuclease Recruited to DNA Damage by Monoubiquitinated FANCD2. *Cell* **142**: 65–76

Mankouri HW & Hickson ID (2007) The RecQ helicase-topoisomerase III-Rmi1 complex: a DNA structure-specific ‘dissolvasome’? *Trends Biochem. Sci.* **32**: 538–546

Matos J & West SC (2014) Holliday junction resolution: Regulation in space and time. *DNA Repair (Amst)*. **19**: 176–181

McCulloch SD & Kunkel TA (2008) The fidelity of DNA synthesis by eukaryotic replicative and translesion synthesis polymerases. *Cell Res.* **18**: 148–161

Meetei AR, De Winter JP, Medhurst AL, Wallisch M, Waisfisz Q, Van de Vrugt HJ, Oostra AB, Yan Z, Ling C, Bishop CE, Hoatlin ME, Joenje H & Wang W (2003) A novel ubiquitin ligase is deficient in Fanconi anemia. *Nat. Genet.* **35**: 165–170

Michl J, Zimmer J & Tarsounas M (2016) Interplay between Fanconi anemia and homologous recombination pathways in genome integrity. *EMBO J.* **35**: 909–923

Miles JA, Frost MG, Carroll E, Rowe ML, Howard MJ, Sidhu A, Chaugule VK, Alpi AF & Walden H (2015) The Fanconi Anemia DNA Repair Pathway Is Regulated by an Interaction between Ubiquitin and the E2-like Fold Domain of FANCL. *J. Biol. Chem.* **290**: 20995–21006

Minko IG, Harbut MB, Kozekov ID, Kozekova A, Jakobs PM, Olson SB, Moses RE, Harris

- TM, Rizzo CJ & Lloyd RS (2008) Role for DNA polymerase κ in the processing of N2-N2-guanine interstrand cross-links. *J. Biol. Chem.* **283**: 17075–17082
- Moder M, Velimezi G, Owusu M, Mazouzi A, Wiedner M, Ferreira Da Silva J, Robinson-Garcia L, Schischlik F, Slavkovsky R, Kralovics R, Schuster M, Bock C, Ideker T, Jackson SP, Menche J & Loizou JI (2017) Parallel genome-wide screens identify synthetic viable interactions between the BLM helicase complex and Fanconi anemia. *Nat. Commun.* **8**: 1–8
- Moldovan G-L & D'andrea AD (2009) How the Fanconi Anemia pathway guards the genome. *Annu. Rev. Genet.* **43**: 223–249
- Moldovan G-L & D'Andrea AD (2009) How the fanconi anemia pathway guards the genome. *Annu. Rev. Genet.* **43**: 223–49
- Moldovan G-L, Madhavan M V., Mirchandani KD, McCaffrey RM, Vinciguerra P & D'Andrea AD (2010) DNA Polymerase POLN Participates in Cross-Link Repair and Homologous Recombination. *Mol. Cell. Biol.* **30**: 1088–1096
- Morales JF, Song T, Auerbach AD & Wittkowski KM (2008) Phenotyping Genetic Diseases Using an Extension of μ -Scores for Multivariate Data. *Stat. Appl. Genet. Mol. Biol.* **7**: 1–21
- Nabet B, Roberts JM, Buckley DL, Paulk J, Dastjerdi S, Yang A, Leggett AL, Erb MA, Lawlor MA, Souza A, Scott TG, Vittori S, Perry JA, Qi J, Winter GE, Wong KK, Gray NS & Bradner JE (2018) The dTAG system for immediate and target-specific protein degradation. *Nat. Chem. Biol.* **14**: 431–441
- Navarro S, Meza NW, Quintana-Bustamante O, Casado JA, Jacome A, McAllister K, Puerto S, Surrallés J, Segovia JC & Bueren JA (2006) Hematopoietic Dysfunction in a Mouse Model for Fanconi Anemia Group D1. *Mol. Ther.* **14**: 525–535
- Neveling K, Endt D, Hoehn H & Schindler D (2009) Genotype-phenotype correlations in Fanconi anemia. *Mutat. Res. - Fundam. Mol. Mech. Mutagen.* **668**: 73–91
- Niedernhofer LJ, Lalai AS & Hoeijmakers JHJ (2005) Fanconi anemia (cross)linked to DNA repair. *Cell* **123**: 1191–1198
- Noll DM, Mason TM & Miller PS (2006) Formation and repair of Interstrand cross-links in DNA. *Chem. Rev.* **106**: 277–301
- Oldham M, Yoon P, Fathi Z, Beyer WF, Adamson J, Liu L, Alcorta D, Xia W, Osada T, Liu C, Yang XY, Dodd RD, Herndon JE, Meng B, Kirsch DG, Lysterly HK, Dewhirst MW, Fecci

- P, Walder H & Spector NL (2016) X-ray psoralen activated cancer therapy (X-PACT). *PLoS One* **11**: 1–13
- Owusu M, Bannauer P, Ferreira Da Silva J, Mourikis TP, Jones A, Májek P, Caldera M, Wiedner M, Lardeau C-H, Mueller AC, Menche J, Kubicek S, Ciccarelli FD & Loizou JI (2019) Mapping the Human Kinome in Response to DNA Damage. *Cell Rep.* **26**: 555-563.e6
- Pace P, Mosedale G, Hodskinson MR, Rosado I V, Sivasubramaniam M & Patel KJ (2010) Ku70 corrupts DNA repair in the absence of the Fanconi anemia pathway. *Sci. (New York, NY)* **329**: 219–223
- Palovcak A, Liu W, Yuan F & Zhang Y (2017) Maintenance of genome stability by Fanconi anemia proteins. *Cell Biosci.* **7**: 4–18
- Panier S & Durocher D (2009) Regulatory ubiquitylation in response to DNA double-strand breaks. *DNA Repair (Amst).* **8**: 436–443
- Park HL, Bai C, Platt KA, Matise MP, Beeghly A, Hui CC, Nakashima M & Joyner AL (2000) Mouse Gli1 mutants are viable but have defects in SHH signaling in combination with a Gli2 mutation. *Development* **127**: 1593–605
- Parmar K, D'Andrea A & Niedernhofer LJ (2009) Mouse models of Fanconi anemia. *Mutat. Res. - Fundam. Mol. Mech. Mutagen.* **668**: 133–140
- Patel KJ, Niedzwiedz W, Mosedale G, Johnson M, Ong CY & Pace P (2004) The Fanconi anaemia gene FANCC promotes homologous recombination and error-prone DNA repair. *Mol. Cell* **15**: 607–620
- Pawlikowska P, Fouchet P, Vainchenker W, Rosselli F & Naim V (2014) Defective endomitosis during megakaryopoiesis leads to thrombocytopenia in Fanca^{-/-} mice. *Blood* **124**: 3613–3623
- Peffault de Latour R & Soulier J (2016) How we diagnose and treat MDS and AML in Fanconi anemia. *Blood* **127**: blood-2016-01-583625
- Qiao F, Mi J, Wilson JB, Zhi G, Bucheimer NR, Jones NJ & Kupfer GM (2004) Phosphorylation of Fanconi anemia (FA) complementation group G protein, FANCG, at serine 7 is important for function of the FA pathway. *J. Biol. Chem.* **279**: 46035–46045
- Rajendra E, Oestergaard VH, Langevin F, Wang M, Dornan GL, Patel KJ & Passmore L a. (2014) The Genetic and Biochemical Basis of FANCD2 Monoubiquitination. *Mol. Cell* **54**: 858–869

- Ramanagoudr-Bhojappa R, Carrington B, Ramaswami M, Bishop K, Robbins GM, Jones MP, Harper U, Frederickson SC, Kimble DC, Sood R & Chandrasekharappa SC (2018) Multiplexed CRISPR/Cas9-mediated knockout of 19 Fanconi anemia pathway genes in zebrafish revealed their roles in growth, sexual development and fertility. *PLoS Genet.* **14**: 1–27
- Räschle M, Knipsheer P, Enoiu M, Angelov T, Sun J, Griffith JD, Ellenberger TE, Schärer OD & Walter JC (2008) Mechanism of Replication-Coupled DNA Interstrand Crosslink Repair. *Cell* **134**: 969–980
- Reid LJ, Shakya R, Modi AP, Lokshin M, Cheng J-T, Jasin M, Baer R & Ludwig T (2008) E3 ligase activity of BRCA1 is not essential for mammalian cell viability or homology-directed repair of double-strand DNA breaks. *Proc. Natl. Acad. Sci.* **105**: 20876–20881
- Río P, Navarro S, Guenechea G, Sánchez-Domínguez R, Lamana ML, Yañez R, Casado JA, Mehta PA, Pujol MR, Surrallés J, Charrier S, Galy A, Segovia JC, Díaz De Heredia C, Sevilla J & Bueren JA (2017) Engraftment and in vivo proliferation advantage of gene-corrected mobilized CD34+ cells from Fanconi anemia patients. *Blood* **130**: 1535–1542
- Rogakou EP, Pilch DR, Orr AH, Ivanova VS & Bonner WM (1998) DNA Double-stranded Breaks Induce DNA Double-stranded Breaks Induce Histone H2AX Phosphorylation on Serine 139 *. *J. Biol. Chem.* **273**: 5858–5868
- Rogers CS, Hao Y, Rokhlina T, Samuel M, Stoltz DA, Li Y, Petroff E, Vermeer DW, Kabel AC, Yan Z, Spate L, Wax D, Murphy CN, Rieke A, Whitworth K, Linville ML, Korte SW, Engelhardt JF, Welsh MJ & Prather RS (2008) Production of CFTR-null and CFTR-ΔF508 heterozygous pigs by adeno-associated virus-mediated gene targeting and somatic cell nuclear transfer. Rogers, C. S., Hao, Y., Rokhlina, T., Samuel, M., Stoltz, D. A., Li, Y., ... Prather, R. S. (2008). Production of CFT. *J. Clin. Invest.* **118**: 1571-1577
- Rosado I V., Langevin F, Crossan GP, Takata M & Patel KJ (2011) Formaldehyde catabolism is essential in cells deficient for the Fanconi anemia DNA-repair pathway. *Nat. Struct. Mol. Biol.* **18**: 1432–1434
- Roy U & Schärer OD (2016) Involvement of translesion synthesis DNA polymerases in DNA interstrand crosslink repair. *DNA Repair (Amst)*. **44**: 33–41
- Sale JE, Lehmann AR & Woodgate R (2012) Y-family DNA polymerases and their role in tolerance of cellular DNA damage. *Nat. Publ. Gr.* **13**: 141–152
- Schunke KJ, Rosati LM, Zahurak M, Herman JM, Narang AK, Usach I, Klein AP, Yeo CJ,

- Korman LT, Hruban RH, Cameron JL, Laheru DA & Abrams RA (2018) Long-term analysis of 2 prospective studies that incorporate mitomycin C into an adjuvant chemoradiation regimen for pancreatic and periampullary cancers. *Adv. Radiat. Oncol.* **3**: 42–51
- Schwab RA, Blackford AN & Niedzwiedz W (2010) ATR activation and replication fork restart are defective in FANCM-deficient cells. *EMBO J.* **29**: 806–818
- Schweitzer K & Naumann M (2015) CSN-associated USP48 confers stability to nuclear NF- κ B/RelA by trimming K48-linked Ub-chains. *Biochim. Biophys. Acta - Mol. Cell Res.* **1853**: 453–469
- Shah Punatar R, Martin MJ, Wyatt HDM, Chan YW & West SC (2017) Resolution of single and double Holliday junction recombination intermediates by GEN1. *Proc. Natl. Acad. Sci.* **114**: 443–450
- Shakya R, Szabolcs M, McCarthy E, Ospina E, Basso K, Nandula S, Murty V, Baer R & Ludwig T (2008) The basal-like mammary carcinomas induced by Brca1 or Bard1 inactivation implicate the BRCA1/BARD1 heterodimer in tumor suppression. *Proc. Natl. Acad. Sci.* **105**: 7040–7045
- Shaloam D & Tchounwou PB (2014) Cisplatin in cancer therapy: Molecular mechanisms of action. *Eur. J. Pharmacol.* **740**: 364–378
- Sheng Y, Saridakis V, Sarkari F, Duan S, Wu T, Arrowsmith CH & Frappier L (2006) Molecular recognition of p53 and MDM2 by USP7/HAUSP. *Nat. Struct. Mol. Biol.* **13**: 285–291
- Shiloh Y (2001) ATM and ATR: Networking cellular responses to DNA damage. *Curr. Opin. Genet. Dev.* **11**: 71–77
- De Silva IU, McHugh PJ, Clingen PH & Hartley JA (2002) Defining the Roles of Nucleotide Excision Repair and Recombination in the Repair of DNA Interstrand Cross-Links in Mammalian Cells. *Mol. Cell. Biol.* **20**: 7980–7990
- Simpson LJ, Ross AL, Szüts D, Alviani CA, Oestergaard VH, Patel KJ & Sale JE (2006) RAD18-independent ubiquitination of proliferating-cell nuclear antigen in the avian cell line DT40. *EMBO Rep.* **7**: 927–932
- Simpson LJ & Sale JE (2003) Rev1 is essential for DNA damage tolerance and non-templated immunoglobulin gene mutation in a vertebrate cell line. *EMBO J.* **22**: 1654–1664

- Singh TR, Ali AM, Paramasivam M, Pradhan A, Wahengbam K, Seidman MM & Meetei AR (2013) ATR-dependent phosphorylation of FANCM at serine 1045 is essential for FANCM functions. *Cancer Res.* **73**: 4300–4310
- Smogorzewska A, Desetty R, Saito TT, Schlabach M, Lach FP, Sowa ME, Clark AB, Kunkel TA, Harper JW, Colaiácovo MP & Elledge SJ (2010) A Genetic Screen Identifies FAN1, a Fanconi Anemia-Associated Nuclease Necessary for DNA Interstrand Crosslink Repair. *Mol. Cell* **39**: 36–47
- Smogorzewska A, Matsuoka S, Vinciguerra P, McDonald ER, Hurov KE, Luo J, Ballif BA, Gygi SP, Hofmann K, D'Andrea AD & Elledge SJ (2007) Identification of the FANCI Protein, a Monoubiquitinated FANCD2 Paralog Required for DNA Repair. *Cell* **129**: 289–301
- Sonoda E, Okada T, Zhao GY, Tateishi S, Araki K, Yamaizumi M, Yagi T, Verkaik NS, Gent DC Van, Takata M & Takeda S (2003) Multiple roles of Rev3, the catalytic subunit of polz in maintaining genome stability in vertebrates. *EMBO J.* **22**: 3188–3197
- Sowa ME, Bennett EJ, Gygi SP & Harper JW (2009) Defining the Human Deubiquitinating Enzyme Interaction Landscape. *Cell* **138**: 389–403
- Stoepker C, Hain K, Schuster B, Hilhorst-Hofstee Y, Rooimans MA, Steltenpool J, Oostra AB, Eirich K, Korthof ET, Nieuwint AWM, Jaspers NGJ, Bettecken T, Joenje H, Schindler D, Rouse J & De Winter JP (2011) SLX4, a coordinator of structure-specific endonucleases, is mutated in a new Fanconi anemia subtype. *Nat. Genet.* **43**: 138–141
- Strathdee CA, Gavish H, Shannon WR & Buchwald M (1992) Cloning of cDNAs for Fanconi's anaemia by functional complementation. *Nature* **356**: 763–767
- Swuec P & Costa A (2014) Molecular mechanism of double Holliday junction dissolution. **4**: 1–5
- Syed A & Tainer JA (2018) The MRE11–RAD50–NBS1 Complex Conducts the Orchestration of Damage Signaling and Outcomes to Stress in DNA Replication and Repair. *Annu. Rev. Biochem.* **87**: 263–294
- Szakal B & Branzei D (2013) Premature Cdk1/Cdc5/Mus81 pathway activation induces aberrant replication and deleterious crossover. *EMBO J.* **32**: 1155–1167
- Taniguchi T, Garcia-Higuera I, Xu B, Andreassen PR, Gregory RC, Kim ST, Lane WS, Kastan MB & D'Andrea AD (2002) Convergence of the Fanconi anemia and ataxia telangiectasia signaling pathways. *Cell* **109**: 459–472

- Tetreault M, Bareke E, Nadaf J, Alirezaie N & Majewski J (2015) Whole-exome sequencing as a diagnostic tool: Current challenges and future opportunities. *Expert Rev. Mol. Diagn.* **15**: 749–760
- Titus TA, Yan YL, Wilson C, Starks AM, Frohnmayer JD, Bremiller RA, Cañestro C, Rodriguez-Mari A, He X & Postlethwait JH (2009) The Fanconi anemia/BRCA gene network in zebrafish: Embryonic expression and comparative genomics. *Mutat. Res. - Fundam. Mol. Mech. Mutagen.* **668**: 117–132
- Toledo LI, Altmeyer M, Rask MB, Lukas C, Larsen DH, Povlsen LK, Bekker-Jensen S, Mailand N, Bartek J & Lukas J (2013) ATR prohibits replication catastrophe by preventing global exhaustion of RPA. *Cell* **155**: 1088
- Trujillo JP & Surrallés J (2015) Savior siblings and Fanconi anemia: Analysis of success rates from the family's perspective. *Genet. Med.* **17**: 935–938
- Tsui V & Crismani W (2019) The Fanconi Anemia Pathway and Fertility. *Trends Genet.* **35**: 199–214
- Tuinmann G, Hegewisch-Becker S, Zschaber R, Kehr A, Schulz J & Hossfeld DK (2004) Gemcitabine and mitomycin C in advanced pancreatic cancer: A single-institution experience. *Anticancer. Drugs* **15**: 575–579
- van Twest S, Murphy VJ, Hodson C, Tan W, Swuec P, O'Rourke JJ, Heierhorst J, Crismani W & Deans AJ (2017) Mechanism of Ubiquitination and Deubiquitination in the Fanconi Anemia Pathway. *Mol. Cell* **65**: 247–259
- Tzimas C, Michailidou G, Arsenakis M, Kieff E, Mosialos G & Hatzivassiliou EG (2006) Human ubiquitin specific protease 31 is a deubiquitinating enzyme implicated in activation of nuclear factor- κ B. *Cell. Signal.* **18**: 83–92
- Uckelmann M, Densham RM, Baas R, Winterwerp HHK, Fish A, Sixma TK & Morris JR (2018) USP48 restrains resection by site-specific cleavage of the BRCA1 ubiquitin mark from H2A. *Nat. Commun.* **9**: 1–8
- Uckelmann M & Sixma TK (2017) Histone ubiquitination in the DNA damage response. *DNA Repair (Amst)*. **56**: 92–101
- Vieira NM, Elvers I, Alexander MS, Moreira YB, Eran A, Gomes JP, Marshall JL, Karlsson EK, Verjovski-Almeida S, Lindblad-Toh K, Kunkel LM & Zatz M (2015) Jagged 1 Rescues the Duchenne Muscular Dystrophy Phenotype. *Cell* **163**: 1204–1213
- Wang AT, Sengerová B, Cattell E, Inagawa T, Hartley JM, Kiakos K, Burgess-Brown NA,

- Swift LP, Enzlin JH, Schofield CJ, Gileadi O, Hartley JA & McHugh PJ (2011) Human SNM1A and XPF-ERCC1 collaborate to initiate DNA interstrand cross-link repair. *Genes Dev.* **25**: 1859–1870
- Wang C, Wang G, Feng X, Shepherd P, Zhang J, Tang M, Chen Z, Srivastava M, McLaughlin ME, Navone NM, Hart GT & Chen J (2018) Genome-wide CRISPR screens reveal synthetic lethality of RNASEH2 deficiency and ATR inhibition. *Oncogene* **38**: 2451–2463
- Wang X, Cheng K, Han Y, Zhang G, Dong J, Cui Y & Yang Z (2016) Effects of Psoralen as an Anti-tumor Agent in Human Breast Cancer MCF-7/ADR Cells. *Biol. Pharm. Bull.* **39**: 815–822
- Wang X, Kennedy RD, Ray K, Stuckert P, Ellenberger T & D'Andrea AD (2007) Chk1-Mediated Phosphorylation of FANCE Is Required for the Fanconi Anemia/BRCA Pathway. *Mol. Cell. Biol.* **27**: 3098–3108
- Ward IM & Chen J (2001) Histone H2AX Is Phosphorylated in an ATR-dependent Manner in Response to Replicational Stress. *J. Biol. Chem.* **276**: 47759–47762
- Williams HL, Gottesman ME & Gautier J (2012) Replication-Independent Repair of DNA Interstrand Crosslinks. *Mol. Cell* **47**: 140–147
- Wu D & Prives C (2018) Relevance of the p53-MDM2 axis to aging. *Cell Death Differ.* **25**: 169–179
- Wu L & Hickson IO (2003) The Bloom's syndrome helicase suppresses crossing over during homologous recombination. *Nature* **426**: 870–874
- Yamamoto KN, Kobayashi S, Tsuda M, Kurumizaka H, Takata M, Kono K, Jiricny J, Takeda S & Hirota K (2011) Involvement of SLX4 in interstrand cross-link repair is regulated by the Fanconi anemia pathway. *Proc. Natl. Acad. Sci.* **108**: 6492–6496
- Yamanaka K, Minko IG, Takata KI, Kolbanovskiy A, Kozekov ID, Wood RD, Rizzo CJ & Lloyd RS (2010) Novel enzymatic function of DNA Polymerase ν in translesion DNA synthesis past major groove DNA-peptide and DNA-DNA cross-links. *Chem. Res. Toxicol.* **23**: 689–695
- Yan Z, Guo R, Paramasivam M, Shen W, Ling C, Fox D, Wang Y, Oostra AB, Kuehl J, Lee DY, Takata M, Hoatlin ME, Schindler D, Joenje H, de Winter JP, Li L, Seidman MM & Wang W (2012) A Ubiquitin-Binding Protein, FAAP20, Links RNF8-Mediated Ubiquitination to the Fanconi Anemia DNA Repair Network. *Mol. Cell* **47**: 61–75

- Youds JL, Barber LJ & Boulton SJ (2009) *C. elegans*: A model of Fanconi anemia and ICL repair. *Mutat. Res. - Fundam. Mol. Mech. Mutagen.* **668**: 103–116
- Zhang F, Fan Q, Ren K, Auerbach AD & Andreassen PR (2010) FANCD2 recruitment and regulation of FANCD2 in DNA damage responses. *Chromosoma* **119**: 637–649
- Zhang P & Wu MX (2018) A clinical review of phototherapy for psoriasis. *Lasers Med. Sci.* **33**: 173–180
- Zhang ZM, Rothbart SB, Allison DF, Cai Q, Harrison JS, Li L, Wang Y, Strahl BD, Wang GG & Song J (2015) An Allosteric Interaction Links USP7 to Deubiquitination and Chromatin Targeting of UHRF1. *Cell Rep.* **12**: 1400–1406
- Zhou A, Lin K, Zhang S, Ma L, Xue J, Morris S, Aldape KD & Huang S (2017) Gli1-induced deubiquitinase USP48 aids glioblastoma tumorigenesis by stabilizing Gli1. *EMBO Rep.* **18**: 1318–1330
- Zhu Q, Sharma N, He J, Wani G & Wani AA (2015) USP7 deubiquitinase promotes ubiquitin-dependent DNA damage signaling by stabilizing RNF168. *Cell Cycle* **14**: 1413–1425

CURRICULUM VITAE

Personal information

Lydia Robinson García

E-mail: LRobinson-garcia@cemm.oeaw.ac.at

Nationality: Spanish

Education

-Molecular Signal Transduction Program Predoctoral Fellow – Medical University of Vienna (Vienna, Austria) (Supported by an awarded Boehringer Ingelheim Fonds Fellowship)
Sept 2015 – Present

-MSc in Biology and Clinics of Cancer – University of Salamanca (Salamanca, Spain)
(Academic record: 9.64/10)
Sept 2014 – June 2015

-BSc/MSc Biotechnology – Polytechnic University of Valencia (Valencia, Spain)
(Academic record: 8/10 with Special Distinction in the Bachelor Thesis)
Sept 2009 – June 2014

Research experience

-Loizou Laboratory, PI: Joanna Loizou

Research Centre for Molecular Medicine of the Austrian Academy of Science (CeMM)
(Vienna, Austria)

Synthetic rescue interactions for the Fanconi anemia pathway of DNA repair
Sept 2015 – Present

-Department of Medicine, PI: Dr Rogelio González Sarmiento

University of Salamanca – Cancer Research Centre (Salamanca, Spain)

Characterization of variants of unknown significance found in patients with breast and ovarian cancer in BRCA1 and BRCA2 genes
Sept 2014 – June 2015

-Lowndes Laboratory, PI: Noel Lowndes

National University of Ireland, Galway, Department of Biochemistry (Galway City, Ireland)

Molecular studies of KIF18B as a possible mediator of the DNA damage response pathway
Aug 2013 – July 2014

-Signal transduction Laboratory, PI: Jerónimo Bravo-Sicilia

Institute of Biomedicine of Valencia, CSIC (Spanish National Science Research Council)
(Valencia, Spain)

Purification of proteins of the apoptosis pathway to achieve their molecular structure

Feb – July 2013

-Department of Biotechnology, PI: Consuelo Sabater Marco

Polytechnic University of Valencia, Department of Biotechnology (Valencia, Spain)

Toxicity studies of *Vibrio fischeri* and *Selenastrum capricornutum*

July 2012

Professional experience

-Demonstrator (National University of Ireland, Galway; October 2013)

Taught in biochemistry practical classes to 1st year students (12 students)

Assisted in any doubts and explained the main focus of the biochemistry techniques

-Member of the Association of Biotechnologists of the region of Valencia

Member of the Management Committee (2011-2013)

Acting Secretary (December 2012-May 2013)

-Member of Scout Group Domingo Savio of Granada (1999-2013)

Instructor for 4 years of children between 5-8 years old

Awards and scholarships

-Boehringer Ingelheim Fonds PhD Fellowship

December 2016 – December 2018

-Erasmus Internship scholarship: National University of Ireland Galway

August 2013 – July 2014

-Language Academic Scholarship from the Junta de Andalucía (Regional Government)

July 2008

Publications

-Robinson-Garcia L*, Ferreira da Silva J*, Loizou JI. *Synthetic lethal interactions for kinase deficiencies to DNA damage chemotherapeutics*. Cancer Research. Accepted (Review)

-Velimezi G*, **Robinson-Garcia L***, Muñoz-Martínez F, Wiegant WW, Ferreira da Silva J, Owusu M, Moder M, Wiedner M, Rosenthal SB, Fisch KM, Moffat J, Menche J, van Attikum H, Jackson SP, Loizou JI. *Map of Synthetic rescue interactions for the Fanconi anemia DNA repair pathway identifies USP48*. Nat. Commun. June 2018

- Moder M*, Velimezi G*, Owusu M, Mazouzi A, Wiedner M, Ferreira da Silva J, **Robinson-Garcia L**, Schischlik F, Slavkovsky R, Kralovics R, Schuster M, Bock C, Ideker T, Jackson SP, Menche J, Loizou JI. *Parallele genome-wide screens identify synthetic viable interactions between the BLM helicase complex and Fanconi anemia*. Nat. Commun. November 2017

*Denotes shared authorship

Conference Presentations

-Velimezi G.*, **Robinson-Garcia L***. et al. EMBO conference on the DNA damage response in cell physiology and disease (2nd-6th October 2017)

“USP48 is a synthetic rescue gene for the Fanconi anemia pathway”

-Frizzell L., Luesing J., **Robinson-Garcia L.** et al. Irish Association for Cancer Research Annual meeting. 27th-28th February 2014 (Awarded First Prize)

“The role of KIF18B, a novel 53BP1 interactor, in the DNA damage repair”

-The Francis Crick Institute Symposium 'DNA repair and genomic instability'. 30th October 2013

*Denotes shared authorship

Languages

-Mother tongues: Spanish and English

-Other languages: French (B2) and German (B1.1)